

involve

a journal of mathematics

Editorial Board

Kenneth S. Berenhaut, *Managing Editor*

Colin Adams	Suzanne Lenhart
John V. Baxley	Chi-Kwong Li
Arthur T. Benjamin	Robert B. Lund
Martin Bohner	Gaven J. Martin
Nigel Boston	Mary Meyer
Amarjit S. Budhiraja	Emil Minchev
Pietro Cerone	Frank Morgan
Scott Chapman	Mohammad Sal Moslehian
Jem N. Corcoran	Zuhair Nashed
Toka Diagana	Ken Ono
Michael Dorff	Timothy E. O'Brien
Sever S. Dragomir	Joseph O'Rourke
Behrouz Emamizadeh	Yuval Peres
Joel Foisy	Y.-F. S. Pétermann
Errin W. Fulp	Robert J. Plemmons
Joseph Gallian	Carl B. Pomerance
Stephan R. Garcia	Bjorn Poonen
Anant Godbole	James Propp
Ron Gould	Józeph H. Przytycki
Andrew Granville	Richard Rebarber
Jerrold Griggs	Robert W. Robinson
Sat Gupta	Filip Saidak
Jim Haglund	James A. Sellers
Johnny Henderson	Andrew J. Sterge
Jim Hoste	Ann Trenk
Natalia Hritonenko	Ravi Vakil
Glenn H. Hurlbert	Antonia Vecchio
Charles R. Johnson	Ram U. Verma
K. B. Kulasekera	John C. Wierman
Gerry Ladas	Michael E. Zieve
David Larson	



involve

msp.org/involve

EDITORS

MANAGING EDITOR

Kenneth S. Berenhaut, Wake Forest University, USA, berenhks@wfu.edu

BOARD OF EDITORS

Colin Adams	Williams College, USA colin.c.adams@williams.edu	David Larson	Texas A&M University, USA larson@math.tamu.edu
John V. Baxley	Wake Forest University, NC, USA baxley@wfu.edu	Suzanne Lenhart	University of Tennessee, USA lenhart@math.utk.edu
Arthur T. Benjamin	Harvey Mudd College, USA benjamin@hmc.edu	Chi-Kwong Li	College of William and Mary, USA ckli@math.wm.edu
Martin Bohner	Missouri U of Science and Technology, USA bohner@mst.edu	Robert B. Lund	Clemson University, USA lund@clemson.edu
Nigel Boston	University of Wisconsin, USA boston@math.wisc.edu	Gaven J. Martin	Massey University, New Zealand g.j.martin@massey.ac.nz
Amarjit S. Budhiraja	U of North Carolina, Chapel Hill, USA budhiraj@email.unc.edu	Mary Meyer	Colorado State University, USA meyer@stat.colostate.edu
Pietro Cerone	Victoria University, Australia pietro.cerone@vu.edu.au	Emil Minchev	Ruse, Bulgaria eminchev@hotmail.com
Scott Chapman	Sam Houston State University, USA scott.chapman@shsu.edu	Frank Morgan	Williams College, USA frank.morgan@williams.edu
Joshua N. Cooper	University of South Carolina, USA cooper@math.sc.edu	Mohammad Sal Moselehian	Ferdowsi University of Mashhad, Iran moslehian@ferdowsi.um.ac.ir
Jem N. Corcoran	University of Colorado, USA corcoran@colorado.edu	Zuhair Nashed	University of Central Florida, USA znashed@mail.ucf.edu
Toka Diagana	Howard University, USA tdiagana@howard.edu	Ken Ono	Emory University, USA ono@mathcs.emory.edu
Michael Dorff	Brigham Young University, USA mdorff@math.byu.edu	Timothy E. O'Brien	Loyola University Chicago, USA tobrie1@luc.edu
Sever S. Dragomir	Victoria University, Australia sever@matilda.vu.edu.au	Joseph O'Rourke	Smith College, USA orourke@cs.smith.edu
Behrouz Emamizadeh	The Petroleum Institute, UAE bemamizadeh@pi.ac.ae	Yuval Peres	Microsoft Research, USA peres@microsoft.com
Joel Foisy	SUNY Potsdam foisyjs@potsteam.edu	Y.-F. S. Pétermann	Université de Genève, Switzerland petermann@math.unige.ch
Errin W. Fulp	Wake Forest University, USA fulp@wfu.edu	Robert J. Plemmons	Wake Forest University, USA rplemmons@wfu.edu
Joseph Gallian	University of Minnesota Duluth, USA jgallian@d.umn.edu	Carl B. Pomerance	Dartmouth College, USA carl.pomerance@dartmouth.edu
Stephan R. Garcia	Pomona College, USA stephan.garcia@pomona.edu	Vadim Ponomarenko	San Diego State University, USA vadim@sciences.sdsu.edu
Anant Godbole	East Tennessee State University, USA godbole@etsu.edu	Bjorn Poonen	UC Berkeley, USA poonen@math.berkeley.edu
Ron Gould	Emory University, USA rg@mathcs.emory.edu	James Propp	U Mass Lowell, USA jpropp@cs.uml.edu
Andrew Granville	Université Montréal, Canada andrew@dms.umontreal.ca	József H. Przytycki	George Washington University, USA przytyck@gwu.edu
Jerrold Griggs	University of South Carolina, USA griggs@math.sc.edu	Richard Rebarber	University of Nebraska, USA rrebarbe@math.unl.edu
Sat Gupta	U of North Carolina, Greensboro, USA sngupta@uncg.edu	Robert W. Robinson	University of Georgia, USA rwr@cs.uga.edu
Jim Haglund	University of Pennsylvania, USA jhaglund@math.upenn.edu	Filip Saidak	U of North Carolina, Greensboro, USA f_saidak@uncg.edu
Johnny Henderson	Baylor University, USA johnny_henderson@baylor.edu	James A. Sellers	Penn State University, USA sellersj@math.psu.edu
Jim Hoste	Pitzer College jhoste@pitzer.edu	Andrew J. Sterge	Honorary Editor andy@ajsterge.com
Natalia Hritonenko	Prairie View A&M University, USA nahritonenko@pvamu.edu	Ann Trenk	Wellesley College, USA atrenk@wellesley.edu
Glenn H. Hurlbert	Arizona State University, USA hurlbert@asu.edu	Ravi Vakil	Stanford University, USA vakil@math.stanford.edu
Charles R. Johnson	College of William and Mary, USA crjohnso@math.wm.edu	Antonia Vecchio	Consiglio Nazionale delle Ricerche, Italy antonia.vecchio@cnr.it
K. B. Kulasekera	Clemson University, USA kk@ces.clemson.edu	Ram U. Verma	University of Toledo, USA verma99@msn.com
Gerry Ladas	University of Rhode Island, USA gladas@math.uri.edu	John C. Wierman	Johns Hopkins University, USA wierman@jhu.edu
		Michael E. Zieve	University of Michigan, USA zieve@umich.edu

PRODUCTION

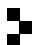
Silvio Levy, Scientific Editor

See inside back cover or msp.org/involve for submission instructions. The subscription price for 2013 is US \$105/year for the electronic version, and \$145/year (+\$35, if shipping outside the US) for print and electronic. Subscriptions, requests for back issues from the last three years and changes of subscribers address should be sent to MSP.

Involve (ISSN 1944-4184 electronic, 1944-4176 printed) at Mathematical Sciences Publishers, 798 Evans Hall #3840, c/o University of California, Berkeley, CA 94720-3840, is published continuously online. Periodical rate postage paid at Berkeley, CA 94704, and additional mailing offices.

Involve peer review and production are managed by EditFLOW[®] from Mathematical Sciences Publishers.

PUBLISHED BY

 **mathematical sciences publishers**
nonprofit scientific publishing

<http://msp.org/>

© 2013 Mathematical Sciences Publishers

Potentially eventually exponentially positive sign patterns

Marie Archer, Minerva Catral, Craig Erickson, Rana Haber,
Leslie Hogben, Xavier Martinez-Rivera and Antonio Ochoa

(Communicated by Chi-Kwong Li)

We introduce the study of potentially eventually exponentially positive (PEEP) sign patterns and establish several results using the connections between these sign patterns and the potentially eventually positive (PEP) sign patterns. It is shown that the problem of characterizing PEEP sign patterns is not equivalent to that of characterizing PEP sign patterns. A characterization of all 2×2 and 3×3 PEEP sign patterns is given.

1. Introduction

A matrix $A \in \mathbb{R}^{n \times n}$ is *eventually positive* if there exists a $k_0 \in \mathbb{Z}^+$ such that for all $k \geq k_0$, $A^k > 0$ (where the inequality is interpreted entrywise). A matrix A is *eventually exponentially positive* if there exists some $t_0 \geq 0$ such that for all $t \geq t_0$,

$$e^{tA} = \sum_{k=0}^{\infty} \frac{t^k A^k}{k!} > 0.$$

Eventually exponentially positive matrices have applications to dynamical systems in situations where it is of interest to determine whether an initial trajectory reaches positivity at a certain time and remains positive thereafter [Noutsos and Tsatsomeros 2008]. There is a characterization of eventual exponential positivity in terms of eventual positivity:

Theorem 1.1 [Noutsos and Tsatsomeros 2008, Theorem 3.3]. *The matrix $A \in \mathbb{R}^{n \times n}$ is eventually exponentially positive if and only if there exists $a \geq 0$ such that $A + aI$ is eventually positive (where I is the $n \times n$ identity matrix).*

MSC2010: 15A18, 15B35, 15B48.

Keywords: potentially eventually exponentially positive, potentially eventually positive, PEEP, PEP, sign pattern, matrix.

This research was supported by NSF grant DMS-0502354.

A *sign pattern* is a matrix having entries in $\{+, -, 0\}$. For a real matrix A , $\text{sgn}(A)$ is the sign pattern having entries that correspond to the signs of the entries in A . If \mathcal{A} is an $n \times n$ sign pattern, the *qualitative class* of \mathcal{A} , denoted $\mathcal{Q}(\mathcal{A})$, is the set of all $A \in \mathbb{R}^{n \times n}$ such that $\text{sgn}(A) = \mathcal{A}$; such a matrix A is called a *realization* of \mathcal{A} . A sign pattern \mathcal{A} is *potentially eventually positive* (PEP) if there exists some realization $A \in \mathcal{Q}(\mathcal{A})$ that is eventually positive. PEP sign patterns were studied in [Berman et al. 2010], and we adapt several techniques from that paper to study potentially eventually exponentially positive sign patterns.

Definition 1.2. A sign pattern \mathcal{A} is *potentially eventually exponentially positive* (PEEP) if there exists some realization $A \in \mathcal{Q}(\mathcal{A})$ that is eventually exponentially positive.

Since an eventually positive matrix is eventually exponentially positive, a PEP sign pattern is PEEP. Theorem 1.1 leads naturally to consideration of a sign pattern with positive diagonal entries.

Definition 1.3. Given an $n \times n$ sign pattern $\mathcal{A} = [\alpha_{ij}]$, we denote by $\mathcal{A}_{D(+)} = [\hat{\alpha}_{ij}]$ the $n \times n$ sign pattern such that $\hat{\alpha}_{ij} = \alpha_{ij}$ for $i \neq j$ and $\hat{\alpha}_{ii} = +$ for $i, j \in \{1, \dots, n\}$. $\mathcal{A}_{D(0)}$ and $\mathcal{A}_{D(-)}$ are defined analogously, with zero and negative diagonal, respectively.

In [Berman et al. 2010] it is noted that if \mathcal{A} is PEP then $\mathcal{A}_{D(+)}$ is also PEP. This observation together with Theorem 1.1 leads to the following observation.

Observation 1.4. If \mathcal{A} is a PEEP sign pattern, then $\mathcal{A}_{D(+)}$ is a PEP sign pattern (and hence $\mathcal{A}_{D(+)}$ is also PEEP).

Given a PEEP sign pattern, we can generate a PEP sign pattern by changing every diagonal element to $+$. However, taking a PEP sign pattern and changing $+$ diagonal entries to 0 or $-$ does not always yield a PEEP sign pattern. For example,

$$\mathcal{B}_{D(+)} = \begin{bmatrix} + & - & 0 \\ + & + & - \\ - & + & + \end{bmatrix} \tag{1}$$

is PEP [Berman et al. 2010], but in Example 2.3 below it is shown that the sign pattern

$$\mathcal{B}_{D(0)} = \begin{bmatrix} 0 & - & 0 \\ + & 0 & - \\ - & + & 0 \end{bmatrix} \tag{2}$$

is not PEEP. Thus the problem of determining which sign patterns are PEEP is not equivalent to the problem of determining which sign patterns are PEP.

Section 2 presents general results on PEEP sign patterns, including those obtained by perturbation analysis and connections with known results on PEP sign patterns.

At the end of Section 2 the open question of the minimum number of positive entries in an $n \times n$ PEEP sign pattern is discussed. In Section 3 small order PEEP sign patterns are characterized. The remainder of this section contains information on eventually exponentially positive matrices and terminology on digraphs and sign patterns.

The *spectrum* of A , denoted $\sigma(A)$, is the multiset of the eigenvalues of A . The *spectral radius* of A is defined as $\rho(A) = \max\{|\lambda| : \lambda \in \sigma(A)\}$ and an eigenvalue $\lambda \in \sigma(A)$ is a *dominant eigenvalue* if $|\lambda| = \rho(A)$. A nonzero vector \mathbf{w} is called a *left eigenvector* of A if $\mathbf{w}^T A = \lambda \mathbf{w}^T$ for some $\lambda \in \sigma(A)$ (or equivalently, \mathbf{w} is a (right) eigenvector of A^T). The matrix A is eventually positive if and only if A has a unique dominant eigenvalue that is positive and simple, and A has positive right and left eigenvectors for $\rho(A)$ [Handelman 1981] (this is called the *strong Perron–Frobenius test* for eventual positivity).

Definition 1.5. A real eigenvalue $\gamma \in \sigma(A)$ is called the *rightmost eigenvalue* if it is simple and for all $\lambda \in \sigma(A)$, $\lambda \neq \gamma$ implies $\operatorname{Re}(\lambda) < \gamma$, where $\operatorname{Re}(\alpha)$ denotes the real part of a complex number α .

Not every matrix has a rightmost eigenvalue. Definition 1.5 was motivated by the following test for eventual exponential positivity, which is implicit in the proof of Theorem 3.3 in [Noutsos and Tsatsomeris 2008] (and also follows immediately from that theorem, which is Theorem 1.1 above).

Proposition 1.6. *Let $A \in \mathbb{R}^{n \times n}$. Then A is eventually exponentially positive if and only if A has a rightmost eigenvalue having positive left and right eigenvectors.*

An eventually positive matrix must have a positive entry in each row and column. This need not be the case for an eventually exponentially positive matrix (for example, an eventually exponentially positive matrix that realizes $\mathcal{B}_{D(-)}$ in (3) will not have a positive entry in each row and column). However, certain conditions on the eigenvalues require an eventually exponentially positive matrix to have a positive entry in each row and column.

Proposition 1.7. *Let A be an eventually exponentially positive matrix.*

1. *If A has an eigenvalue with nonnegative real part, then each row and column of A has a positive entry.*
2. *If A does not have an eigenvalue with positive real part, then each row and column of A has a negative entry.*

Proof. If A has an eigenvalue with nonnegative real part, then the rightmost eigenvalue γ of A is nonnegative. By Proposition 1.6, A has positive right and left eigenvectors corresponding to γ . Suppose that row k of A has no positive entry. Since A is an eventually exponentially positive matrix, A is irreducible, so row k

has a negative entry. But then if $\mathbf{x} > 0$, $(A\mathbf{x})_k < 0$ and $(\gamma\mathbf{x})_k \geq 0$, so \mathbf{x} is not a (right) eigenvector. Thus every row of A has a positive entry. The result for column k of A is established with the left eigenvector. Similarly, if A has no eigenvalue with positive real part, then $\gamma \leq 0$ and every row and every column of A has a negative entry. \square

A square sign pattern \mathcal{A} (or matrix) is *reducible* if there exists a permutation matrix P such that

$$P\mathcal{A}P^T = \begin{bmatrix} \mathcal{A}_{11} & 0 \\ \mathcal{A}_{21} & \mathcal{A}_{22} \end{bmatrix},$$

where \mathcal{A}_{11} and \mathcal{A}_{22} are nonempty square sign patterns (or matrices) and 0 is a (possibly rectangular) block consisting entirely of zero entries. If \mathcal{A} is not reducible, then \mathcal{A} is called *irreducible* (note any 1×1 matrix is irreducible). Since an eventually exponentially positive matrix must be irreducible, a PEEP sign pattern must be irreducible.

For an $n \times n$ sign pattern $\mathcal{A} = [\alpha_{ij}]$, the *digraph of \mathcal{A}* , denoted $\Gamma(\mathcal{A})$, has vertex set $\{1, \dots, n\}$ and arc set $\{(i, j) : \alpha_{ij} \neq 0\}$. A nonnegative sign pattern \mathcal{A} is *primitive* if \mathcal{A} is irreducible and the greatest common divisor of the lengths of the cycles of $\Gamma(\mathcal{A})$ is one; for a nonnegative matrix the definition of primitive is analogous. It is well known that a primitive (necessarily nonnegative) matrix is eventually positive.

Let $\mathcal{A} = [\alpha_{ij}]$, $\hat{\mathcal{A}} = [\hat{\alpha}_{ij}]$ be sign patterns. If $\alpha_{ij} \neq 0$ implies $\alpha_{ij} = \hat{\alpha}_{ij}$, then \mathcal{A} is a *subpattern* of $\hat{\mathcal{A}}$ and $\hat{\mathcal{A}}$ is a *superpattern* of \mathcal{A} . Define the *positive part* of \mathcal{A} to be $\mathcal{A}^+ = [\alpha_{ij}^+]$, where

$$\alpha_{ij}^+ = \begin{cases} + & \text{if } \alpha_{ij} = +, \\ 0 & \text{if } \alpha_{ij} = 0 \text{ or } \alpha_{ij} = -. \end{cases}$$

Note \mathcal{A}^+ is a subpattern of \mathcal{A} .

2. PEEP sign patterns

In this section we establish general properties of PEEP sign patterns. Some of these results will be used in Section 3 to determine which sign patterns of order at most 3 are PEEP.

Remark 2.1. If $\mathcal{A}_{D(+)}$ is a PEP sign pattern, then $\mathcal{A}_{D(-)}$ is a PEEP sign pattern, because if $A \in \mathcal{Q}(\mathcal{A}_{D(+)})$ is eventually positive, there exists $t > 0$ such that $A - tI \in \mathcal{Q}(\mathcal{A}_{D(-)})$.

A PEP sign pattern must have a positive entry in each row and column. This need not be the case for an eventually exponentially positive matrix. The sign pattern

$$\mathcal{B}_{D(-)} = \begin{bmatrix} - & - & 0 \\ + & - & - \\ - & + & - \end{bmatrix} \tag{3}$$

is PEEP because the sign pattern $\mathcal{B}_{D(+)}$ in (1) is PEP. But $\mathcal{B}_{D(-)}$ does not have a + entry in row 1 nor in column 3. If $A \in \mathbb{R}^{n \times n}$ is an eventually exponentially positive matrix with nonnegative trace, then A has an eigenvalue with nonnegative real part. As a consequence of Proposition 1.7, we have the following observation.

Observation 2.2. If \mathcal{A} is a PEEP sign pattern with no – on the diagonal, then \mathcal{A} has a + in each row and column.

The next example shows that the problem of determining which sign patterns are PEEP is not equivalent to the problem of determining which sign patterns are PEP, because the fact that $\mathcal{A}_{D(+)}$ is PEP does not guarantee that \mathcal{A} is PEEP.

Example 2.3. The sign pattern

$$\mathcal{B}_{D(0)} = \begin{bmatrix} 0 & - & 0 \\ + & 0 & - \\ - & + & 0 \end{bmatrix}$$

is not PEEP by Observation 2.2, because $\mathcal{B}_{D(0)}$ has no – on the diagonal and no + in row 1. Note that $(\mathcal{B}_{D(0)})_{D(+)} = \mathcal{B}_{D(+)}$ from (1) is PEP.

Related sign patterns are discussed in Corollary 3.4 and Theorem 3.5 below.

Matrix perturbations are used extensively in the study of potential eventual positivity. It is well known that for any matrix $A \in \mathbb{R}^{n \times n}$, the eigenvalues of A are continuous functions of the entries of A . For a simple eigenvalue, the same is true of the eigenvector [Golub and Van Loan 1996, p. 323]. Because a matrix is eventually positive if and only if it passes the strong Perron–Frobenius test, eventual positivity is inherited by matrices that are small perturbations of eventually positive matrices. That is, if $A \in \mathbb{R}^{n \times n}$ is eventually positive and $C \in \mathbb{R}^{n \times n}$ is any matrix, then for ε sufficiently small, $A(\varepsilon) = A + \varepsilon C$ is eventually positive (see, for example, [Ellison et al. 2010] for applications of this technique). The analogous result for eventually exponentially positive matrices follows from Proposition 1.6 and perturbation theory.

Theorem 2.4. *If $A \in \mathbb{R}^{n \times n}$ is eventually exponentially positive and $C \in \mathbb{R}^{n \times n}$ is any matrix, then for ε sufficiently small, $A(\varepsilon) = A + \varepsilon C$ is eventually exponentially positive.*

If $\hat{\mathcal{A}}$ is a superpattern of a PEEP sign pattern \mathcal{A} , and $A \in \mathcal{Q}(\mathcal{A})$ is eventually exponentially positive, then a matrix \hat{A} realizing $\hat{\mathcal{A}}$ can be obtained by a small perturbation of A .

Corollary 2.5. *If \mathcal{A} is a PEEP sign pattern, then every superpattern of \mathcal{A} is PEEP. If $\hat{\mathcal{A}}$ is a sign pattern that is not PEEP, then no subpattern of $\hat{\mathcal{A}}$ is a PEEP sign pattern.*

If a sign pattern \mathcal{A} has a primitive positive part, it is PEP. There is an analogous result for PEEP sign patterns.

Theorem 2.6. *Let \mathcal{A} be a sign pattern such that \mathcal{A}^+ is irreducible. Then \mathcal{A} is PEEP.*

Proof. Let B be the matrix obtained from \mathcal{A}^+ by replacing $+$ by 1. Since $B + I \geq 0$, has positive entries on its diagonal, and is irreducible, $B + I$ is primitive and thus eventually positive. So B is eventually exponentially positive and \mathcal{A}^+ is PEEP. Since \mathcal{A} is a superpattern of \mathcal{A}^+ , \mathcal{A} is PEEP. \square

The converse of Theorem 2.6 is false because the sign pattern $\mathcal{B}_{D(+)}(1)$ is a PEP sign pattern with reducible positive part.

Several necessary or sufficient conditions for PEP sign patterns were established in [Berman et al. 2010]. The sign patterns

$$\mathcal{B}_1 = \begin{bmatrix} - & - & + \\ + & - & - \\ - & + & - \end{bmatrix}, \quad \mathcal{B}_2 = \begin{bmatrix} - & - & - \\ + & - & - \\ - & + & - \end{bmatrix}$$

are PEEP and demonstrate that the following statements about PEP sign patterns do not necessarily hold for PEEP sign patterns:

1. For $n \geq 2$, an $n \times n$ sign pattern that has exactly one positive entry in each row and each column is not PEP.
2. If $n \geq 2$, the minimum number of $+$ entries in an $n \times n$ PEP sign pattern is $n+1$.
3. If A is PEP, then $\Gamma(\mathcal{A})$ has a cycle (of length one or more) consisting entirely of $+$ entries.

Certain conditions that prevent a sign pattern from being PEP also prevent a sign pattern from being PEEP:

Theorem 2.7 [Berman et al. 2010]. *Let $\mathcal{A} = [\alpha_{ij}]$ be an $n \times n$ sign pattern with $n \geq 2$ such that for every $k = 1, \dots, n$,*

1. $\alpha_{kk} = +$, and
2. (a) no off-diagonal entry in row k is $+$, or
(b) no off-diagonal entry in column k is $+$.

Then \mathcal{A} is not PEP.

Corollary 2.8. Let $\mathcal{A} = [\alpha_{ij}]$ be an $n \times n$ sign pattern with $n \geq 2$ such that for every $k = 1, \dots, n$,

- (a) no off-diagonal entry in row k is $+$, or
- (b) no off-diagonal entry in column k is $+$.

Then \mathcal{A} is not PEEP.

Proof. By Theorem 2.7, $\mathcal{A}_{D(+)}$ is not PEP, so \mathcal{A} is not PEEP. □

Corollary 2.9. If \mathcal{A} is a PEEP sign pattern, then there exists k such that both row and column k have an off-diagonal $+$. Hence, a PEEP sign pattern must have at least 2 positive off-diagonal entries.

A square sign pattern \mathcal{A} is a Z sign pattern if $\alpha_{ij} \neq +$ for all $i \neq j$.

Corollary 2.10. If \mathcal{A} is an $n \times n$ Z sign pattern with $n \geq 2$, then \mathcal{A} is not PEEP.

Proposition 2.11 [Berman et al. 2010]. Let

$$\mathcal{K} = \begin{bmatrix} [+ & - & + & \dots \\ [- & + & - & \dots \\ [+ & - & + & \dots \\ \vdots & \vdots & \vdots & \ddots \end{bmatrix}$$

be a square checkerboard block sign pattern where the block $+$ (respectively, $-$) consists of entirely positive (respectively, entirely negative) entries, and the diagonal blocks are square. Then $-\mathcal{K}$ is not PEP, and if \mathcal{K} has a negative entry, then \mathcal{K} is not PEP.

Corollary 2.12. No subpattern of a checkerboard pattern \mathcal{K} that contains a negative entry is PEEP.

Remark 2.13. Provided the sign pattern \mathcal{K} contains a negative entry,

$$-\mathcal{K} = \begin{bmatrix} [- & + & - & \dots \\ [+ & - & + & \dots \\ [- & + & - & \dots \\ \vdots & \vdots & \vdots & \ddots \end{bmatrix}$$

is PEEP because the positive part of $(-\mathcal{K})_{D(+)}$ is primitive.

For a PEP sign pattern \mathcal{A} , Lemma 4.3 in [Berman et al. 2010] establishes the existence of a standard form of a matrix $C \in \mathcal{Q}(\mathcal{A})$ with $\rho(C) = 1$ and $C\mathbf{1} = \mathbf{1}$. We have a related result for PEEP sign patterns.

Proposition 2.14. Let \mathcal{A} be a PEEP sign pattern. There is an eventually exponentially positive matrix $C \in \mathcal{Q}(\mathcal{A})$ such that the rightmost eigenvalue $\gamma(C)$ lies in $\{-1, 0, 1\}$ and $C\mathbf{1} = \gamma(C)\mathbf{1}$.

Proof. There exists $A \in \mathcal{Q}(\mathcal{A})$ that is eventually exponentially positive. Let $\gamma(A)$ be the rightmost eigenvalue of A and $\mathbf{v} = [v_1, \dots, v_n]^T$ be the corresponding positive eigenvector. If $\gamma(A) \neq 0$, let $B = (1/|\gamma(A)|)A$; otherwise, $B = A$. Then $B \in \mathcal{Q}(\mathcal{A})$, B is eventually exponentially positive, $\gamma(B) \in \{-1, 0, 1\}$, and $B\mathbf{v} = \gamma(B)\mathbf{v}$. Let $C = D^{-1}BD$ for $D = \text{diag}(v_1, \dots, v_n)$. Then $C \in \mathcal{Q}(\mathcal{A})$ is eventually exponentially positive and $\gamma(C) \in \{-1, 0, 1\}$ with $C\mathbf{1} = \gamma(C)\mathbf{1}$. \square

We have only started the study of PEEP sign patterns and there are many open questions. Here we highlight one particular question.

Question 2.15. What is the minimum number of positive entries in an $n \times n$ PEEP sign pattern, or equivalently, what is the minimum number of positive entries in an eventually exponentially positive $n \times n$ matrix?

This question is motivated by Corollary 4.5 in [Berman et al. 2010], which states that the minimum number of positive entries in an $n \times n$ PEP sign pattern is $n + 1$ (for $n \geq 2$). An upper bound for the minimum number of $+$ entries in a PEEP sign pattern is given by the following example.

Example 2.16. Let \mathcal{C}_n be the $n \times n$ sign pattern

$$\mathcal{C}_n = \begin{bmatrix} 0 & + & 0 & \cdots & 0 \\ 0 & 0 & + & \cdots & 0 \\ \vdots & \vdots & \vdots & \ddots & \vdots \\ 0 & 0 & 0 & \cdots & + \\ + & 0 & 0 & \cdots & 0 \end{bmatrix}.$$

Since \mathcal{C}_n is nonnegative and irreducible, it is PEEP; note that \mathcal{C}_n has n positive entries.

Corollary 2.17. *The minimum number of positive entries in an $n \times n$ PEEP sign pattern is at most n .*

The sign pattern $\mathcal{B}_{D(-)}$ in (3) is a 3×3 pattern that has only 2 positive entries, and from Theorem 3.5 in the next section it follows that the minimum number of positive entries in a 3×3 PEEP sign pattern is exactly 2. But we do not have examples of PEEP sign patterns having fewer than n positive entries for $n > 3$.

3. Classification of small order PEEP sign patterns

In this section we classify all 2×2 and 3×3 sign patterns as to whether the pattern is PEEP.

Two $n \times n$ sign patterns \mathcal{A} and \mathcal{A}' are *equivalent* if $\mathcal{A}' = P^T \mathcal{A} P$ or $\mathcal{A}' = P^T \mathcal{A}^T P$ (where P is a permutation matrix). Throughout this section: $?$ is one of $0, +, -$; \oplus is one of $0, +$; \ominus is one of $0, -$.

It is clear that every 1×1 sign pattern is PEEP. The classification of 2×2 sign patterns as to whether they are PEEP is immediate from the classification as to whether they are PEP.

Proposition 3.1. *A 2×2 sign pattern is PEEP if and only if it is of the form*

$$\begin{bmatrix} ? & + \\ + & ? \end{bmatrix}. \tag{4}$$

Proof. Sign patterns of the form (4) have \mathcal{A}^+ irreducible and so by Theorem 2.6, they are PEEP. For the converse, let \mathcal{A} be a 2×2 PEEP sign pattern. Then $\mathcal{A}_{D(+)}$ is PEP. In [Berman et al. 2010] it was shown that any 2×2 PEP sign pattern has both off-diagonal entries equal to $+$, so \mathcal{A} must also have both off-diagonal entries equal to $+$. \square

The classification of 3×3 sign patterns as to whether they are PEEP makes use of the following classification as to whether they are PEP.

Theorem 3.2 [Berman et al. 2010]. *A 3×3 sign pattern \mathcal{A} is PEP if and only if \mathcal{A}^+ is primitive or \mathcal{A} is equivalent to a sign pattern of the form*

$$\mathcal{B} = \begin{bmatrix} + & - & \ominus \\ + & ? & - \\ - & + & + \end{bmatrix}. \tag{5}$$

Theorem 3.3. *Let*

$$B = \begin{bmatrix} x_1 & -b_{12} & -b_{13} \\ b_{21} & x_2 & -b_{23} \\ -b_{31} & b_{32} & x_3 \end{bmatrix}, \quad \text{with } b_{ij} > 0 \text{ for all } i, j = 1, 2, 3,$$

be an eventually exponentially positive matrix (note there is no restriction on the signs of $x_i, i = 1, 2, 3$). Then $x_2 < \min\{x_1, x_3\}$.

Proof. Let γ be the rightmost eigenvalue of B . Observe that $B - \gamma I$ is eventually exponentially positive with rightmost eigenvalue 0. By Proposition 1.7, $B - \gamma I$ must have a positive entry in each row and column, so $x_1, x_3 > \gamma$. Since the rightmost eigenvalue of $B - \gamma I$ is simple, $0 > \text{tr}(B - \gamma I) = (x_1 - \gamma) + (x_2 - \gamma) + (x_3 - \gamma)$. The first and third term in this sum are positive, so $\text{tr}(B - \gamma I) < 0$ implies that $x_2 < \gamma$. \square

Corollary 3.4. *A sign pattern equivalent to one of the forms*

$$\mathcal{M}_1 = \begin{bmatrix} - & - & - \\ + & + & - \\ - & + & - \end{bmatrix} \quad \text{or} \quad \mathcal{M}_2 = \begin{bmatrix} - & - & - \\ + & + & - \\ - & + & + \end{bmatrix}$$

is not PEEP.

Theorem 3.5. *A 3×3 sign pattern is PEEP if and only if it is equivalent to one of the following four forms:*

$$\begin{aligned} \mathcal{A}_1 &= \begin{bmatrix} ? & + & ? \\ ? & ? & + \\ + & ? & ? \end{bmatrix}, & \mathcal{A}_2 &= \begin{bmatrix} ? & + & + \\ + & ? & \ominus \\ + & \ominus & ? \end{bmatrix}, \\ \mathcal{A}_3 &= \begin{bmatrix} ? & - & \ominus \\ + & - & - \\ - & + & ? \end{bmatrix}, & \mathcal{A}_4 &= \begin{bmatrix} + & - & \ominus \\ + & \oplus & - \\ - & + & + \end{bmatrix}. \end{aligned}$$

Proof. The sign patterns \mathcal{A}_1 and \mathcal{A}_2 are PEEP by Theorem 2.6. Note that \mathcal{A}_4 is of the form \mathcal{B} from Theorem 3.2; therefore \mathcal{A}_4 is PEP and hence is PEEP. Let

$$A = \begin{bmatrix} 0 & -10 & 0 \\ 22 & -33 & -8 \\ -16 & 22 & 0 \end{bmatrix}.$$

Since the spectrum of A is $\{-5, -14 + 2i\sqrt{15}, -14 - 2i\sqrt{15}\}$, $\gamma = -5$ is the rightmost eigenvalue of A , and γ has the right and left eigenvectors $[2, 1, 2]^T$ and $[18, 25, 40]^T$ respectively. Thus A is eventually exponentially positive by Proposition 1.6. Note that $A \in \mathcal{Q}(\mathcal{A}_3(0))$ where $\mathcal{A}_3(0)$ is the form of \mathcal{A}_3 with all flexible entries set to zero. Therefore $\mathcal{A}_3(0)$ is PEEP, and by Corollary 2.5 every superpattern of $\mathcal{A}_3(0)$ is PEEP. Hence every sign pattern of the form \mathcal{A}_3 is PEEP.

Let \mathcal{A} be a 3×3 PEEP sign pattern. Then by Observation 1.4, $\mathcal{A}_{D(+)}$ is PEP. By Theorem 3.2 either $(\mathcal{A}_{D(+)})^+$ is primitive or $\mathcal{A}_{D(+)}$ is of the form \mathcal{B} in (5). If $(\mathcal{A}_{D(+)})^+$ is primitive, then \mathcal{A} is of the form \mathcal{A}_1 or \mathcal{A}_2 . Now suppose that $(\mathcal{A}_{D(+)})^+$ is not primitive. Then we must consider all possible sign patterns \mathcal{A} such that

$$\mathcal{A}_{D(+)} = \begin{bmatrix} + & - & \ominus \\ + & + & - \\ - & + & + \end{bmatrix}.$$

The sign patterns \mathcal{M}_1 and \mathcal{M}_2 in Corollary 3.4 and their subpatterns rule out all of the sign patterns that could possibly have this $\mathcal{A}_{D(+)}$ except for those of the form \mathcal{A}_3 and \mathcal{A}_4 . Therefore if \mathcal{A} is a 3×3 PEEP sign pattern, it must be of one of the forms $\mathcal{A}_1, \mathcal{A}_2, \mathcal{A}_3$ or \mathcal{A}_4 . □

The symbols \ominus and \oplus are used in Theorem 3.5 so that the listed patterns are disjoint classes. For example, if the $(2, 2)$ -entry of \mathcal{A}_4 were changed to $?$, then one sign pattern of that form would be equivalent to one sign pattern of the form of \mathcal{A}_3 .

References

- [Berman et al. 2010] A. Berman, M. Catral, L. M. DeAlba, A. Elhashash, F. J. Hall, L. Hogben, I.-J. Kim, D. D. Olesky, P. Tarazaga, M. J. Tsatsomeros, and P. van den Driessche, “Sign patterns that allow eventual positivity”, *Electron. J. Linear Algebra* **19** (2010), 108–120. MR 2011c:15089 Zbl 1190.15031
- [Ellison et al. 2010] E. M. Ellison, L. Hogben, and M. J. Tsatsomeros, “Sign patterns that require eventual positivity or require eventual nonnegativity”, *Electron. J. Linear Algebra* **19** (2010), 98–107. MR 2011a:15048 Zbl 1193.15031
- [Golub and Van Loan 1996] G. H. Golub and C. F. Van Loan, *Matrix computations*, 3rd ed., Johns Hopkins University Press, Baltimore, MD, 1996. MR 97g:65006 Zbl 0865.65009
- [Handelman 1981] D. Handelman, “Positive matrices and dimension groups affiliated to C^* -algebras and topological Markov chains”, *J. Operator Theory* **6**:1 (1981), 55–74. MR 84i:46058 Zbl 0495.06011
- [Noutsos and Tsatsomeros 2008] D. Noutsos and M. J. Tsatsomeros, “Reachability and holdability of nonnegative states”, *SIAM J. Matrix Anal. Appl.* **30**:2 (2008), 700–712. MR 2009e:93006 Zbl 1159.93004

Received: 2011-07-11 Accepted: 2013-05-25

- | | |
|-----------------------|--|
| mariemtz@iastate.edu | <i>Mathematics and Computing, Columbia College, 1301 Columbia College Drive, Columbia, SC 29203, United States</i> |
| catralm@xavier.edu | <i>Department of Mathematics and Computer Science, Xavier University, 3800 Victory Parkway, Cincinnati, OH 45207, United States</i> |
| craig@iastate.edu | <i>Department of Mathematics, Iowa State University of Science and Technology, 396 Carver Hall, Ames, IA 50011-2064, United States</i> |
| rhaber2010@my.fit.edu | <i>Department of Mathematics and Statistics, California State Polytechnic University, Pomona, 3801 West Temple Avenue, Pomona, CA 91768, United States</i> |
| hogben@aimath.org | <i>Department of Mathematical Sciences, Florida Institute of Technology, 3366 Mazur Drive, Melbourne, FL 32901, United States</i> |
| xaviermr@iastate.edu | <i>Department of Mathematics, Iowa State University, Ames, IA 50011, United States</i> |
| adjochoa@gmail.com | <i>American Institute of Mathematics, 360 Portage Avenue, Palo Alto, CA 94306, United States</i> |
| | <i>Department of Mathematical Sciences, University of Puerto Rico, Highway no. 2, Post 259 North, Mayagüez, Puerto Rico 00681, United States</i> |
| | <i>Department of Mathematics and Statistics, California State Polytechnic University, Pomona, 3801 West Temple Avenue, Pomona, CA 91768, United States</i> |

The surgery unknotting number of Legendrian links

Bianca Boranda, Lisa Traynor and Shuning Yan

(Communicated by Kenneth S. Berenhaut)

The surgery unknotting number of a Legendrian link is defined as the minimal number of particular oriented surgeries that are required to convert the link into a Legendrian unknot. Lower bounds for the surgery unknotting number are given in terms of classical invariants of the Legendrian link. The surgery unknotting number is calculated for every Legendrian link that is topologically a twist knot or a torus link and for every positive, Legendrian rational link. In addition, the surgery unknotting number is calculated for every Legendrian knot in the Legendrian knot atlas of Chongchitmate and Ng whose underlying smooth knot has crossing number 7 or less. In all these calculations, as long as the Legendrian link of j components is not topologically a slice knot, its surgery unknotting number is equal to the sum of $j-1$ and twice the smooth 4-ball genus of the underlying smooth link.

1. Introduction

A classical invariant for smooth knots is the unknotting number: the unknotting number of a diagram of a knot K is the minimum number of crossing changes required to change the diagram into a diagram of the unknot; the unknotting number of K is the minimum of the unknotting numbers of all diagrams of K . In the following, we will define a surgery unknotting number for Legendrian knots and links.

Legendrian links are smooth links that satisfy an additional geometric condition imposed by a contact structure. We will focus on Legendrian links in \mathbb{R}^3 with its standard contact structure. The notion of Legendrian equivalence is more refined than smooth equivalence: there is only one smooth unknot, but there are an infinite number of Legendrian unknots. Figure 1 shows the front projections of three

MSC2010: primary 53D35, 57R17; secondary 57M25.

Keywords: Legendrian links, unknotting number, genus, Lagrangian cobordism.

Lisa Traynor is partially supported by NSF grant DMS-0909021. Bianca Boranda and Shuning Yan completed this work as Bryn Mawr College undergraduates; they received support from NSF grant DMS-0909021 to pursue this research.

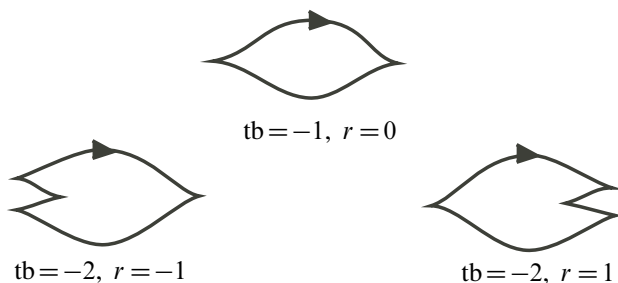


Figure 1. Three different Legendrian knots that are topologically the unknot.

different Legendrian unknots; the infinite structure representing all Legendrian unknots is depicted in Figure 7 on page 281.

The act of changing a crossing (smoothly passing a knot through itself) is not a natural operation in a contact manifold. Instead, given a Legendrian link, we will attempt to arrive at a Legendrian unknot through a Legendrian “surgery” operation in which two oppositely oriented strands in a Legendrian 0-tangle are replaced by an oriented, Legendrian ∞ -tangle as illustrated in Figure 2. It is shown in Proposition 3.5 that every Legendrian link can become a Legendrian unknot after a finite number of surgeries. The surgery unknotting number of a Legendrian link Λ , $\sigma_0(\Lambda)$, measures the minimal number of these surgeries that are required to convert Λ to a Legendrian unknot; see Definitions 3.1 and 3.6. In the following, our goal is to study and calculate this Legendrian invariant $\sigma_0(\Lambda)$.

Main results. Lower bounds on $\sigma_0(\Lambda)$ exist in terms of the classical invariants of Λ . These invariants include invariants of the underlying smooth link type L_Λ and the classical Legendrian invariants of Λ : the Thurston–Bennequin, $tb(\Lambda)$, and rotation number, $r(\Lambda)$, as defined in Section 2.

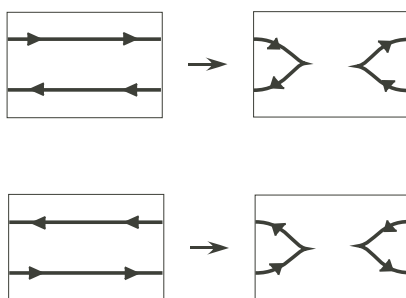


Figure 2. Oriented Legendrian surgeries: a basic, compatibly oriented 0-tangle is replaced by a basic, compatibly oriented ∞ -tangle.

Theorem 1.1. *Let Λ be a Legendrian link. Then:*

- (1) $\text{tb}(\Lambda) + |r(\Lambda)| + 1 \leq \sigma_0(\Lambda)$.
- (2) *If Λ has j components, L_Λ denotes the underlying smooth link type of Λ , and $g_4(L_\Lambda)$ denotes the smooth 4-ball genus of L_Λ ,¹ then*

$$2g_4(L_\Lambda) + (j - 1) \leq \sigma_0(\Lambda).$$

Remark 1.2. In parallel to Theorem 1.1 (1), when Λ is a Legendrian knot with underlying smooth knot type K_Λ , the well known slice-Bennequin inequality says that

$$\text{tb}(\Lambda) + |r(\Lambda)| + 1 \leq 2g_4(K_\Lambda). \tag{1-1}$$

There are now a number of proofs of this result, but all use deep theory. Lisca and Matic [1998] prove this using their adjunction inequality obtained by Seiberg–Witten theory. See also [Akbulut and Matveyev 1997; Rudolph 1995]. In contrast, the proof of Theorem 1.1 is elementary and is given in Lemmas 3.8 and 3.9.

When Λ is a knot, combining Theorem 1.1(2) and the slice-Bennequin inequality (1-1), we find:

Corollary 1.3. *For any Legendrian knot Λ , if K_Λ denotes the smooth knot type of Λ then*

$$\text{tb}(\Lambda) + |r(\Lambda)| + 1 \leq 2g_4(K_\Lambda) \leq \sigma_0(\Lambda).$$

Thus $\sigma_0(\Lambda) = 2g_4(K_\Lambda)$ when $\sigma_0(\Lambda) = \text{tb}(\Lambda) + |r(\Lambda)| + 1$.

As we will see below, this corollary sometimes allows us to calculate the smooth 4-ball genus of a knot.

Using the established lower bounds, we can calculate $\sigma_0(\Lambda)$ when the underlying smooth link type of Λ falls within some important families.

Theorem 1.4. (1) *If Λ is a Legendrian knot that is topologically a nontrivial twist knot, then $\sigma_0(\Lambda) = 2$.*

- (2) *If Λ is a j -component Legendrian link that is topologically a (jp, jq) -torus link, $|p| > q > 1$ and $\text{gcd}(p, q) = 1$, then*

$$\sigma_0(\Lambda) = (|jp| - 1)(jq - 1).$$

Theorem 1.4 is proved in Section 4 as Theorems 4.1 and 4.2. The proof of this theorem relies heavily on the classification of Legendrian twist knots given by Etnyre, Ng and Vértesi [Etnyre et al. 2013], and the classification of Legendrian torus knots by Etnyre and Honda [2001], which was extended to a classification of Legendrian torus links by Dalton [2008]. When Λ is topologically a positive torus

¹That is, $g_4(L_\Lambda)$ denotes the minimal genus of a smooth, compact, connected, oriented surface $\Sigma \subset B^4$ with $\partial\Sigma = L_\Lambda \subset \mathbb{R}^3 \subset S^3 = \partial B^4$.

link, $p > 0$, of maximal Thurston–Bennequin invariant, the calculation of $\sigma_0(\Lambda)$ is obtained realizing the lower bound given in Theorem 1.1 by the Legendrian invariants of Λ . Thus by Corollary 1.3, which employs the deep slice–Bennequin inequality in (1-1), we are able to deduce the Milnor conjecture about torus knots, originally proved by Kronheimer and Mrowka:

Corollary 1.5 [Kronheimer and Mrowka 1993]. *If $T(p, q)$ is a (p, q) -torus knot, $|p| > q > 1$, then*

$$2g_4(T(p, q)) = (|p| - 1)(q - 1).$$

By comparing σ_0 of the Legendrian and g_4 of the underlying smooth link type, we can rephrase the conclusions of Theorem 1.4 as:

Corollary 1.6. *If Λ is a Legendrian link that is topologically a nonslice twist knot² or a j -component torus link, L_Λ , then*

$$\sigma_0(\Lambda) = 2g_4(L_\Lambda) + (j - 1).$$

As an additional family of Legendrian links, we consider *positive, Legendrian rational links*. These links are defined as Legendrian numerator closures of the Legendrian rational tangles studied, for example, in [Traynor 1998] and [Schneider 2011]. These links are positive in the sense that an orientation is chosen on the components so that all the crossings have a positive sign. Such Legendrian links are specified by a vector (c_n, \dots, c_1) of positive integers; see Definition 4.4 and Figure 18. Lemma 4.5 gives conditions on the c_i that guarantee that the link is positive.

Theorem 1.7. *If $\Lambda(c_n, \dots, c_2, c_1)$ is a positive, Legendrian rational link, then*

$$\sigma_0(\Lambda(c_n, \dots, c_2, c_1)) = \sum_{i \text{ odd}} c_i - p(n),$$

where $p(n)$ equals 1 when n is odd and equals 0 when n is even.

This is proved in Section 4; see Theorem 4.6.

Remark 1.8. When Λ is a positive, Legendrian rational link, the calculation of $\sigma_0(\Lambda)$ is obtained realizing the lower bound given in Theorem 1.1 given by the classical Legendrian invariants of Λ . Thus by Corollary 1.3, when $\Lambda(c_n, \dots, c_1)$ is a positive, Legendrian rational knot, Theorem 1.7 gives a formula for twice the smooth 4-ball genus of the underlying smooth knot. This can be used to get

²Casson and Gordon [1986] proved that the only twist knots that are slice are the unknot, 6_1 , and $m(6_1)$.

formulas for the smooth 4-ball genus of a knot in terms of its rational notation. In particular,

$$\begin{aligned}
 g_4(5_2) &= g_4(N(3, 2)) = \frac{1}{2}\sigma_0(\Lambda(3, 2)) = \frac{1}{2}(2) = 1, \\
 g_4(7_5) &= g_4(N(3, 2, 2)) = \frac{1}{2}\sigma_0(\Lambda(3, 2, 2)) = \frac{1}{2}(2 + 3 - 1) = 2, \\
 g_4(N(5, 244, 4, 16, 3, 104, 2, 12, 1)) &= \frac{1}{2}(1 + 2 + 3 + 4 + 5 - 1).
 \end{aligned}$$

This is an alternate to formulas for calculating the smooth 4-ball genus in terms of crossings and Seifert circles as given by Nakamura in [2000]. In turn, using Nakamura’s formula, we see that when the underlying link type of $\Lambda(c_n, \dots, c_2, c_1)$ is a 2-component link L_Λ ,

$$\sigma_0(\Lambda(c_n, \dots, c_2, c_1)) = 2g_4(L_\Lambda) + 1;$$

see Remark 4.7.

Given the above calculations, it is natural to ask:

Question 1.9. If Λ is a Legendrian knot that is topologically a nonslice knot K_Λ , is $\sigma_0(\Lambda) = 2g_4(K_\Lambda)$? More generally, if Λ is a Legendrian link of $j \geq 2$ components that is topologically the link L_Λ , is $\sigma_0(\Lambda) = 2g_4(L_\Lambda) + (j - 1)$?

To investigate the knot portion of this question, we examined Legendrian representatives of knots with crossing number 7 or less. There is not yet a Legendrian classification of all these knot types, but a conjectured classification is given by Chongchitmate and Ng [2013].

Proposition 1.10. *Assuming the conjectured classification of Legendrian knots in [Chongchitmate and Ng 2013],³ if Λ is a Legendrian knot that is topologically a nonslice knot K_Λ with crossing number 7 or less, $\sigma_0(\Lambda) = 2g_4(K_\Lambda)$.*

The only non-torus and non-twist knots with crossing number at most 7 are $6_2, m(6_2), 6_3 = m(6_3), 7_3, m(7_3), 7_4, m(7_4), 7_5, m(7_5), 7_6, m(7_6), 7_7$, and $m(7_7)$. While doing the calculations for Legendrians with these knot types, in general we found that for a Legendrian Λ whose underlying smooth knot type K_Λ satisfies $g_3(K_\Lambda) = g_4(K_\Lambda)$, where $g_3(K_\Lambda)$ denotes the (3-dimensional) genus of the knot, it is fairly straight forward to show that $\sigma_0(\Lambda) = 2g_4(K_\Lambda)$. Legendrians that are topologically $7_3, m(7_3), 7_4, m(7_4), 7_5$, and $m(7_5)$ fall into this category. For the remaining knot types under consideration, the calculation of the smooth 4-ball genus follows from the fact that the topological unknotting number of these knots is equal to 1. We show that in a front projection of a Legendrian knot, it is possible to locally change any negative crossing to a positive one by 2 surgeries; see Lemma 5.2. This allowed us to prove Proposition 1.10 in the cases where Λ is

³Potential duplications in their atlas will not affect the statement.

topologically $6_2, 6_3 = m(6_3), 7_6$, or 7_7 . For the remaining cases of $m(6_2), m(7_6)$, and $m(7_7)$, results of [Soteros et al. 2011] show that it is not possible to find a front projection that can be unknotted at a negative crossing. However, we found front projections that could be unknotted at a positive crossing in a special “S” or “hooked-X” form: a positive crossing in one of these special forms can be locally changed to a negative crossing by 2 surgeries; see Lemma 5.5.

The Lagrangian motivation and discussion. All of our calculations indicate that $\sigma_0(\Lambda)$ is measuring an invariant of the underlying smooth link type and that this invariant will be the same for Λ and Λ' when they represent smooth knots that differ by the topological mirror operation. Below is an explanation for why this may be true.

Although the definition of the surgery unknotting number has been formulated above combinatorially, the motivation comes from trying to understand the flexibility and rigidity of Lagrangian submanifolds of a symplectic manifold. From [Bourgeois et al. ≥ 2013] (see also [Ekholm et al. 2012]) the existence of an unknotting surgery string $(\Lambda_n, \dots, \Lambda_0)$, as defined in Definition 3.1, implies the existence of an oriented Lagrangian cobordism Σ in $(\mathbb{R} \times \mathbb{R}^3 = \{(s, x, y, z)\}) \cap \{0 \leq s \leq n\}$ so that $(\Sigma \cap \{s = i\}) = \Lambda_i$, for $i = n, \dots, 0$. Furthermore, if Λ_0 is the Legendrian unknot with maximal Thurston–Bennequin invariant, this cobordism can be “filled in” with a Lagrangian $\bar{\Sigma} \subset \{s \leq n\}$ so that $\partial \bar{\Sigma} = \Lambda_n$. In fact, it is shown in [Chantraine 2010] that if Λ_0 is not the Legendrian unknot with maximal Thurston–Bennequin invariant, then the cobordism Σ cannot be filled in to $\bar{\Sigma}$; moreover, when there does exist the filling to $\bar{\Sigma}$ and the smooth underlying knot type of Λ_n is K_n , then the genus of $\bar{\Sigma}$ agrees with the smooth 4-ball genus of K_n .

From this Lagrangian perspective, it is a bit more natural to consider surgery strings $(\Lambda_n, \dots, \Lambda_0)$ where Λ_0 is a Legendrian unlink (a trivial link of Legendrian unknots), and define a corresponding “surgery unlinking number”; this is a project that the second author has begun to pursue with other undergraduates. A Lagrangian analogue of Question 1.9 is:

Question 1.11. If Λ is a Legendrian knot with underlying smooth knot type K_Λ , does there exist a Lagrangian cobordism constructed from Legendrian isotopy and oriented Legendrian surgeries between Λ and Λ_0 , a Legendrian that is a smooth unlink, that realizes $g_4(K_\Lambda)$?

Any Lagrangian constructed from Legendrian isotopy and oriented Legendrian surgeries would be in ribbon form; this means that the restriction of the height function, given by the s coordinate, to the cobordism would not have any local maxima in the interior of the cobordism. So a positive answer to Question 1.11 would imply that the slice genus agrees with the ribbon genus; for some background on this and related problems, see, for example, [Livingston 2005].

2. Background information on Legendrian links

Below is some basic background on Legendrian links. More information can be found, for example, in [Etnyre 2005].

The *standard contact structure* on \mathbb{R}^3 is the field of hyperplanes ξ where $\xi_p = \ker(dz - ydx)_p$. A *Legendrian link* is a submanifold, L , of \mathbb{R}^3 diffeomorphic to a disjoint union of circles so that for all $p \in L$, $T_p L \subset \xi_p$. It is common to examine Legendrian links from their xz -projections, known as their *front projections*. A Legendrian link will generically have an immersed front projection with semicubical cusps and no vertical tangents; conversely, any such projection can be uniquely lifted to a Legendrian link using $y = dz/dx$. Figure 3 shows Legendrian versions of the trefoils 3_1 and $m(3_1)$.

Λ_0 and Λ_1 are *equivalent Legendrian links* if there exists a 1-parameter family of Legendrian links Λ_t joining Λ_0 and Λ_1 . In fact, Legendrian links Λ_0, Λ_1 are equivalent if and only if their front projections are equivalent by planar isotopies that do not introduce vertical tangents and the *Legendrian Reidemeister moves* as shown in Figure 4.

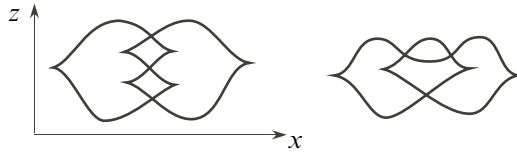


Figure 3. Left: front projection of a Legendrian knot that is topologically the (negative/left) trefoil 3_1 . Right: front projection of a Legendrian knot that is topologically the mirror trefoil $m(3_1)$. At crossings, it is not necessary to specify which strand is the overstrand: the strand with lesser slope will always be on top.

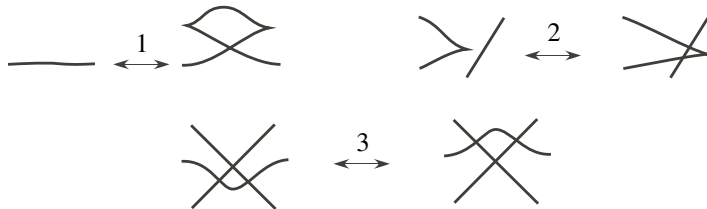


Figure 4. The three Legendrian Reidemeister moves. There is another type 1 move obtained by flipping the planar figure about a horizontal line, and there are three additional type 2 moves obtained by flipping the planar figure about a vertical, a horizontal, and both a vertical and horizontal line.



Figure 5. Negative (left) and positive (right) crossings.

Every Legendrian knot and link has a Legendrian representative. In fact, every Legendrian knot and link has an infinite number of different Legendrian representatives. For example, Figure 1 shows three different Legendrians that are all topologically the unknot. These unknots can be distinguished by classical Legendrian invariants, the Thurston–Bennequin and rotation number. These invariants can easily be computed from a front projection of the Legendrian link once we understand how to assign a \pm sign to each crossing and an up/down direction to each cusp.

A *positive (negative) crossing* of a front projection of an oriented Legendrian link is a crossing where the strands point to the same side (opposite sides) of a vertical line passing through the crossing point; see Figure 5. Each cusp can also be assigned an *up* or *down* direction; see Figure 6. Then for an oriented Legendrian link Λ , we have the following formulas for the *Thurston–Bennequin*, $\text{tb}(\Lambda)$, and *rotation number*, $r(\Lambda)$, invariants:

$$\text{tb}(\Lambda) = P - N - R, \quad r(\Lambda) = \frac{1}{2}(D - U), \quad (2-1)$$

where P is the number of positive crossings, N is the number of negative crossings, R is the number of right cusps, D is the number of down cusps, and U is the number of up cusps in a front projection of Λ . Given that two front projections of equivalent Legendrian links differ by the Legendrian Reidemeister moves described in Figure 4, it is easy to verify that $\text{tb}(\Lambda)$ and $r(\Lambda)$ are Legendrian link invariants.

The two unknots in the second line of Figure 1 are obtained from the one at the top by adding an up or down *zig-zag* (also known as a \mp *stabilization*). In general, this stabilization procedure will not change the underlying smooth knot type but will decrease the Thurston–Bennequin number by 1; adding an up (down) zig-zag will decrease (increase) the rotation number by 1. If Λ is a Legendrian knot, we will use the notation $S_{\pm}(\Lambda)$ to denote the *double stabilization* of Λ , the Legendrian knot obtained by adding both a positive and negative zig-zag.

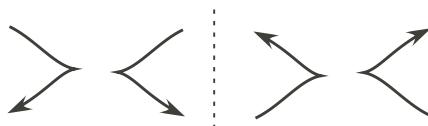


Figure 6. Right and left down cusps (left) and right and left up cusps (right).

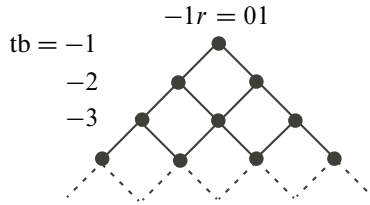


Figure 7. The single-peaked mountain of all Legendrian unknots.

In fact, as discovered by Eliashberg and Fraser, all Legendrian unknots are classified by their Thurston–Bennequin and rotation numbers:

Theorem 2.1 [Eliashberg and Fraser 2009; Etnyre and Honda 2001]. *Suppose Λ_0 and Λ'_0 are oriented Legendrian knots that are both topologically the unknot. Then Λ_0 is equivalent to Λ'_0 if and only if $\text{tb}(\Lambda_0) = \text{tb}(\Lambda'_0)$ and $r(\Lambda_0) = r(\Lambda'_0)$.*

Figure 7 describes all the Legendrian unknots. Notice that any Legendrian unknot is equivalent to one that is obtained by adding up and/or down zig-zags to the unknot with Thurston–Bennequin number equal to -1 and rotation number equal to 0 shown in Figure 1.

In general, it is an important question to understand the “geography” of other knot types. By [Etnyre and Honda 2001; Etnyre et al. 2013], we understand the mountain ranges for all torus and twist knots. The Legendrian knot atlas [Chongchitmate and Ng 2013] gives the known and conjectured mountain ranges for all Legendrian knots with arc index at most 9; this includes all knot types with crossing number at most 7 and all non-alternating knots with crossing number at most 9.

3. The surgery unknotting number

In this section, we define the surgery operation, show that every Legendrian link can be unknotted by surgeries, define the surgery unknotting number, and give some basic properties of the surgery unknotting number.

The surgery operation can be viewed as a *tangle surgery*: the replacement of one Legendrian tangle by another. A *basic, compatibly oriented Legendrian 0-tangle* is a Legendrian tangle that is topologically the 0-tangle where the strands are oppositely oriented and each strand has neither crossings nor cusps; the two basic, compatibly oriented Legendrian 0-tangles can be seen on the left side of Figure 2. A *basic, compatibly oriented Legendrian ∞ -tangle* is Legendrian tangle that is topologically the ∞ -tangle where the strands are oppositely oriented and each strand has precisely one cusp and no crossings; the two basic, compatibly oriented Legendrian ∞ -tangles can be seen on the right side of Figure 2.

Definition 3.1. An *oriented, Legendrian surgery* of an oriented, Legendrian link is the Legendrian link obtained by replacing a basic, compatibly oriented Legendrian

0-tangle with a basic, compatibly oriented Legendrian ∞ -tangle; see Figure 2. An *oriented surgery string* consists of a vector of oriented, Legendrian links

$$(\Lambda_n, \Lambda_{n-1}, \dots, \Lambda_0),$$

where, for all $j \in \{n-1, \dots, 0\}$, Λ_j is obtained from Λ_{j+1} by Legendrian isotopy and an oriented, Legendrian surgery. An *oriented, unknotting surgery string of length n for Λ* consists of an oriented surgery string $(\Lambda_n, \Lambda_{n-1}, \dots, \Lambda_0)$ where $\Lambda_n = \Lambda$ and Λ_0 is topologically an unknot.

To start, we have the following relationships between the classic invariants of two Legendrian links related by surgery:

Lemma 3.2. *If Λ is an oriented, Legendrian link and Λ' is obtained from Λ by an oriented, Legendrian surgery, then:*

- (1) *the parity of the number of components of Λ and Λ' differ;*
- (2) *$\text{tb}(\Lambda') = \text{tb}(\Lambda) - 1$, and $r(\Lambda') = r(\Lambda)$.*

Proof. The statements about the Thurston–Bennequin and rotation numbers are easily verified using Equation (2-1). Regarding the parity, one surgery to a knot will always produce a link of two components, while doing a surgery to a link will increase or decrease the number of components by 1 depending on whether or not the strands in the 0-tangle belong to the same component of the link. \square

Recall that for any Legendrian knot Λ , the Legendrian knot $\Lambda' = S_{\pm}(\Lambda)$ obtained as the double \pm stabilization of Λ will have $r(\Lambda') = r(\Lambda)$ and $\text{tb}(\Lambda') = \text{tb}(\Lambda) - 2$. Thus it is potentially possible that Λ' can be obtained from Λ by two oriented Legendrian surgeries. In fact, it is possible.

Lemma 3.3. *For any oriented, Legendrian knot Λ there exists an oriented surgery string $(\Lambda_2, \Lambda_1, \Lambda_0)$ with $\Lambda_2 = \Lambda$ and $\Lambda_0 = S_{\pm}(\Lambda)$.*

Proof. These surgeries are illustrated in Figure 8. Every Legendrian link Λ must have a right cusp. By a Legendrian isotopy, we can pull a right cusp far to the right and perform one surgery near this right cusp. This produces a link consisting of the original link and a Legendrian unknot. After a Legendrian isotopy, a second surgery can be done using one strand near the same cusp of the original link and a strand from the unknot. The result is $S_{\pm}(\Lambda)$. \square

In the chart of Legendrian unknots given in Figure 7, we see that any two unknots with the same rotation number are related by a sequence of double \pm stabilizations. Thus we get:

Corollary 3.4. *If Λ and Λ' are oriented, Legendrian unknots with $r(\Lambda) = r(\Lambda')$ and $\text{tb}(\Lambda) = \text{tb}(\Lambda') + 2m$, for $m \geq 0$, then there exists an oriented surgery string $(\Lambda_{2m}, \Lambda_{2m-1}, \dots, \Lambda_0)$, where $\Lambda_{2m} = \Lambda$, and $\Lambda_0 = \Lambda'$.*

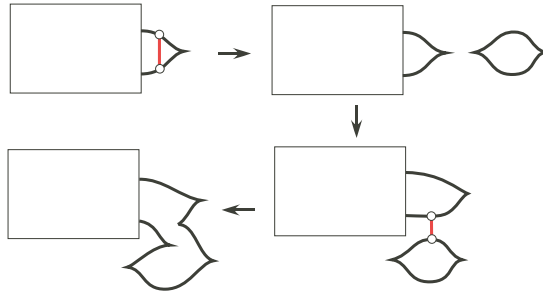


Figure 8. Two oriented, Legendrian surgeries produce $S_{\pm}(\Lambda)$ from Λ .

Thus if we can reach a Legendrian unknot by surgeries, then we can reach an infinite number of Legendrian unknots by surgery. The basis for our new invariant is the fact that every Legendrian link can be “unknotted” by a string of surgeries:

Proposition 3.5. *For any oriented, Legendrian link Λ , there exists an oriented, unknotting surgery string $(\Lambda = \Lambda_u, \Lambda_{u-1}, \dots, \Lambda_0)$. Moreover, if Λ has j components and there exists a front projection of Λ with m crossings, then $u \leq 2m + j - 1$.*

Proof. Assume that there is a front projection of Λ with m crossings. We will first show that there is an oriented surgery string $(\tilde{\Lambda}_m, \tilde{\Lambda}_{m-1}, \dots, \tilde{\Lambda}_0)$, where $\tilde{\Lambda}_m = \Lambda$ and $\tilde{\Lambda}_0$ is a trivial link of Legendrian unknots. If $\tilde{\Lambda}_0$ has c components, we will then show that it is possible to do an additional $c - 1$ surgeries to get this into a single component unknot.

Given the initial Legendrian link Λ having a projection with m crossings, assume that n of these crossings are negative. It is then possible to construct a surgery string $(\tilde{\Lambda}_m, \tilde{\Lambda}_{m-1}, \dots, \tilde{\Lambda}_{m-n})$ where $\tilde{\Lambda}_m = \Lambda$ and $\tilde{\Lambda}_{m-n}$ has a front projection with $m - n$ crossings, all of which are positive. This surgery string is obtained by doing a surgery to the right of each negative crossing and then doing a Legendrian isotopy to remove the positive crossing introduced by the surgery, as shown in Figure 9. Next, by applying a planar Legendrian isotopy, it is possible to assume that all the crossings of $\tilde{\Lambda}_{m-n}$ have distinct x -coordinates. The left cusps associated to the leftmost positive crossing are either nested or stacked and fall into one of the 6 cases listed in Figure 10; by an additional Legendrian planar isotopy, we can assume that all other left cusps occur to the right of this crossing. For each case, it is possible

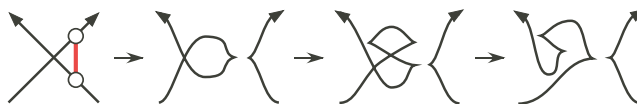


Figure 9. A negative crossing can be removed by an oriented Legendrian surgery and then Legendrian isotopy.

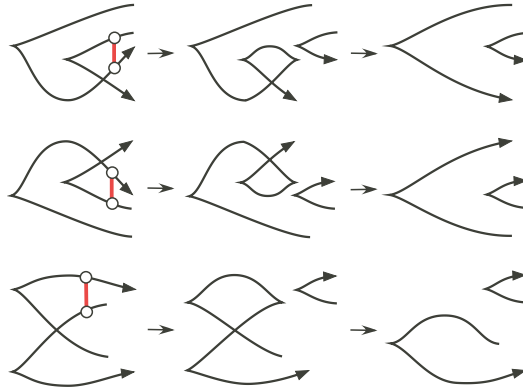


Figure 10. Three cases for the leftmost positive crossing and their associated left cusps; three additional cases are obtained by reversing the orientations on both strands.

to do a surgery immediately to the right of this leftmost crossing. After Legendrian Reidemeister moves, the crossing is eliminated and the number of crossings of the projection of the resulting link has decreased by 1; see Figure 10. What was the second leftmost positive crossing is now the leftmost positive crossing and the procedure can be repeated. In this way, we obtain a surgery string of Legendrian links $(\tilde{\Lambda}_m, \dots, \tilde{\Lambda}_{m-n}, \tilde{\Lambda}_{m-n-1}, \dots, \tilde{\Lambda}_0)$ where $\tilde{\Lambda}_0$ has a front projection with no crossings. It follows that $\tilde{\Lambda}_0$ is topologically a trivial link of unknots. By applying a Legendrian isotopy, we can assume that $\tilde{\Lambda}_0$ consists of c Legendrian unknots which are vertically stacked and where each unknot is oriented “clockwise”; an example of this is shown in Figure 11. It is then easy to see that after applying $c - 1$ additional surgeries, we can obtain a Legendrian unknot. Thus there is a length $u = m + c - 1$ unknotting surgery sequence for Λ . By Lemma 3.2, if $\Lambda = \tilde{\Lambda}_m$ has j components, $\tilde{\Lambda}_0$ has at most $c = j + m$ components. Thus we see that $u \leq 2m + j - 1$, as claimed. \square

Definition 3.6. Given a Legendrian link Λ , the (oriented) *Legendrian surgery unknotting number* of Λ , $\sigma_0(\Lambda)$, is defined as the minimal length of an oriented, unknotting surgery string for Λ .

Remark 3.7. Here are some basic properties of $\sigma_0(\Lambda)$:

- (1) By Lemma 3.2, for any Legendrian link Λ , the parity of $\sigma_0(\Lambda)$ is opposite the parity of the number of components of Λ ;
- (2) For any oriented, Legendrian link Λ with j components, $j - 1 \leq \sigma_0(\Lambda) < \infty$, with $0 = \sigma_0(\Lambda)$ if and only if Λ is topologically an unknot.

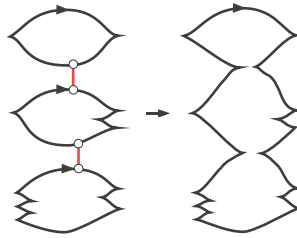


Figure 11. After all crossings are eliminated, a Legendrian isotopy can be applied so that Λ_0 is a stack of c Legendrian unknots oriented clockwise. After $c - 1$ additional surgeries, a Legendrian unknot is obtained.

- (3) If Λ is a topologically nontrivial Legendrian knot and there exists an oriented unknotting surgery string for Λ of length 2, then $\sigma_0(\Lambda) = 2$.
- (4) If Λ' is obtained from Λ by stabilization(s), then $\sigma_0(\Lambda') \leq \sigma_0(\Lambda)$.

Proposition 3.5 and, more importantly, explicit calculations will give upper bounds for $\sigma_0(\Lambda)$. Now we turn to examining some lower bounds for $\sigma_0(\Lambda)$.

First, by Theorem 2.1, if Λ' is a Legendrian unknot, then

$$\text{tb}(\Lambda') + |r(\Lambda')| \leq -1.$$

Thus if Λ is a Legendrian link with a “large” Thurston–Bennequin and/or rotation number, one is forced to do a certain number of Legendrian surgeries. More precisely, Lemma 3.2 implies:

Lemma 3.8. *For any Legendrian link Λ ,*

$$\text{tb}(\Lambda) + |r(\Lambda)| + 1 \leq \sigma_0(\Lambda).$$

Lemma 3.8 gives us improved lower bounds over those given in Remark 3.7 when $2 \leq \text{tb}(\Lambda) + |r(\Lambda)|$.⁴ For example, there exists a Legendrian whose underlying smooth knot type is $m(5_1)$ and whose classical invariants satisfy

$$\text{tb}(\Lambda) + |r(\Lambda)| = 3;$$

see, for example, [Chongchitmate and Ng 2013]. Thus Lemma 3.8 implies that $4 \leq \sigma_0(\Lambda)$. However for many links, $\text{tb}(\Lambda) + |r(\Lambda)| \leq 2$. For example, for any Legendrian Λ that is topologically the 5_1 knot, $\text{tb}(\Lambda) + |r(\Lambda)| \leq -5$. Although Lemma 3.8 will not help us, in this case we can make use of another result:

⁴The parity of $\text{tb}(\Lambda) + |r(\Lambda)|$ agrees with the parity of the number of components of Λ , so for knots, we get interesting new bounds when $3 \leq \text{tb}(\Lambda) + |r(\Lambda)|$.

Lemma 3.9. *For a Legendrian link Λ with j components, let L_Λ denote the underlying smooth link type of Λ , and let $g_4(L_\Lambda)$ denote the smooth 4-ball genus of L_Λ . Then*

$$2g_4(L_\Lambda) + (j - 1) \leq \sigma_0(\Lambda).$$

Proof. From a Legendrian surgery string of length n that ends at an unknot, one can construct a smooth, orientable, compact, and connected 2-dimensional surface in B^4 with boundary equal to L_Λ and Euler characteristic equal to $1 - n$; the genus, g , of this surface satisfies $1 - n = 2 - 2g - j$. Thus, by definition of the smooth 4-ball genus,

$$(j - 1) + 2g_4(L_\Lambda) \leq (j - 1) + 2g = n.$$

Since $\sigma_0(\Lambda)$ is the minimum length of a surgery unknotting string, the claim follows. \square

A convenient table of smooth 4-ball genera of knots can be found at KnotInfo [Cha and Livingston 2012].

4. The surgery unknotting number for families of knots

In this section we will calculate the surgery unknotting numbers for Legendrian twist knots, Legendrian torus links, and positive, Legendrian rational links. The fact that we can precisely calculate these numbers for the first two families rests upon classification results of [Etnyre et al. 2013; Etnyre and Honda 2001; Dalton 2008].

Legendrian twist knots. A twist knot is a knot that is smoothly equivalent to a knot K_m in the form of Figure 12. In other words, a twist knot is a twisted Whitehead double of the unknot.

Theorem 4.1. *If Λ is a Legendrian knot that is topologically a nontrivial twist knot then $\sigma_0(\Lambda) = 2$.*

Proof. Etnyre, Ng and Vértesi [Etnyre et al. 2013] have classified all Legendrian twist knots. In particular, every Legendrian knot Λ with maximal Thurston–Bennequin invariant that is topologically K_m , for some $m \leq -2$, is Legendrian isotopic to one

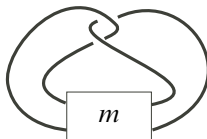


Figure 12. The twist knot K_m ; the box contains m right-handed half twists if $m \geq 0$, and $|m|$ left-handed twists if $m < 0$. Notice that K_0 and K_{-1} are unknots.

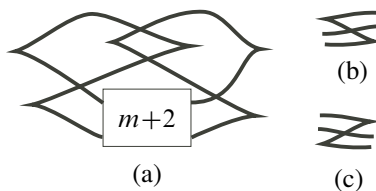


Figure 13. Any Legendrian knot that is topologically a negative twist knot, K_m with $m \leq -2$, and has maximal Thurston–Bennequin invariant is Legendrian isotopic to one of the form in (a) where the box contains $|m + 2|$ half twists, each of form S as shown in (b) or of form Z as shown in (c).

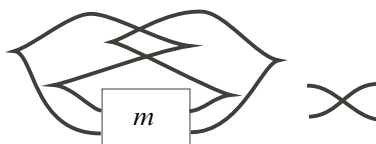


Figure 14. Any Legendrian knot that is topologically a positive twist knot, K_m with $m \geq 0$, and has maximal Thurston–Bennequin invariant is Legendrian isotopic to one of the form on the left. The box contains m half twists, each of form X as shown on the right.

of the form in Figure 13, and every Legendrian knot Λ with maximal Thurston–Bennequin invariant that is topologically K_m , for $m \geq 1$ with maximal Thurston–Bennequin invariant is Legendrian isotopic to one of the form in Figure 14.⁵ Every Legendrian knot Λ that is topologically a nontrivial twist knot is obtained by stabilization of one of these with maximal Thurston–Bennequin invariant. By Remark 3.7, it suffices to show for any Legendrian knot Λ^+ that is topologically a nontrivial twist knot and has maximal Thurston–Bennequin invariant, $\sigma_0(\Lambda^+) = 2$. For Λ^+ , we can do the two unknotting surgeries near the “clasp”. The sign of the crossings in the clasp will depend on whether m is even or odd: Figure 15 shows the positions of two surgeries that result in an unknot. \square

Legendrian torus links. A torus link is a link that can be smoothly isotoped so that it lies on the surface of an unknotted torus in \mathbb{R}^3 . Every torus knot can be specified by a pair (p, q) of coprime integers: we will use the convention that the (p, q) -torus knot, $T(p, q)$, winds p times around a meridional curve of the torus and q times in the longitudinal direction. See, for example, [Adams 2004]. In fact, $T(p, q)$ is equivalent to $T(q, p)$ and to $T(-p, -q)$. So we will always assume that $|p| > q > 0$; in addition we will assume $q > 1$ since we are interested in nontrivial

⁵We omit $m = 0, -1$ since those correspond to the unknot.

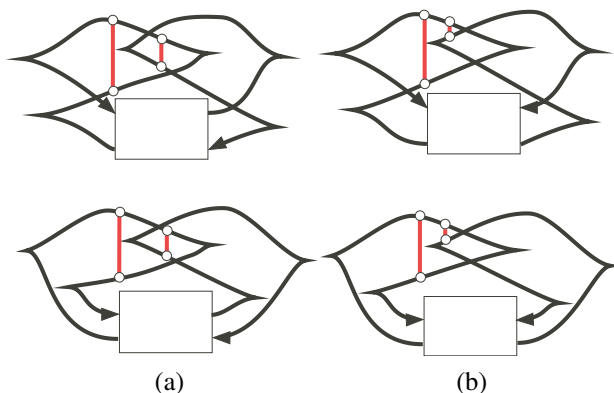


Figure 15. For a Legendrian knot with maximal Thurston–Bennequin invariant that is topologically K_m , (a) gives the surgery points when m is even, and (b) gives the surgery points when m is odd.

torus knots. For $j \geq 2$, $T(jp, jq)$, with $|p| > q > 1$ and $\gcd(p, q) = 1$, will be a j -component link where each component is a $T(p, q)$ torus link. We will only consider torus links of nontrivial components.

Theorem 4.2. *If Λ is a j -component Legendrian link that is topologically the (jp, jq) -torus link, $|p| > q > 1$, then $\sigma_0(\Lambda) = (|jp| - 1)(jq - 1)$.*

Proof. First consider the case where Λ is topologically a positive torus knot, $T(p, q)$ with $p > 0$. As shown by Etnyre and Honda [2001], the list of different Legendrian representations of a positive torus knot can be represented as a “single-peaked mountain” in parallel to the mountain of unknots shown in Figure 7. Namely, for fixed $p > q > 1$, there is a unique Legendrian knot Λ^+ that is topologically $T(p, q)$ with maximal Thurston–Bennequin invariant $\text{tb}(\Lambda^+) = pq - p - q$ and $r(\Lambda^+) = 0$; any Legendrian knot Λ that is topologically $T(p, q)$ is obtained by stabilizations of Λ^+ . By Remark 3.7, it suffices to show that if Λ^+ is a Legendrian knot that is topologically $T(p, q)$ and has maximal Thurston–Bennequin invariant, then $\sigma_0(\Lambda^+) = (p - 1)(q - 1)$. By Lemma 3.8,

$$\text{tb}(\Lambda^+) + |r(\Lambda^+)| + 1 = (p - 1)(q - 1) \leq \sigma_0(\Lambda).$$

In fact, it is possible to unknot with $(p - 1)(q - 1)$ surgeries. Starting from the left most string of crossings, do $(q - 1)$ successive surgeries as illustrated for the $(5, 3)$ -torus knot in Figure 16; in this sequence of surgeries, one begins with the surgery on the innermost strands, and then performs a Legendrian isotopy so that it is possible to do a surgery on the next set of innermost strands. In general, this

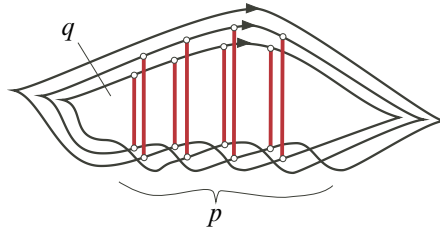


Figure 16. The Legendrian $(5, 3)$ -torus knot with maximal tb invariant. The general, positive Legendrian (p, q) -torus knot with maximal Thurston–Bennequin invariant is constructed using q strands and a length p string of crossings. Shown are the $(p - 1)(q - 1)$ oriented Legendrian surgeries that unknot the Legendrian positive (p, q) -torus knot with maximal tb .

takes the (p, q) -torus knot to the $(p - 1, q)$ -torus link. Repeating this $p - 1$ times results in the $(1, q)$ -torus knot, which is an unknot.⁶

The above proof easily generalizes to positive torus links of nontrivial components. Dalton [2008] showed that there is a unique Legendrian link Λ^+ that is topologically $T(jp, jq)$ with maximal Thurston–Bennequin invariant $tb(\Lambda^+) = jpjq - jp - jq$. The construction of this one exactly parallels the construction in Figure 16, and so the same pattern of $(jp - 1)(jq - 1)$ surgeries will produce a Legendrian unknot.

Next consider the case where Λ is topologically a negative torus knot, $T(p, q)$ with $p < 0$. In this case, Etnyre and Honda have shown that the list of different Legendrian representations of a negative torus knots, $T(p, q)$ for $p < 0$ and $|p| > q > 1$, can be represented as a many-peaked “mountain range” where the number of representatives with maximal Thurston–Bennequin invariant depends on the divisibility of p by q . Namely, if $|p| = mq + e$, $0 < e < q$, then there will be $2m$ Legendrian representatives of $T(p, q)$ with maximal Thurston–Bennequin invariant of $pq < 0$. Half of these different representatives with maximal Thurston–Bennequin invariant are obtained by writing $m = 1 + n_1 + n_2$, where $n_1, n_2 \geq 0$, and then $\Lambda^+_{(n_1, n_2)}$ is constructed using the form shown in Figure 17 with n_1 and n_2 copies of the tangle B inserted as indicated:

$$r(\Lambda^+_{(n_1, n_2)}) = q(n_2 - n_1) + e.$$

The other m Legendrian versions of $T(p, q)$ with maximal Thurston–Bennequin invariant are obtained by reversing the orientation. For negative torus knots, Lemma 3.8 will not be a useful lower bound. However, since the calculation of the 4-ball genus is the same for both the knot and its mirror, the calculations in

⁶By Corollary 1.3, we can now deduce the Milnor conjecture as mentioned in Corollary 1.5.

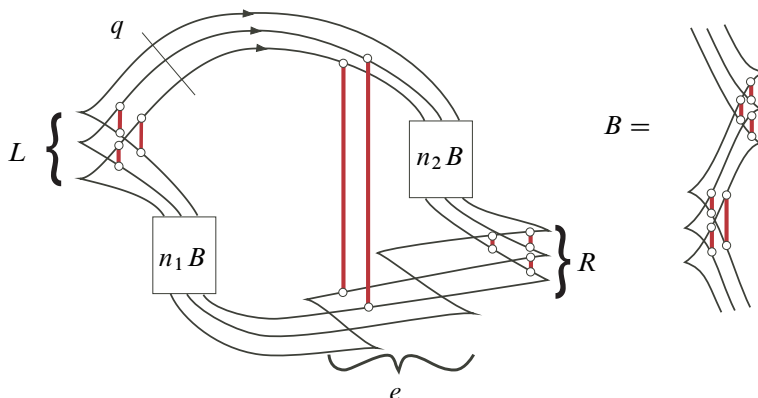


Figure 17. The $(|p|-1)(q-1)$ oriented Legendrian surgeries that unknot a Legendrian negative (p, q) -torus knot with maximal Thurston–Bennequin invariant.

the positive torus knot case and Corollary 1.3, (or [Kronheimer and Mrowka 1993]), show that for a negative torus knot $T(p, q)$, $2g_4(T(p, q)) = (|p|-1)(q-1)$. Thus, by Lemma 3.9

$$(|p|-1)(q-1) \leq \sigma_0(\Lambda).$$

In fact, it is possible to arrive at an unknot with $(|p|-1)(q-1)$ surgeries. Figure 17 shows the claimed surgeries: a surgery is done to the right of all crossings in the L , R , and B regions (contributing $\frac{1}{2}q(q-1) + \frac{1}{2}q(q-1) + (n_1 + n_2)q(q-1)$ surgeries), and between each Z in the e string one does $q-1$ successive surgeries (contributing $(e-1)(q-1)$ surgeries). Thus the total number of surgeries is

$$(1 + n_1 + n_2)q(q-1) + (e-1)(q-1) = (mq + e - 1)(q-1) = (|p|-1)(q-1).$$

The proof easily generalizes to negative torus links. It follows from [Nakamura 2000] that $g_4(T(jp, jq)) + (j-1) = (j|p|-1)(jq-1)$; see Remark 4.3. It was shown in [Dalton 2008] that there are $2m$ Legendrian links Λ^+ that are topologically $T(jp, jq)$ with maximal Thurston–Bennequin invariant, and all Legendrians that are topologically $T(jp, jq)$ are obtained by stabilizations of one of these. Each of these with maximal Thurston–Bennequin invariant can be constructed as in Figure 17, and so the same pattern of $(j|p|-1)(jq-1)$ surgeries will produce a Legendrian unknot. \square

Remark 4.3. Nakamura’s formula [2000] for the smooth 4-ball genus of a j -component positive link L is that

$$2g_4(L) = 2 - j - s(D) + c(D),$$

where $s(D)$ is the number of Seifert circles and $c(D)$ is the number of crossings in a non-split positive diagram D for L . It is straightforward to see that when L is the positive torus link $T(jp, jq)$, using the diagram D corresponding to Figure 16, $s(D) = jq$ and $c(D) = jp(jq - 1)$. So,

$$2g_4(T(jp, jq)) = 2 - j - jq + jp(jq - 1) = (1 - j) + (jp - 1)(jq - 1).$$

Thus for any Legendrian link Λ that is topologically $T(jp, jq)$, for either p positive or negative,

$$2g_4(T(jp, jq)) + (j - 1) = \sigma_0(\Lambda).$$

Positive, Legendrian rational links.

Definition 4.4. Given a vector of integers (c_n, \dots, c_2, c_1) , where $c_n \geq 2$, and $n \geq 2$ implies $c_i \geq 1$ for $i = 1, \dots, n - 1$, we construct the *rational Legendrian link* $\Lambda(c_n, \dots, c_2, c_1)$ to be the Legendrian numerator closure of the Legendrian tangle (c_n, \dots, c_2, c_1) as demonstrated in Figure 18; see also [Adams 2004; Traynor 1998; Schneider 2011]. The rational Legendrian link $\Lambda(c_n, \dots, c_2, c_1)$ is *positive* if all crossings are positive.

This Legendrian link $\Lambda(c_n, \dots, c_1)$ is topologically the numerator closure of the rational tangle associated to the rational number q with continued fraction expansion $q = c_1 + 1/(c_2 + 1/(c_3 + \dots))$; see [Conway 1970].

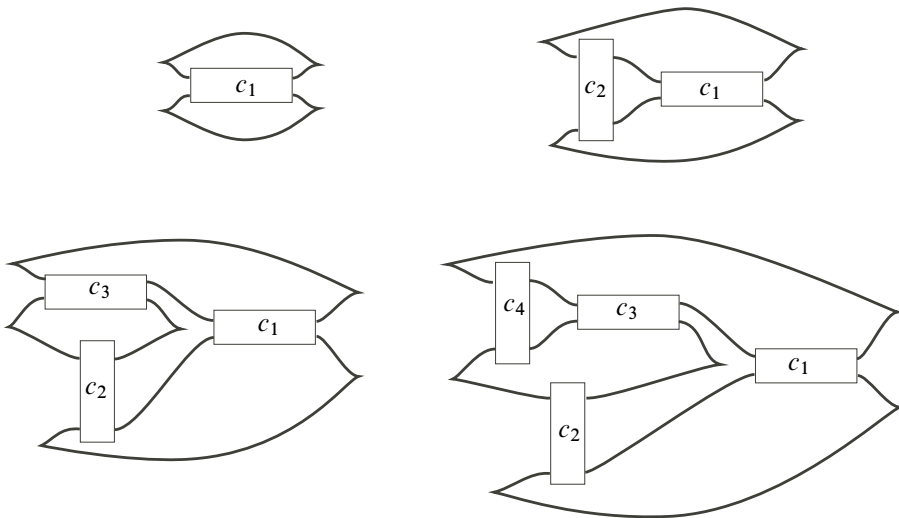


Figure 18. The general form of $\Lambda(c_1)$, $\Lambda(c_2, c_1)$, $\Lambda(c_3, c_2, c_1)$, and $\Lambda(c_4, c_3, c_2, c_1)$.

The “even” entries c_2, c_4, \dots of the vector (c_n, \dots, c_2, c_1) denote the strings of vertical crossings. It is straightforward to verify that the parity of these vertical entries determine when $\Lambda(c_n, \dots, c_1)$ is a positive link:

Lemma 4.5. (1) *When n is odd, there exists an orientation on the components of $\Lambda(c_n, \dots, c_1)$ so that it is a positive link if and only if c_i is even, for all i even. Moreover, $\Lambda(c_n, \dots, c_1)$ is a knot when $\sum_{i \text{ odd}} c_i$ is odd.*

(2) *When n is even, there exists an orientation on the components of $\Lambda(c_n, \dots, c_1)$ so it is a positive link if and only if c_n is odd and $c_{n-2}, c_{n-4}, \dots, c_2$ are all even. Moreover, $\Lambda(c_n, \dots, c_1)$ is a knot when $\sum_{i \text{ odd}} c_i$ is even.*

The Legendrian surgery unknotting number of a positive link has a convenient formula in terms of the “odd” entries, which correspond to the strings of horizontal crossings. There will be some differences in following formulas depending on whether Λ is constructed from an odd or an even length vector. Define

$$p(n) = \begin{cases} 1, & n \text{ odd,} \\ 0, & n \text{ even;} \end{cases}$$

$p(n)$ measures the parity of the “length” of the vector (c_n, \dots, c_1) .

Theorem 4.6. *If $\Lambda(c_n, \dots, c_2, c_1)$ is a positive, Legendrian rational link, then*

$$\sigma_0(\Lambda(c_n, \dots, c_2, c_1)) = \sum_{i \text{ odd}} c_i - p(n).$$

Proof. This will be proved using the lower bound on $\sigma_0(\Lambda)$ provided by Lemma 3.8, and explicit calculations.

We will first show that

$$r(\Lambda(c_n, \dots, c_2, c_1)) = 0 \quad \text{and} \quad \text{tb}(\Lambda(c_n, \dots, c_2, c_1)) = \sum_{i \text{ odd}} c_i - p(n) - 1.$$

It is easy to verify that when all the crossings are positive, the up and down cusps cancel in pairs and thus the rotation number vanishes. To calculate $\text{tb}(\Lambda(c_n, \dots, c_1))$, notice that when n is odd the number of right cusps is 2 more than the number of vertical crossings, $\sum_{i \text{ even}} c_i$, while when n is even, the number of rights cusps is 1 more than the number of vertical crossings. Thus:

$$\text{tb}(\Lambda(c_n, \dots, c_2, c_1)) = \sum_{i=1}^n c_i - \left(\sum_{i \text{ even}} c_i + 1 + p(n) \right) = \sum_{i \text{ odd}} c_i - 1 - p(n).$$

Thus, by Lemma 3.8,

$$\sum_{i \text{ odd}} c_i - p(n) \leq \sigma_0(\Lambda(c_n, \dots, c_2, c_1)).$$

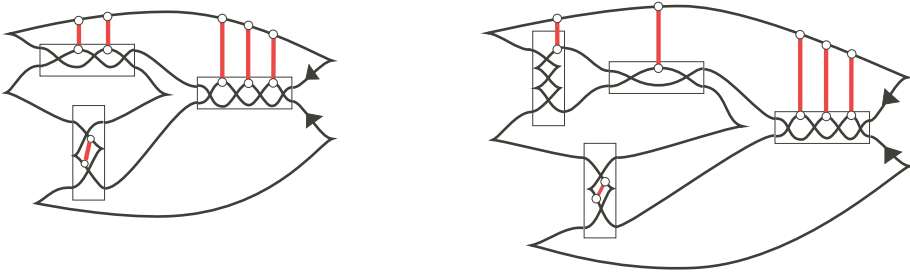


Figure 19. Two positive, Legendrian rational knots of odd and even lengths. In both cases, it is possible to unknot by doing $c_i - 1$ surgeries in each horizontal segment (i odd) and 1 surgery in each vertical segment.

In fact, it is possible to unknot $\Lambda(c_n, \dots, c_2, c_1)$ by doing $c_i - 1$ surgeries in each horizontal component and 1 surgery in each vertical segment; Figure 19 illustrates some examples of this. When $n = 1$, there are no vertical segments; for other odd n , the number of vertical components is one less than the number of horizontal components, and when n is even, the number of vertical components agrees with the number of horizontal components. Thus

$$\sigma_0(\Lambda(c_n, \dots, c_1)) \leq \sum_{i \text{ odd}} c_i - p(n),$$

and the desired calculation of $\sigma_0(\Lambda(c_n, \dots, c_1))$ follows. □

Remark 4.7. In the above proof, $\sigma_0(\Lambda(c_n, \dots, c_1))$ is obtained by realizing the lower bound given by the classical Legendrian invariants. Thus, by Corollary 1.3, we see that when $\Lambda(c_n, \dots, c_1)$ has an underlying topological type of the knot K_Λ , $\sigma_0(\Lambda(c_n, \dots, c_1)) = 2g_4(K_\Lambda)$. Moreover, when $\Lambda(c_n, \dots, c_1)$ has an underlying topological type of a 2-component link L_Λ , we can compare $\sigma_0(\Lambda(c_n, \dots, c_1))$ to the smooth 4-ball genus of L_Λ using Nakamura’s formula (see Remark 4.3) for the smooth 4-ball genus of a positive link. When n is odd, the number of Seifert circles is $s(D) = 2 + \sum_{i \text{ even}} c_i$, while when n is even, $s(D) = 1 + \sum_{i \text{ even}} c_i$. Thus we find that for a 2-component, positive, Legendrian rational link $\Lambda(c_n, \dots, c_1)$,

$$2g_4(L_\Lambda) + 1 = c(D) - s(D) + 1 = \sum_{i \text{ odd}} c_i - p(n) = \sigma_0(\Lambda(c_n, \dots, c_1)).$$

5. The surgery unknotting number for small crossing knots

Given the calculations of the previous section, it is natural to ask Question 1.9 in the Introduction. To investigate the knot portion of this question, we examined Legendrian representatives of low-crossing knots. There is not a Legendrian

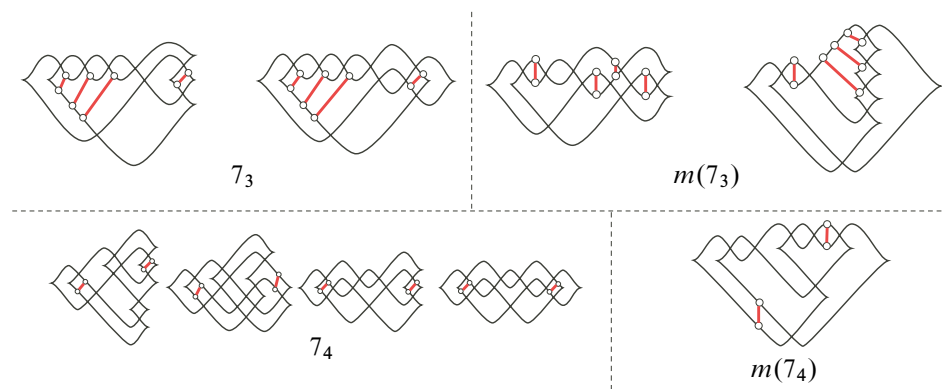


Figure 20. Front projections representing all conjectured Legendrian representatives of 7_3 , $m(7_3)$, 7_4 , and $m(7_4)$ with maximal Thurston–Bennequin invariant. For all of these knot types, $g_3(K_\Lambda) = g_4(K_\Lambda)$; the indicated surgery points realize $\sigma_0(\Lambda) = 2g_4(K_\Lambda)$.

classification of all these knot types, but a conjectured classification of these knot types can be found in [Chongchitmate and Ng 2013]. In the following, we prove Proposition 1.10, which says that the surgery unknotting number of the Legendrian agrees with twice the smooth 4-ball genus of the underlying smooth knot for all Legendrians that are topologically a nonslice knot with crossing number at most 7.

In Section 4, Proposition 1.10 is verified for all torus and twist knots. The only non-torus and non-twist knots with 7 or fewer crossings are 6_2 , $m(6_2)$, $6_3 = m(6_3)$, 7_3 , $m(7_3)$, 7_4 , $m(7_4)$, 7_5 , $m(7_5)$, 7_6 , $m(7_6)$, 7_7 , and $m(7_7)$. The needed calculations fall into three categories as described below.

Example 5.1. For the smooth knots 7_3 , $m(7_3)$, 7_4 , $m(7_4)$, 7_5 , and $m(7_5)$, the genus, g_3 , agrees with the smooth 4-ball genus g_4 .⁷ In general, we find that for a Legendrian Λ whose underlying knot type K_Λ satisfied $g_3(K_\Lambda) = g_4(K_\Lambda)$, it is fairly straightforward to show that $\sigma_0(\Lambda) = 2g_4(K_\Lambda)$. For example, Figure 20 shows all conjectured representatives of 7_3 , $m(7_3)$, 7_4 , $m(7_4)$, 7_5 , and $m(7_5)$ with maximal Thurston–Bennequin invariant (after perhaps selecting alternate orientations and/or performing the Legendrian mirror operation, which consists of rotating the diagram 180°). For each of these with maximal Thurston–Bennequin invariant, it is possible to unknot with $2g_4(K_\Lambda)$ surgeries as indicated.

In general, we found that for a Legendrian Λ whose underlying knot type K_Λ satisfied $g_4(K_\Lambda) < g_3(K_\Lambda)$, it is more difficult to calculate $\sigma_0(\Lambda)$. To do calculations for our remaining cases, we made use of the well known fact that the

⁷This is also the situation for the torus and nonslice twist knots studied in Section 4.

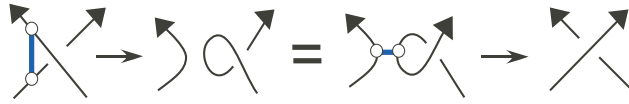


Figure 21. A sequence of two topological surgeries in a neighborhood of a negative crossing that topologically change the crossing. An analogous picture shows that a positive crossing can be changed into a negative crossing by two topological surgeries.

unknotting number of a knot, $u(K)$, gives an upper bound to the smooth 4-ball genus:

$$g_4(K) \leq u(K). \tag{5-1}$$

Figure 21 demonstrates two topological surgeries that produce a crossing change; an argument as in the proof of Lemma 3.9 then proves inequality (5-1). Notice that the topological Reidemeister moves used in the equivalence are not Legendrian Reidemeister moves. However, near a negative crossing, it is possible to “Legendrify” this construction:

Lemma 5.2. *If the Legendrian knot Λ has a front projection that can be topologically unknotted by changing a negative crossing, then*

$$\sigma_0(\Lambda) \leq 2.$$

Proof. Figure 22 demonstrates how two surgeries can locally produce a topological crossing change. □

Example 5.3. Using Lemma 5.2, it is possible to show that for any conjectured Legendrian representative Λ of 6_2 , 6_3 , 7_6 , or 7_7 , $\sigma_0(\Lambda) = 2g_4(K_\Lambda)$. Figure 23 shows the conjectured Legendrian representatives of these knot types with maximal Thurston–Bennequin invariant (after perhaps selecting alternate orientations and/or performing a mirror operation, which corresponds to a rotation of the front diagram

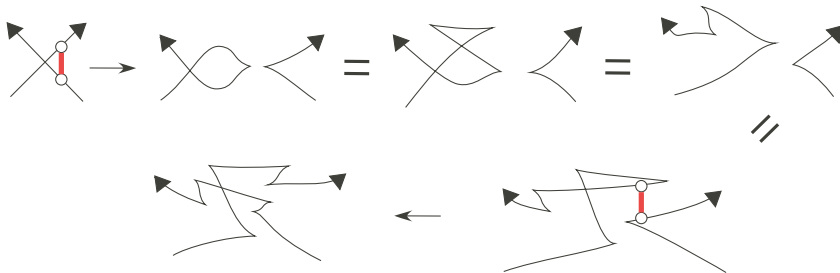


Figure 22. A sequence of two oriented surgeries in a neighborhood of a negative crossing that topologically change the crossing.

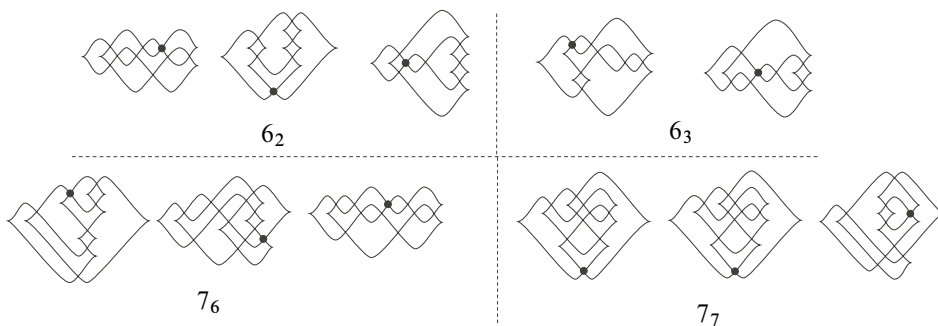


Figure 23. Front projections representing all conjectured Legendrian representatives of 6_2 , 6_3 , 7_6 , and 7_7 with maximal Thurston–Bennequin invariant. These projections can be topologically unknotted at the indicated negative crossing.

by 180°), and the negative crossing that when topologically changed produces an unknot.

We were not able to find front projections of the conjectured maximal Thurston–Bennequin representatives of $m(6_2)$, $m(7_6)$, or $m(7_7)$ that could be topologically unknotted by changing a negative crossing; in fact, by [Soteros et al. 2011], it is *not* possible to do this even in the smooth setting. Luckily, sometimes we can topologically change a positive crossing when it has a special form.

Definition 5.4. A positive crossing is of *S form*, *Z form*, or *hooked-X form* if it takes the form as shown in Figure 24.

Lemma 5.5. *If Λ is a nontrivial Legendrian knot that has a projection that can be topologically unknotted by changing a positive crossing in S, Z, or hooked-X form, then*

$$\sigma_0(\Lambda) \leq 2.$$

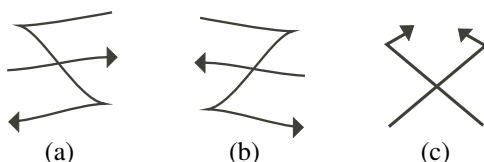


Figure 24. A positive crossing of (a) S form, (b) Z form, and (c) hooked-X form. Reversing the orientations on both strands keeps the respective forms. Also reflecting the planar figure in (c) about a horizontal line produces another hooked-X form.

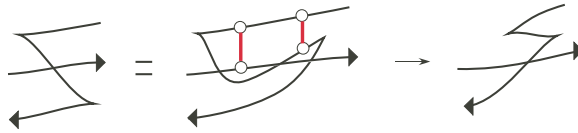


Figure 25. A positive crossing of S form can be transformed into a negative crossing with 2 surgeries. Similarly, a positive crossing of Z form can be transformed into a negative crossing with 2 surgeries.

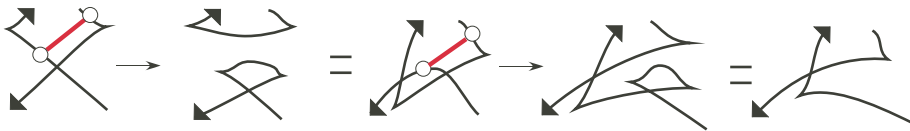


Figure 26. A positive crossing of hooked- X form can be transformed into a negative crossing with 2 Legendrian surgeries.

Proof. Figures 25 and 26 show how a positive crossing in S , Z , or hooked- X form can be transformed into a negative crossing using two surgeries and Legendrian isotopies. \square

Example 5.6. Using Lemma 5.5, it is possible to show that for any conjectured Legendrian representative Λ of $m(6_2)$, $m(7_6)$, or $m(7_7)$, $\sigma_0(\Lambda) = 2g_4(K_\Lambda)$. Figure 27 shows the conjectured Legendrian representatives of these knot types with maximal Thurston–Bennequin invariant (after perhaps selecting alternate orientations and/or

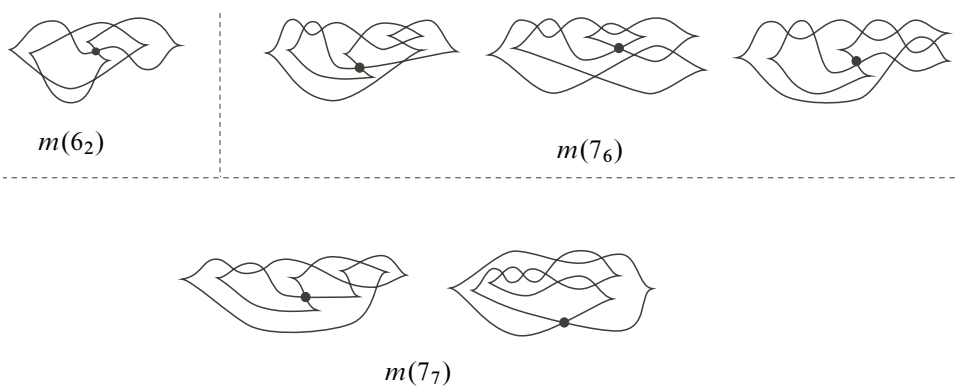


Figure 27. Front projections representing all conjectured Legendrian representatives of $m(6_2)$, $m(7_6)$ and $m(7_7)$ with maximal Thurston–Bennequin invariant. Each of these can be topologically unknotted by changing the indicated positive crossing in S form or hooked- X form.

performing a mirror operation). These projections differ from those in [Chongchitmate and Ng 2013] by Legendrian Reidemeister moves of type II and III. The black dot indicates a positive crossing that when topologically changed produces an unknot.

The proofs of Lemmas 5.2 and 5.5 in fact show that if the Legendrian knot Λ has a front projection that can be topologically unknotted by changing ν negative crossings and ρ crossings in S, Z, or hooked-X form, then $\sigma_0(\Lambda) \leq 2\nu + 2\rho$. However, for our calculations we did not need this more general form.

Acknowledgements

The ideas of this project were inspired by joint work of Josh Sabloff and the second author. We are extremely grateful for the many fruitful discussions we have had with Sabloff throughout this project. We also gained much by discussions with Chuck Livingston about the smooth 4-ball genus; we are very thankful for his clear explanations. We also thank Paul Melvin and other members of our PACT (Philadelphia Area Contact/Topology) seminar for useful comments during a series of presentations on this work.

References

- [Adams 2004] C. C. Adams, *The knot book: an elementary introduction to the mathematical theory of knots*, American Mathematical Society, Providence, RI, 2004. MR 2005b:57009 Zbl 1065.57003
- [Akbulut and Matveyev 1997] S. Akbulut and R. Matveyev, “Exotic structures and adjunction inequality”, *Turkish J. Math.* **21**:1 (1997), 47–53. MR 98d:57053 Zbl 0885.57011 arXiv math/0011055
- [Bourgeois et al. \geq 2013] F. Bourgeois, J. Sabloff, and L. Traynor, “Lagrangian cobordisms via generating families: constructions and geography”. In preparation.
- [Casson and Gordon 1986] A. J. Casson and C. M. Gordon, “Cobordism of classical knots”, pp. 181–199 in *À la recherche de la topologie perdue*, edited by L. Guillou and A. Marin, Progr. Math. **62**, Birkhäuser, Boston, 1986. MR 900252
- [Cha and Livingston 2012] J. C. Cha and C. Livingston, “Knotinfo: table of knot invariants”, web site, 2012, <http://www.indiana.edu/~knotinfo>.
- [Chantraine 2010] B. Chantraine, “Lagrangian concordance of Legendrian knots”, *Algebr. Geom. Topol.* **10**:1 (2010), 63–85. MR 2011f:57049 Zbl 1203.57010
- [Chongchitmate and Ng 2013] W. Chongchitmate and L. Ng, “An atlas of Legendrian knots”, *Exp. Math.* **22**:1 (2013), 26–37. MR 3038780 Zbl 06180370
- [Conway 1970] J. H. Conway, “An enumeration of knots and links, and some of their algebraic properties”, pp. 329–358 in *Computational problems in abstract algebra* (Oxford, 1967), edited by J. Leech, Pergamon, Oxford, 1970. MR 41 #2661 Zbl 0202.54703
- [Dalton 2008] J. Dalton, *Legendrian torus links*, Ph.D. thesis, Bryn Mawr College, Bryn Mawr, PA, 2008, <http://repository.brynmawr.edu/dissertations/6>. MR 2712646
- [Ekholm et al. 2012] T. Ekholm, K. Honda, and T. Kálmán, “Legendrian knots and exact Lagrangian cobordisms”, preprint, 2012. arXiv 1212.1519

- [Eliashberg and Fraser 2009] Y. Eliashberg and M. Fraser, “Topologically trivial Legendrian knots”, *J. Symplectic Geom.* **7**:2 (2009), 77–127. MR 2010d:57024 Zbl 1179.57040
- [Etnyre 2005] J. B. Etnyre, “Legendrian and transversal knots”, pp. 105–185 in *Handbook of knot theory*, edited by W. Menasco and M. Thistlethwaite, Elsevier, Amsterdam, 2005. MR 2006j:57050 Zbl 1095.57006
- [Etnyre and Honda 2001] J. B. Etnyre and K. Honda, “Knots and contact geometry, I: Torus knots and the figure eight knot”, *J. Symplectic Geom.* **1**:1 (2001), 63–120. MR 2004d:57032 Zbl 1037.57021
- [Etnyre et al. 2013] J. B. Etnyre, L. Ng, and V. Vértesi., “Legendrian and transverse twist knots”, *J. Eur. Math. Soc.* **15**:3 (2013), 969–995. arXiv 1002.2400
- [Kronheimer and Mrowka 1993] P. B. Kronheimer and T. S. Mrowka, “Gauge theory for embedded surfaces, I”, *Topology* **32**:4 (1993), 773–826. MR 94k:57048 Zbl 0799.57007
- [Lisca and Matić 1998] P. Lisca and G. Matić, “Stein 4-manifolds with boundary and contact structures”, *Topology Appl.* **88**:1-2 (1998), 55–66. MR 99f:57037 Zbl 0978.53122
- [Livingston 2005] C. Livingston, “A survey of classical knot concordance”, pp. 319–347 in *Handbook of knot theory*, edited by W. Menasco and M. Thistlethwaite, Elsevier, Amsterdam, 2005. MR 2006k:57020 Zbl 1098.57006 arXiv math/0307077
- [Nakamura 2000] T. Nakamura, “Four-genus and unknotting number of positive knots and links”, *Osaka J. Math.* **37**:2 (2000), 441–451. MR 2001e:57005 Zbl 0968.57008
- [Rudolph 1995] L. Rudolph, “An obstruction to sliceness via contact geometry and “classical” gauge theory”, *Invent. Math.* **119**:1 (1995), 155–163. MR 95k:57013 Zbl 0843.57011
- [Schneider 2011] G. R. Schneider, *On the classification of Legendrian rational tangles via characteristic foliations of compressing discs*, Ph.D. thesis, State University of New York, Buffalo, NY, 2011, <http://tinyurl.com/schneider-thesis>. MR 2898627
- [Soteros et al. 2011] C. Soteros, K. Ishihara, K. Shimokawa, M. Szafron, and M. Vazquez, “Signed unknotting number and knot chirality discrimination via strand passage”, *Prog. Theor. Phys. Suppl.* **191** (2011), 78–95.
- [Traynor 1998] L. Traynor, “A Legendrian stratification of rational tangles”, *J. Knot Theory Ramifications* **7**:5 (1998), 659–700. MR 2000c:57020 Zbl 0912.57003

Received: 2012-05-07 Revised: 2013-05-20 Accepted: 2013-05-25

aboranda@brynmawr.edu *Bryn Mawr College, Bryn Mawr, PA 19010, United States*

ltraynor@brynmawr.edu *Department of Mathematics, Bryn Mawr College,
Bryn Mawr, PA 19010, United States*

syam@brynmawr.edu *Bryn Mawr College, Bryn Mawr, PA 19010, United States*

On duals of p -frames

Ali Akbar Arefijamaal and Leili Mohammadkhani

(Communicated by Mohammad Sal Moslehian)

The concept of frames in a Banach space has been introduced by Gröchenig and developed by several authors. The main feature of a frame is to present every element of the underlying Banach space as a norm-convergent series. In this decomposition, the dual frame plays an essential role. The existence of a dual p -frame is not guaranteed in general. Some characterizations of duals of p -frames are given in this paper.

1. Introduction and preliminaries

A sequence $\{f_i\}_{i=1}^{\infty}$ in a Hilbert space \mathcal{H} is called a *frame* if there exist constants $A, B > 0$ such that

$$A\|f\|^2 \leq \sum_{i=1}^{\infty} |\langle f, f_i \rangle|^2 \leq B\|f\|^2 \quad (f \in \mathcal{H}). \quad (1-1)$$

The numbers A and B are called *frame bounds*. A frame is called *tight* if $A = B$. In frame theory, the operator $T : l^2 \rightarrow \mathcal{H}$ given by $T\{c_i\}_{i=1}^{\infty} = \sum_{i=1}^{\infty} c_i f_i$ is useful in analyzing various properties of frames. It is called the *synthesis* or *preframe operator*. Its adjoint $T^* : \mathcal{H} \rightarrow l^2; f \mapsto \{\langle f, f_i \rangle\}_{i=1}^{\infty}$ is called the *analysis operator*. By composing T and T^* , we obtain the frame operator

$$S : \mathcal{H} \rightarrow \mathcal{H}, \quad Sf = \sum_{i=1}^{\infty} \langle f, f_i \rangle f_i \quad (f \in \mathcal{H}).$$

The frame operator S is invertible and the reconstruction formula

$$f = S^{-1}Sf = \sum_{i=1}^{\infty} \langle f, S^{-1}f_i \rangle f_i \quad (f \in \mathcal{H}) \quad (1-2)$$

MSC2010: primary 42C15; secondary 46B15.

Keywords: frame, Banach space, dual frame, p -frame, alternate dual.

holds. The sequence $\{S^{-1}f_i\}_{i=1}^{\infty}$ which plays the same role as the dual in the theory of bases is also a frame. It is called the *canonical dual* of $\{f_i\}_{i=1}^{\infty}$. In general, the Bessel sequence $\{g_i\}_{i=1}^{\infty}$ is called a *dual* of $\{f_i\}_{i=1}^{\infty}$ if

$$f = \sum_{i=1}^{\infty} \langle f, g_i \rangle f_i \quad (f \in \mathcal{H}). \quad (1-3)$$

For general references on this theory, we refer the reader to [Christensen 2008, Section 5.1]. Recently, various generalizations of frames have been proposed: continuous frames [Ali et al. 1993; Askari-Hemmat et al. 2001; Gabardo and Han 2003], g -frames [Sun 2006], fusion frames [Casazza et al. 2008], von Neumann-Schatten frames [Sadeghi and Arefijamaal 2012], and so on. Frames for Banach spaces were first introduced in [Gröchenig 1991] and were developed in [Aldroubi et al. 2001; Cazassa and Christensen 1997; Casazza et al. 1999; 2005]. In particular, Christensen and Stoeva [2003] studied p -frames in Banach spaces and obtained a lot of interesting and important results.

In applications of frame theory the goal is to recognize the finer properties of functions by means of the magnitudes of the frame coefficients [Benedetto et al. 2006; Bolcskei et al. 1998; Candès and Donoho 2004; Heath and Paulraj 2002]. These properties, typically smoothness and decay properties or phase-space localization of functions, are measured by the Banach space norm. Dual frames have a key role in the decomposition of elements in the underlying space. Casazza et al. [2005] present some equivalent conditions for the existence of reconstruction formulas in Banach spaces. Moreover, sufficient conditions for the existence of dual frames are studied in [Aldroubi et al. 2001]. In this article, at the first, we review the definition and basic properties of p -frames, and then express some characterizations of duals of p -frames. The analogous results concerning frames in Hilbert spaces may be found in [Li 1995]. Finally, we discuss a stability theorem for duals of p -frames.

2. Elementary properties of p -frames

Throughout this paper, X is a separable Banach space with dual X^* , $1 < p, q < \infty$ and $\frac{1}{p} + \frac{1}{q} = 1$. A sequence $\{g_i\}_{i=1}^{\infty} \subseteq X^*$ is called a p -frame for X if there exist constants $A, B > 0$ such that

$$A\|x\| \leq \left(\sum_{i=1}^{\infty} |g_i(x)|^p \right)^{\frac{1}{p}} \leq B\|x\| \quad (x \in X). \quad (2-1)$$

The sequence $\{g_i\}_{i=1}^{\infty}$ is a p -Bessel sequence if at least the upper p -frame condition is satisfied. Analogous to frame theory in Hilbert spaces, one can define

the synthesis operator as

$$T : l^q \rightarrow X^*, \quad T\{d_i\} := \sum_{i=1}^{\infty} d_i g_i.$$

A straightforward calculation shows that $\{g_i\}_{i=1}^{\infty} \subseteq X^*$ is a p -Bessel sequence with bound B if and only if T is well-defined and $\|T\| \leq B$; see [Christensen and Stoeva 2003, Proposition 2.2].

The following result shows other aspects of the synthesis operator:

Proposition 2.1 [Christensen and Stoeva 2003]. *Let $\{g_i\} \subseteq X^*$ be a p -frame. Then*

- (i) *the adjoint of T given by $T^* : X \rightarrow l^p; f \mapsto \{g_i(f)\}_{i=1}^{\infty}$ has closed range;*
- (ii) *X is reflexive;*
- (iii) *T is onto.*

The next proposition deals with preservation of the p -frame property under the action of various operators. Its proof is straightforward and we omit it.

Proposition 2.2. *Let X and Y be two Banach spaces and $\Psi : Y \rightarrow X$ be a bounded operator. Then*

- (i) *if $\{g_i\}_{i=1}^{\infty} \subseteq X^*$ is a p -Bessel sequence for X , then $\{\Psi^* g_i\}_{i=1}^{\infty}$ is a p -Bessel sequence for Y ;*
- (ii) *if $\{g_i\}_{i=1}^{\infty}$ is a p -frame for X , and Ψ is one-to-one with closed range, then $\{\Psi^* g_i\}_{i=1}^{\infty}$ is a p -frame for Y .*

Definition 2.3. Let X be a Banach space and $1 < p < \infty$. A sequence $\{f_i\}_{i=1}^{\infty} \subseteq X$ is called a p -Riesz basis for X if the closed linear span of $\{f_i\}_{i=1}^{\infty}$ is X and there exist constants A and B such that, for any finite scalars $\{c_i\}$,

$$A(\sum |c_i|^p)^{\frac{1}{p}} \leq \|\sum c_i f_i\| \leq B(\sum |c_i|^p)^{\frac{1}{p}}. \tag{2-2}$$

Clearly, if $\{g_i\}_{i=1}^{\infty} \subseteq X^*$ is a p -Riesz basis for X^* then its synthesis operator has a bounded inverse. In particular, every p -Riesz basis for X^* is a q -frame for X with the same bounds.

If $\{g_i\}_{i=1}^{\infty} \subseteq X^*$ is a p -frame for X , then Proposition 2.1 shows that every $g \in X^*$ can be written as $g = \sum_{i=1}^{\infty} d_i g_i$ for some $\{d_i\}_{i=1}^{\infty} \in l^q$. Our aim is to find such a decomposition for the elements of X .

3. Main results

Let $\{f_i\}_{i=1}^{\infty}$ be a frame in a Hilbert space \mathcal{H} with the synthesis operator T . The canonical dual $\{S^{-1} f_i\}_{i=1}^{\infty}$ deals with the frame operator S ; see (1-2). It is not guaranteed that the canonical dual frame has the same structure as the frame itself

[Daubechies 1990]. Alternate duals are now presented as being a good candidate to apply the reconstruction formula (1-2).

Unfortunately, in p -frames, the frame operator cannot be defined. Hence, we first try to describe the canonical dual with respect to the synthesis operator. In fact, let $\{f_i\}_{i=1}^\infty$ be a frame in a Hilbert space \mathcal{H} with the analysis operator T^* . Then the frame condition (1-1) implies that T^* is injective and has closed range [Christensen 2008, Corollary 5.4.3]. Hence, the operator $(T^*)^{-1} : \mathcal{R}(T^*) \rightarrow \mathcal{H}$ can be extended to a bounded operator $\Phi : l^2 \rightarrow \mathcal{H}$. Therefore,

$$S^{-1} f_i = S^{-1} T \delta_i = S^{-1} T T^* \Phi \delta_i = \Phi \delta_i,$$

where $\{\delta_i\}_{i=1}^\infty$ is the canonical orthonormal basis for l^2 .

We summarize this fact in the following lemma.

Lemma 3.1. *Let $\{f_i\}_{i=1}^\infty$ be a frame in \mathcal{H} with the analysis operator T^* . The canonical dual $\{f_i\}_{i=1}^\infty$ can be represented as $\{\Phi \delta_i\}_{i=1}^\infty$, where $\Phi : l^2 \rightarrow \mathcal{H}$ is the unique extension of $(T^*)^{-1}$ and $\{\delta_i\}_{i=1}^\infty$ is the canonical orthonormal basis of l^2 .*

Let X be a Banach space with dual X^* and $1 < p < \infty$. The usual duality between X and X^* allows us to consider p -frames for X^* . In fact, a sequence $\{f_i\}_{i=1}^\infty \subseteq X$ is a p -frame if there exist constants A and B such that

$$A \|g\| \leq \left(\sum_{i=1}^{\infty} |g(f_i)|^p \right)^{\frac{1}{p}} \leq B \|g\| \quad (g \in X^*).$$

If the upper frame condition is satisfied we call $\{f_i\}_{i=1}^\infty$ a p -Bessel sequence.

Definition 3.2. Let $\{g_i\}_{i=1}^\infty \subseteq X^*$ be a p -Bessel sequence for X . A q -Bessel sequence $\{f_i\}_{i=1}^\infty \subseteq X$ for X^* is called a *dual* for $\{g_i\}_{i=1}^\infty$ if

$$g = \sum g(f_i) g_i \quad (g \in X^*) \quad \text{or} \quad f = \sum g_i(f) f_i \quad (f \in X). \quad (3-1)$$

If $\{g_i\}_{i=1}^\infty$ is p -frame, by using the Cauchy–Schwarz inequality, $\{f_i\}_{i=1}^\infty$ is automatically a q -frame for X^* , and vice versa. For more details see Theorem 2.10 of [Christensen and Stoeva 2003].

Denote the synthesis operators of $\{g_i\}_{i=1}^\infty$ and $\{f_i\}_{i=1}^\infty$ by T and U , respectively. Also let X be reflexive. Then (3-1) holds if and only if $TU^* = I_{X^*}$ or $UT^* = I_X$. Although, for every $p \neq 2$, there exist a Banach space X and a p -frame for X without any dual [Casazza et al. 1999], Christensen and Stoeva [2003] showed that a p -frame $\{g_i\}_{i=1}^\infty$ has a dual if and only if $\mathcal{R}(T^*)$, the range of T^* , is complemented in l^p . Obviously, every p -Riesz basis for X^* has a unique dual.

Now we give a characterization of dual p -frames:

Proposition 3.3. *Let $\{g_i\}_{i=1}^\infty \subseteq X^*$ be a p -frame for X with the synthesis operator T . Then there exists a one-to-one correspondence between duals of $\{g_i\}_{i=1}^\infty$ and bounded left inverses of T^* .*

Proof. Suppose that $\Phi : l^p \rightarrow X$ is a bounded left inverse of T^* and consider $\{\delta_i\}_{i=1}^\infty$ as the canonical basis of l^p . It is obvious that $\{f_i\}_{i=1}^\infty := \{\Phi\delta_i\}_{i=1}^\infty$ is a q -Bessel sequence and

$$f = \Phi T^* f = \Phi \sum_{i=1}^\infty g_i(f)\delta_i = \sum_{i=1}^\infty g_i(f)f_i \quad (f \in X).$$

Thus $\{f_i\}_{i=1}^\infty$ is a q -frame for X^* . Conversely, let $\{f_i\}_{i=1}^\infty \subseteq X$ be a dual for $\{g_i\}_{i=1}^\infty$. Consider $\Phi : l^p \rightarrow X$ as the synthesis operator of $\{f_i\}_{i=1}^\infty$. Then Φ is bounded and for each $f \in X$ we have

$$f = \sum_{i=1}^\infty g_i(f)f_i = \sum_{i=1}^\infty g_i(f)\Phi\delta_i = \Phi(\{g_i(f)\}_{i=1}^\infty) = \Phi T^* f. \quad \square$$

As a consequence, we show that a p -frame $\{g_i\}_{i=1}^\infty \subseteq X^*$ with a unique dual is a q -Riesz basis for X^* . In fact, by Proposition 3.3 there exists a one-to-one correspondence between the dual frames of $\{g_i\}_{i=1}^\infty$ and all bounded left inverse operators of T^* , in which T is the synthesis operator of $\{g_i\}_{i=1}^\infty$. Hence, $\{g_i\}_{i=1}^\infty$ has a unique dual if and only if T is injective. T is also surjective by Proposition 2.1. Thus T is invertible and $\|T^{-1}\| < \infty$. This implies that $\{g_i\}_{i=1}^\infty$ is a q -Riesz basis for X^* .

Proposition 3.4. *Assume that p -frame $\{g_i\}_{i=1}^\infty \subseteq X^*$ has a dual. Then the q -Bessel sequence $\{f_i\}_{i=1}^\infty \subseteq X$ is a dual for $\{g_i\}_{i=1}^\infty$ if there exists a bounded operator $\Psi : X^* \rightarrow l^q$ such that $T\Psi = 0$. Conversely, all duals of $\{g_i\}_{i=1}^\infty$ (provided existence) can be described in this manner.*

Proof. Let $\{g_i\}_{i=1}^\infty$ be a p -frame. As a consequence of Proposition 2.1, the operator $(T^*)^{-1} : \mathcal{R}(T^*) \rightarrow X$ is well-defined. If $\{g_i\}_{i=1}^\infty$ has a dual, then $\mathcal{R}(T^*)$ is complemented and so this operator can be extended to a bounded linear operator $W : l^p \rightarrow X$. Now assume that $\{f_i\}_{i=1}^\infty \subseteq X$ is a dual for $\{g_i\}_{i=1}^\infty$ with the synthesis operator U . Then (3-1) immediately implies that $TU^* = I$. Define $\Psi : X^* \rightarrow l^q$ by $\Psi = U^* - W^*$. Clearly, Ψ is a bounded operator and

$$T\Psi = TU^* - TW^* = I - (WT^*)^* = 0.$$

Conversely, suppose that $\Psi : X^* \rightarrow l^q$ is a bounded operator via $T\Psi = 0$. Take $\Phi = W - \psi^*$. Then Φ is a bounded operator and $\Phi T^* = I$. Using Proposition 3.3 we conclude that $\{\Phi\delta_i\}_{i=1}^\infty$ is a dual for $\{g_i\}_{i=1}^\infty$. \square

Suppose that $\{g_i\}_{i=1}^\infty \subseteq X^*$ is a p -frame with the synthesis operator T such that $\mathcal{R}(T^*) \subseteq l^p$ is complemented. Then $\{W\delta_i\}_{i=1}^\infty$ is called the *canonical dual* of $\{g_i\}_{i=1}^\infty$, where $W : l^p \rightarrow X$ is the extension of $(T^*)^{-1}$. Other duals, which are characterized by Proposition 3.3, are called *alternate duals*. In other words, the canonical dual is associated to the bounded inverse of T^* whereas alternate duals are in fact obtained by the left inverses of T^* .

Now we are ready to state a perturbation theorem about duals.

Theorem 3.5. *Let $\{g_i\}_{i=1}^\infty \subseteq X^*$ be a p -frame for X with bounds A_1 and B_1 . The p -frames sufficiently close to $\{g_i\}_{i=1}^\infty$ have a dual. More precisely, let $\{f_i\}_{i=1}^\infty \subseteq X$ be a dual for $\{g_i\}_{i=1}^\infty$ with bounds A_2 and B_2 , and let $\{g'_i\}_{i=1}^\infty$ be another p -frame with bounds A' and B' such that $\{g_i - g'_i\}_{i=1}^\infty$ is a p -Bessel sequence with constant sufficiently small ϵ . Then there exists a dual q -frame $\{f'_i\}_{i=1}^\infty$ for $\{g'_i\}_{i=1}^\infty$ such that $\{f_i - f'_i\}_{i=1}^\infty$ is also a q -Bessel sequence with bound multiplied by ϵ .*

Proof. Denote by T_1 and T_2 the synthesis operators of $\{g_i\}_{i=1}^\infty$ and $\{g'_i\}_{i=1}^\infty$, respectively. Then $\|T_1 - T_2\| < \epsilon$ by Proposition 2.2 of [Christensen and Stoeva 2003]. Moreover, $(T_1^*)^{-1} : \mathcal{R}(T_1^*) \rightarrow X$ can be extended to a bounded operator $W : l^p \rightarrow X$ by the assumption. Hence

$$\|I - T_2^*W\| = \|(T_1 - T_2)^*W\| \leq \|W\|\|T_1 - T_2\| \leq \epsilon\|W\|.$$

Consequently T_2^*W is invertible. It follows that T_2^* has a bounded right inverse. A similar argument shows that its left inverse also exists. Consider $U_1 : l^p \rightarrow X$ as the synthesis operator of $\{f_i\}_{i=1}^\infty$. Then

$$\|I - U_1T_2^*\| = \|U_1(T_1 - T_2)^*\| \leq \|U_1\|\|T_1 - T_2\| \leq \epsilon\|U_1\|.$$

Therefore, the p -frame $\{g'_i\}_{i=1}^\infty$ has a dual. We are looking for the desired dual. First by Proposition 3.4 there exists a bounded operator $\Psi : X^* \rightarrow l^q$ such that $T_1\Psi = 0$. Assume that $W_2 : l^p \rightarrow X$ is an extension of $(T_2^*)^{-1}$. Put

$$h_i = (W_2 + \Psi^*)\delta_i.$$

Then $\{h_i\}_{i=1}^\infty$ is a q -Bessel sequence with the synthesis operator $U_2 := W_2 + \Psi^*$ by Proposition 2.2. Moreover, for each $f \in X$ we have

$$\begin{aligned} \|f - U_2T_2^*f\| &= \|\Psi^*T_2^*f\| \\ &= \|\Psi^*T_1^*f - \Psi^*T_2^*f\| \\ &\leq \|T_1 - T_2\|\|\Psi\|\|f\| \leq \epsilon\|\Psi\|\|f\|. \end{aligned}$$

Therefore, $U_2T_2^*$ is invertible for sufficiently small $\epsilon > 0$. In particular,

$$\|I - U_2T_2^*\| \leq \epsilon\|\Psi\|.$$

It remains to show that the q -frame $\{f'_i\}_{i=1}^\infty := \{(U_2 T_2^*)^{-1} f_i\}_{i=1}^\infty$ satisfies the theorem. It is easy to see that

$$U_2 T_2^* = I + \Psi^*(T_1^* - T_2^*). \quad (3-2)$$

Hence,

$$1 - \epsilon \|\Psi\| \leq \|U_2 T_2^*\|. \quad (3-3)$$

For each sequence $\{d_i\}_{i=1}^\infty$ in l^p by using (3-2) and (3-3) we get

$$\begin{aligned} \left\| \sum_{i=1}^\infty d_i (f_i - f'_i) \right\| &= \|U_1 \{d_i\} - (U_2 T_2^*)^{-1} U_1 \{d_i\}\| \\ &\leq \|U_1\| \|I - (U_2 T_2^*)^{-1}\| \left(\sum_{i=1}^\infty |d_i|^p \right)^{\frac{1}{p}} \\ &\leq \|U_1\| \|(U_2 T_2^*)^{-1}\| \|U_2 T_2^* - I\| \left(\sum_{i=1}^\infty |d_i|^p \right)^{\frac{1}{p}} \\ &\leq \frac{\epsilon \|\Psi\| B_2}{1 - \epsilon \|\Psi\|} \left(\sum_{i=1}^\infty |d_i|^p \right)^{\frac{1}{p}}. \end{aligned}$$

This means that $\{f_i - f'_i\}_{i=1}^\infty$ is a q -Bessel sequence and its bound is a multiple of ϵ . \square

Let $\{g_i\}_{i=1}^\infty \subseteq X^*$ be a p -Bessel sequence for X with the synthesis operator T . We say that a q -Bessel sequence $\{f_i\}_{i=1}^\infty \subseteq X$ with the synthesis operator U is an *approximately dual* of $\{g_i\}_{i=1}^\infty$ if

$$\|I - T U^*\| < 1 \quad \text{or} \quad \|I - U T^*\| < 1. \quad (3-4)$$

Obviously, $\{f_i\}_{i=1}^\infty$ is a dual of $\{g_i\}_{i=1}^\infty$ when $T U^* = I$ or $U T^* = I$. Approximate duals are studied in a Hilbert space setting in [Christensen and Laugesen 2010]. They are easier to construct than the classical dual frames. For p -frames, which don't have duals in general, it is natural to ask whether we can exploit the approximate duals instead of duals. Unfortunately, the answer is negative. In fact, if $\{g_i\}_{i=1}^\infty$ is a p -frame for X with an approximate dual $\{f_i\}_{i=1}^\infty$, then, with notation as above, the operator $U T^*$ is invertible. Hence, $\{U T^* f_i\}_{i=1}^\infty$ is a p -frame by Proposition 2.2. Moreover,

$$f = (U T^*)^{-1} U T^* f = (U T^*)^{-1} \sum_{i=1}^\infty g_i(f) f_i = \sum_{i=1}^\infty g_i(f) (U T^*)^{-1} f_i.$$

Therefore, $\{(U T^*)^{-1} f_i\}$ is a dual of $\{g_i\}_{i=1}^\infty$.

Acknowledgements

Part of this work was done while the first author was visiting the Numerical Harmonic Analysis Group at the Faculty of Mathematics, University of Vienna. He thanks Professor Hans G. Feichtinger for helpful comments and suggestions. The authors also thank the referees for useful comments.

References

- [Aldroubi et al. 2001] A. Aldroubi, Q. Sun, and W.-S. Tang, “ p -frames and shift invariant subspaces of L^p ”, *J. Fourier Anal. Appl.* **7**:1 (2001), 1–21. MR 2002c:42046 Zbl 0983.46027
- [Ali et al. 1993] S. T. Ali, J.-P. Antoine, and J.-P. Gazeau, “Continuous frames in Hilbert space”, *Ann. Physics* **222**:1 (1993), 1–37. MR 94e:81107 Zbl 0782.47019
- [Askari-Hemmat et al. 2001] A. Askari-Hemmat, M. A. Dehghan, and M. Radjabalipour, “Generalized frames and their redundancy”, *Proc. Amer. Math. Soc.* **129**:4 (2001), 1143–1147. MR 2001m:42054 Zbl 0976.42022
- [Benedetto et al. 2006] J. J. Benedetto, A. M. Powell, and Ö. Yılmaz, “Sigma-Delta ($\Sigma\Delta$) quantization and finite frames”, *IEEE Trans. Inform. Theory* **52**:5 (2006), 1990–2005. MR 2007a:94030
- [Bolcskei et al. 1998] H. Bolcskei, F. Hlawatsch, and H. G. Feichtinger, “Frame-theoretic analysis of oversampled filter banks”, *IEEE Trans. Signal Process.* **46**:12 (1998), 3256–3268.
- [Candès and Donoho 2004] E. J. Candès and D. L. Donoho, “New tight frames of curvelets and optimal representations of objects with piecewise C^2 singularities.”, *Commun. Pure Appl. Math.* **57**:2 (2004), 219–266. MR 2012649 Zbl 1038.94502
- [Casazza et al. 1999] P. G. Casazza, D. Han, and D. R. Larson, “Frames for Banach spaces”, pp. 149–182 in *The functional and harmonic analysis of wavelets and frames* (San Antonio, TX, 1999), edited by L. W. Baggett and D. R. Larson, Contemp. Math. **247**, Amer. Math. Soc., Providence, RI, 1999. MR 2000m:46015 Zbl 0947.46010
- [Casazza et al. 2005] P. Casazza, O. Christensen, and D. T. Stoeva, “Frame expansions in separable Banach spaces”, *J. Math. Anal. Appl.* **307**:2 (2005), 710–723. MR 2006e:42044 Zbl 1091.46007
- [Casazza et al. 2008] P. G. Casazza, G. Kutyniok, and S. Li, “Fusion frames and distributed processing”, *Appl. Comput. Harmon. Anal.* **25**:1 (2008), 114–132. MR 2009d:42094 Zbl 05295258
- [Cazassa and Christensen 1997] P. G. Cazassa and O. Christensen, “Perturbation of operators and applications to frame theory”, *J. Fourier Anal. Appl.* **3**:5 (1997), 543–557. MR 98j:47028 Zbl 0895.47007
- [Christensen 2008] O. Christensen, *Frames and bases: An introductory course*, Birkhäuser, Boston, MA, 2008. MR 2010i:42001 Zbl 1152.42001
- [Christensen and Laugesen 2010] O. Christensen and R. S. Laugesen, “Approximately dual frames in Hilbert spaces and applications to Gabor frames”, *Sampl. Theory Signal Image Process.* **9**:1-3 (2010), 77–89. MR 2012f:42053 Zbl 1228.42031
- [Christensen and Stoeva 2003] O. Christensen and D. T. Stoeva, “ p -frames in separable Banach spaces”, *Adv. Comput. Math.* **18**:2-4 (2003), 117–126. MR 2004b:42060 Zbl 1012.42024
- [Daubechies 1990] I. Daubechies, “The wavelet transform, time-frequency localization and signal analysis”, *IEEE Trans. Inform. Theory* **36**:5 (1990), 961–1005. MR 91e:42038 Zbl 0738.94004
- [Gabardo and Han 2003] J.-P. Gabardo and D. Han, “Frames associated with measurable spaces”, *Adv. Comput. Math.* **18**:2-4 (2003), 127–147. MR 2004b:42062 Zbl 1033.42036

- [Gröchenig 1991] K. Gröchenig, “Describing functions: atomic decompositions versus frames”, *Monatsh. Math.* **112**:1 (1991), 1–42. MR 92m:42035 Zbl 0736.42022
- [Heath and Paulraj 2002] R. W. Heath and A. J. Paulraj, “Linear dispersion codes for MIMO systems based on frame theory”, *IEEE Trans. Signal Process.* **50**:10 (2002), 2429–2441.
- [Li 1995] S. Li, “On general frame decompositions”, *Numer. Funct. Anal. Optim.* **16**:9-10 (1995), 1181–1191. MR 97b:42055 Zbl 0849.42023
- [Sadeghi and Arefijamaal 2012] G. Sadeghi and A. Arefijamaal, “von Neumann–Schatten frames in separable Banach spaces”, *Mediterr. J. Math.* **9**:3 (2012), 525–535. MR 2954506 Zbl 06107826
- [Sun 2006] W. Sun, “ G -frames and g -Riesz bases”, *J. Math. Anal. Appl.* **322**:1 (2006), 437–452. MR 2007b:42047 Zbl 1129.42017

Received: 2012-05-09 Revised: 2012-10-03 Accepted: 2012-10-06

arefijamaal@hsu.ac.ir

*Department of Mathematics and Computer Sciences,
Hakim Sabzevari University, Sabzevar, Iran*

leili.mohamadkhani@gmail.com

*Department of Mathematics and Computer Sciences,
Hakim Sabzevari University, Sabzevar, Iran*

Shock profile for gas dynamics in thermal nonequilibrium

Wang Xie

(Communicated by John Baxley)

In this paper, we study the existence and the properties of a shock profile for a system of thermal nonequilibrium gas dynamics. We find a neat condition to ensure the existence of the shock profile. Moreover, we calculate the shock profile solution explicitly.

1. Introduction

The motion of a gas in local thermodynamic equilibrium is governed by the compressible Euler equations. In Lagrangian coordinates, the equations for one-dimensional flow read (see [Courant and Friedrichs 1948])

$$\begin{cases} v_t - u_x = 0, \\ u_t + p_x = 0, \\ (e + \frac{1}{2}u^2)_t + (pu)_x = 0, \end{cases} \quad (1-1)$$

where v , u , p and e are, respectively, the specific volume, velocity, pressure and internal energy of the gas. For an ideal gas,

$$e = \frac{1}{\gamma - 1}pv, \quad (1-2)$$

where $\gamma > 1$ is the adiabatic constant. During rapid changes in the flow the internal energy e may lag behind the equilibrium value corresponding to the ambient pressure and density. The translational energy adjusts quickly, but the rotational and vibrational energy may take an order of magnitude longer. If we suppose that α of the degrees of freedom adjust instantaneously but a further α_f degrees of freedom take longer to relax, we may take (see [Whitham 1974])

$$e = \frac{\alpha}{2}pv + q, \quad (1-3)$$

MSC2010: 35Q31.

Keywords: shock profile, thermal nonequilibrium.

where q is the energy in the lagging degrees of freedom. In equilibrium, q would have the value

$$q_{\text{equil}} = \frac{\alpha_f}{2} pv. \quad (1-4)$$

A simple overall equation to represent the relaxation is (in Lagrangian coordinates)

$$q_t = -\frac{1}{\tau} \left(q - \frac{\alpha_f}{2} pv \right), \quad (1-5)$$

where $\tau > 0$ is the relaxation time. Therefore, in thermal nonequilibrium, we have the following system of equations to model the gas motion:

$$\begin{cases} v_t - u_x = 0, \\ u_t + p_x = 0, \\ \left(\frac{1}{2} \alpha pv + q + \frac{1}{2} u^2 \right)_t + (pu)_x = 0, \\ q_t = -\frac{1}{\tau} \left(q - \frac{1}{2} \alpha_f pv \right). \end{cases} \quad (1-6)$$

If the relaxation time τ is taken to be so short that $q = (\alpha_f/2)pv$ is an adequate approximation to the last equation in (1-6), we have the following equilibrium theory:

$$\begin{cases} v_t - u_x = 0, \\ u_t + p_x = 0, \\ \left(\frac{1}{2} (\alpha + \alpha_f) pv + \frac{1}{2} u^2 \right)_t + (pu)_x = 0. \end{cases} \quad (1-7)$$

The three characteristic speeds for (1-7) are

$$\lambda_1 = -\sqrt{\left(1 + \frac{2}{\alpha + \alpha_f}\right) \frac{p}{v}}, \quad \lambda_2 = 0, \quad \lambda_3 = \sqrt{\left(1 + \frac{2}{\alpha + \alpha_f}\right) \frac{p}{v}}.$$

For the system (1-7), the setup $((v_-, u_-, p_-), (v_+, u_+, p_+), \sigma)$ with two constant states (v_-, u_-, p_-) and (v_+, u_+, p_+) and speed σ is called a shock wave (see [Courant and Friedrichs 1948]) if the Rankine–Hugoniot conditions

$$\begin{cases} -\sigma(v_+ - v_-) = (u_+ - u_-), \\ \sigma(u_+ - u_-) = (p_+ - p_-), \\ \sigma \left(\left(\frac{1}{2} (\alpha + \alpha_f) p_+ v_+ + \frac{1}{2} u_+^2 \right) - \left(\frac{1}{2} (\alpha + \alpha_f) p_- v_- + \frac{1}{2} u_-^2 \right) \right) = (p_+ u_+ - p_- u_-) \end{cases} \quad (1-8)$$

hold, and some other entropy conditions hold, where v_-, v_+, p_-, p_+ are positive constants, u_- and u_+ are constants. A shock wave is called a 1-shock wave if

$$-\sqrt{\left(1 + \frac{2}{\alpha + \alpha_f}\right) \frac{p_-}{v_-}} > \sigma > -\sqrt{\left(1 + \frac{2}{\alpha + \alpha_f}\right) \frac{p_+}{v_+}}. \quad (1-9)$$

A shock wave is called a 3-shock wave if

$$\sqrt{\left(1 + \frac{2}{\alpha + \alpha_f}\right) \frac{p_-}{v_-}} > \sigma > \sqrt{\left(1 + \frac{2}{\alpha + \alpha_f}\right) \frac{p_+}{v_+}}. \tag{1-10}$$

In this paper, we consider a 3-shock wave, because a 1-shock wave can be handled by the same method. For a 3-shock wave, it follows from (1-8) and (1-10) that

$$v_- < v_+, \quad u_- > u_+, \quad p_- > p_+. \tag{1-11}$$

A shock profile for the 3-shock wave $((v_-, u_-, p_-), (v_+, u_+, p_+), \sigma)$ is a traveling-wave solution for system (1-6) of the form $(v, u, p, q)((x - \sigma t)/\tau)$ satisfying

$$(v, u, p, q)(\pm\infty) = (v_{\pm}, u_{\pm}, p_{\pm}, (\alpha_f/2)p_{\pm}v_{\pm}). \tag{1-12}$$

So we have

$$\begin{cases} -\sigma v' - u' = 0, \\ -\sigma u' + p' = 0, \\ -\sigma\left(\frac{1}{2}\alpha p v + q + \frac{1}{2}u^2\right)' + (p u)' = 0, \\ -\sigma q' = -(q - \frac{1}{2}\alpha_f p v), \end{cases} \tag{1-13}$$

where $' = d/d\xi$ and $\xi = (x - \sigma t)/\tau$.

In this paper, we are interested in the existence and properties of the shock profile. For a general hyperbolic system with relaxation, the existence of the shock profile has been proved in [Yong and Zumbrun 2000] by using the center manifold method with the assumption that the shock strength is sufficiently small. In this paper, we find the sufficient and necessary condition, which is

$$\frac{p_-}{p_+} < 1 + \frac{2\alpha_f}{\alpha(1 + \alpha + \alpha_f)},$$

to ensure the existence of the shock profile. Moreover, we can calculate the shock profile solution in some explicit details. This is in sharp contrast to the abstract construction in [Yong and Zumbrun 2000]. Before we state our theorem, we introduce some notation. Let

$$\begin{aligned} m &= \sigma v_- + u_- = \sigma v_+ + u_+, \\ P &= -\sigma u_- + p_- = -\sigma u_+ + p_+, \\ Q &= -\sigma\left(\frac{1}{2}\alpha + \alpha_f p_- v_- + \frac{1}{2}u_-^2\right) + p_- u_- \\ &= -\sigma\left(\frac{1}{2}\alpha + \alpha_f p_+ v_+ + \frac{1}{2}u_+^2\right) + p_+ u_+, \\ f(v) &= -\sigma^2(1 + \alpha)v + \left(1 + \frac{1}{2}\alpha\right)(\sigma^2 v_- + p_-) \\ &= -\sigma^2(1 + \alpha)v + \left(1 + \frac{1}{2}\alpha\right)(\sigma^2 v_+ + p_+). \end{aligned} \tag{1-14}$$

Theorem. *Suppose the two constant states (v_-, u_-, p_-) , (v_+, u_+, p_+) and the speed σ satisfy the Rankine–Hugoniot conditions (1-8) and the Lax shock condition (1-10).*

(1) *If*

$$\frac{p_-}{p_+} < 1 + \frac{2\alpha_f}{\alpha(1 + \alpha + \alpha_f)}, \tag{1-15}$$

then there exists a solution to the problem (1-13) and (1-12).

(2) *If*

$$\frac{p_-}{p_+} \geq 1 + \frac{2\alpha_f}{\alpha(1 + \alpha + \alpha_f)}, \tag{1-16}$$

the problem (1-13) and (1-12) does not admit a smooth solution.

(3) *In case (1), that is, if (1-15) holds, the solution of the problem (1-13) and (1-12) satisfying $v(0) = v_0$ for some constant v_0 satisfying $v_- < v_0 < v_+$ is given by*

$$\begin{aligned} 2f(v_+)(\ln(v_+ - v) - \ln(v_+ - v_0)) - 2f(v_-)(\ln(v - v_-) - \ln(v_0 - v_-)) \\ = -\sigma\xi(1 + \alpha + \alpha_f)(v_+ - v_-), \end{aligned} \tag{1-17}$$

$$u(\xi) = m - \sigma v(\xi), \quad p(\xi) = m\sigma + P - \sigma^2 v(\xi) \tag{1-18}$$

for $-\infty < \xi < +\infty$. For this solution, we have

$$v'(\xi) > 0, \quad u'(\xi) < 0, \quad p'(\xi) < 0 \tag{1-19}$$

for $-\infty < \xi < +\infty$, and

$$C_1 v'(\xi) \leq \exp\left(-\frac{1 + \alpha + \alpha_f}{2f(v_+)}\sigma(v_+ - v_-)\xi\right) \leq C_2(v_+ - v(\xi)) \tag{1-20}$$

for $\xi > 0$, and

$$C_3 v'(\xi) \leq \exp\left(\frac{1 + \alpha + \alpha_f}{2f(v_-)}\sigma(v_+ - v_-)\xi\right) \leq C_4(v(\xi) - v_-) \tag{1-21}$$

for $\xi < 0$, where C_i ($i = 1, 2, 3, 4$) are some positive constants. For $u(\xi)$ and $p(\xi)$, we have similar estimates.

2. Proofs

To prove our theorem, we start by integrating (1-13) to get

$$\begin{cases} \sigma v + u = m, \\ -\sigma u + p = P, \\ -\sigma\left(\frac{1}{2}\alpha p v + q + \frac{1}{2}u^2\right) + pu = Q, \end{cases} \tag{2-1}$$

where m , P and Q are given by (1-14). By the third equation of (2-1), we have

$$q = -\left(\frac{\alpha}{2}pv + \frac{u^2}{2}\right) + \frac{pu - Q}{\sigma}. \tag{2-2}$$

Substituting (2-2) into the fourth equation of (1-13), using (2-1) and (2-2), we get

$$f(v)\frac{dv}{d\xi} = \frac{1}{\sigma}\left(\frac{\alpha + \alpha_f}{2}pv + \frac{u^2}{2} - \frac{pu - Q}{\sigma}\right), \tag{2-3}$$

where $f(v)$ is given by (1-14). So

$$f(v_-) = v_- \left(-\frac{\alpha}{2}\sigma^2 + \left(1 + \frac{\alpha}{2}\right)\frac{p_-}{v_-}\right). \tag{2-4}$$

In view of (1-10), we have

$$\begin{aligned} -\frac{\alpha}{2}\sigma^2 + \left(1 + \frac{\alpha}{2}\right)\frac{p_-}{v_-} &> -\frac{\alpha}{2}\left(1 + \frac{2}{\alpha + \alpha_f}\right)\frac{p_-}{v_-} + \left(1 + \frac{\alpha}{2}\right)\frac{p_-}{v_-} \\ &= \left(1 - \frac{\alpha}{\alpha + \alpha_f}\right)\frac{p_-}{v_-} > 0. \end{aligned} \tag{2-5}$$

Therefore

$$f(v_-) > 0.$$

By (1-14), we get

$$f(v_+) = v_+ \left(-\frac{1}{2}\alpha\sigma^2 + \left(1 + \frac{1}{2}\alpha\right)\frac{p_+}{v_+}\right). \tag{2-6}$$

Let

$$\bar{v} = \frac{1 + \frac{1}{2}\alpha}{1 + \alpha} \frac{\sigma^2 v_+ + p_+}{\sigma^2}. \tag{2-7}$$

Then

$$f(\bar{v}) = 0. \tag{2-8}$$

So, if

$$v_+ < \bar{v}, \tag{2-9}$$

then, because f is a decreasing function,

$$f(v_+) > 0. \tag{2-10}$$

In the next lemma, we will give a neat condition to ensure (2-10).

Lemma. (1) If $\frac{p_-}{p_+} < 1 + \frac{2\alpha_f}{\alpha(1 + \alpha + \alpha_f)}$, then $v_+ < \bar{v}$ and thus $f(v_+) > 0$.

(2) If $\frac{p_-}{p_+} = 1 + \frac{2\alpha_f}{\alpha(1 + \alpha + \alpha_f)}$, then $v_+ = \bar{v}$ and $f(v_+) = 0$.

(3) If $\frac{p_-}{p_+} > 1 + \frac{2\alpha_f}{\alpha(1 + \alpha + \alpha_f)}$, then $v_+ > \bar{v}$ and $f(v_+) < 0$.

Proof. First, we use (1-8) to show that

$$\frac{1}{2}(\alpha + \alpha_f)(p_+v_+ - p_-v_-) = (v_- - v_+)\frac{1}{2}(p_+ + p_-). \quad (2-11)$$

In fact, by the third equation of (1-8), we have

$$\begin{aligned} \frac{1}{2}(\alpha + \alpha_f)(p_+v_+ - p_-v_-) &= \frac{1}{\sigma}(p_+u_+ - p_-u_-) - \frac{1}{2}(u_+^2 - u_-^2) \\ &= \frac{1}{\sigma}(p_+u_+ - p_-u_-) - \frac{1}{2}(u_+ + u_-)(u_+ - u_-). \end{aligned} \quad (2-12)$$

By the second equation of (1-8), we have $(u_+ - u_-) = (1/\sigma)(p_+ - p_-)$. This, together with (2-12), implies that

$$\begin{aligned} \frac{1}{2}(\alpha + \alpha_f)(p_+v_+ - p_-v_-) &= \frac{1}{\sigma}(p_+u_+ - p_-u_- - \frac{1}{2}(p_+ - p_-)(u_+ + u_-)) \\ &= \frac{1}{\sigma}(\frac{1}{2}p_+u_+ - \frac{1}{2}p_-u_- - \frac{1}{2}p_+u_- + \frac{1}{2}p_-u_+) \\ &= \frac{1}{\sigma}(u_+ - u_-)(p_+ + p_-). \end{aligned} \quad (2-13)$$

This proves (2-11). Dividing by p_-v_+ both sides of (2-11), we get

$$\frac{\alpha + \alpha_f}{2} \left(\frac{p_+}{p_-} - \frac{v_-}{v_+} \right) = \left(\frac{v_-}{v_+} - 1 \right) \frac{(p_+/p_-) + 1}{2}.$$

We solve for v_-/v_+ from this to get

$$\frac{v_-}{v_+} = \frac{(\alpha + \alpha_f)(p_+/p_-) + (p_+/p_-) + 1}{(\alpha + \alpha_f) + (p_+/p_-) + 1}. \quad (2-14)$$

It is easy to verify that $v_+ < \bar{v}$ is equivalent to

$$\sigma^2 < \left(1 + \frac{2}{\alpha} \right) \frac{p_+}{v_+}. \quad (2-15)$$

From the first and second equations of (1-8), we know that

$$\sigma^2 = \frac{p_- - p_+}{v_+ - v_-}. \quad (2-16)$$

So $v_+ < \bar{v}$ is equivalent to

$$\frac{p_- - p_+}{v_+ - v_-} < \left(1 + \frac{2}{\alpha} \right) \frac{p_+}{v_+}. \quad (2-17)$$

Now we use (2-14) to show (2-17) if (1-15) is true.

By (2-14), we have

$$\begin{aligned}
 \frac{p_- - p_+}{v_+ - v_-} &= \frac{(p_-/p_+) - 1}{1 - (v_-/v_+)} (p_+/v_+) \\
 &= \frac{(p_-/p_+) - 1}{1 - \frac{(\alpha + \alpha_f)(p_+/p_-) + (p_+/p_-) + 1}{(\alpha + \alpha_f) + (p_+/p_-) + 1}} \left(\frac{p_+}{v_+} \right) \\
 &= \frac{(p_-/p_+) - 1}{(\alpha + \alpha_f)(1 - (p_+/p_-))} [(\alpha + \alpha_f) + (p_+/p_-) + 1] \left(\frac{p_+}{v_+} \right) \\
 &= \frac{(p_-/p_+) - 1}{1 - (p_+/p_-)} \left(1 + \frac{(p_+/p_-) + 1}{\alpha + \alpha_f} \right) \left(\frac{p_+}{v_+} \right) \\
 &= \frac{(p_-/p_+)(p_-/p_+ - 1)}{(p_-/p_+) - 1} \left(1 + \frac{(p_+/p_-) + 1}{\alpha + \alpha_f} \right) \left(\frac{p_+}{v_+} \right) \\
 &= \left(\frac{p_-}{p_+} \right) \left(1 + \frac{(p_+/p_-) + 1}{\alpha + \alpha_f} \right) \left(\frac{p_+}{v_+} \right) \\
 &= \left(\frac{p_-}{p_+} + \frac{1}{\alpha + \alpha_f} \left(1 + \frac{p_-}{p_+} \right) \right) \left(\frac{p_+}{v_+} \right) \\
 &= \left(\left(1 + \frac{1}{\alpha + \alpha_f} \right) \left(\frac{p_-}{p_+} \right) + \frac{1}{\alpha + \alpha_f} \right) \left(\frac{p_+}{v_+} \right). \tag{2-18}
 \end{aligned}$$

So, if (1-15) holds, then we have

$$\begin{aligned}
 &\left(1 + \frac{1}{\alpha + \alpha_f} \right) \frac{p_-}{p_+} + \frac{1}{\alpha + \alpha_f} \\
 &< \left(1 + \frac{1}{\alpha + \alpha_f} \right) \left(1 + \frac{2\alpha_f}{\alpha(1 + \alpha + \alpha_f)} \right) + \frac{1}{\alpha + \alpha_f} \\
 &= 1 + \frac{1}{\alpha + \alpha_f} \left(2 + \frac{2\alpha_f}{\alpha(1 + \alpha + \alpha_f)} \right) + \frac{2\alpha_f}{\alpha(1 + \alpha + \alpha_f)} \\
 &= 1 + \frac{1}{\alpha + \alpha_f} \left(\frac{2\alpha(1 + \alpha + \alpha_f) + 2\alpha_f}{\alpha(1 + \alpha + \alpha_f)} \right) + \frac{2\alpha_f}{\alpha(1 + \alpha + \alpha_f)} \\
 &= 1 + \frac{2}{\alpha + \alpha_f} \frac{(\alpha + \alpha_f)(1 + \alpha)}{\alpha(1 + \alpha + \alpha_f)} + \frac{2\alpha_f}{\alpha(1 + \alpha + \alpha_f)} \\
 &= 1 + \frac{2(1 + \alpha)}{\alpha(1 + \alpha + \alpha_f)} + \frac{2\alpha_f}{\alpha(1 + \alpha + \alpha_f)} \\
 &= 1 + \frac{2}{\alpha}. \tag{2-19}
 \end{aligned}$$

Inequality (2-17) follows from (2-18) and (2-19). This proves item (1) of the Lemma. Items (2) and (3) follow from the same arguments. \square

Proof of the Theorem. Let

$$G(v, u, p) = (\alpha + \alpha_f)pv + u^2 - \frac{2(pu - Q)}{\sigma}. \quad (2-20)$$

It follows from (2-1) and (2-20) that

$$G(v, u, p) = (\alpha + \alpha_f)(m\sigma + P - \sigma^2v)v + (m - \sigma v)^2 - \frac{2}{\sigma}((m - \sigma v)(m\sigma + P - \sigma^2v) - Q), \quad (2-21)$$

where m, P, Q are given in (1-14). Therefore, $G(v, u, p)$ is a function of the single variable v , and we simply write it $G(v)$ from now on. It is a quadratic function. Moreover, by (1-14), we have

$$G(v_+) = G(v_-) = 0. \quad (2-22)$$

Therefore,

$$G(v) = -\beta(v - v_-)(v - v_+) \quad (2-23)$$

for some constant β . By comparing (2-23) with (2-21), we get $\beta = \sigma^2(1 + \alpha + \alpha_f)$. Hence,

$$G(v) = -\sigma^2(1 + \alpha + \alpha_f)(v - v_-)(v - v_+). \quad (2-24)$$

So

$$G(v) > 0 \quad (2-25)$$

as $v_- < v < v_+$.

In case (1) of the Theorem, we choose a constant v_0 satisfying $v_- < v_0 < v_+$ and set $v(0) = v_0$. Then we have from (2-3) that

$$\int_{v_0}^v \frac{2\sigma f(v)}{G(v)} dv = \xi, \quad (2-26)$$

and consider the expression

$$\int_{v_0}^v \frac{2\sigma f(s)}{G(s)} dv = F(v),$$

where $F(v) = \xi$.

Also, by the Lemma, and (2-24), we have, if

$$\frac{p_-}{p_+} < 1 + \frac{2\alpha_f}{\alpha(1 + \alpha + \alpha_f)},$$

then $f(v)/G(v) > 0$ for $v_- < v < v_+$, and

$$\int_{v_0}^{v_+} \frac{2\sigma f(v)}{G(v)} dv = +\infty, \tag{2-27}$$

$$\int_{v_0}^{v_-} \frac{2\sigma f(v)}{G(v)} dv = -\infty. \tag{2-28}$$

Therefore, $\xi = F(v)$ is an increasing mapping of (v_-, v_+) onto (∞_-, ∞_+) , which clearly maps v_0 to 0. Thus the inverse mapping $\xi \rightarrow v(\xi)$ is a differentiable function (with a positive derivative) and is one-to-one and onto from $(-\infty, +\infty)$ to (v_-, v_+) with $v(0) = v_0$. Moreover, it follows from (2-26) and (2-27) that

$$v(-\infty) = v_-, \quad v(+\infty) = v_+.$$

Therefore the substitution $s = v(t)$ gives

$$\xi = \int_0^\xi \frac{2\sigma f(v(t))}{G(v(t))} v'(t) dt$$

and differentiation gives

$$1 = \frac{2\sigma f(v(\xi))}{G(v(t))} v'(\xi),$$

and so we have a solution v of (2-3), which proves part (1) of the Theorem.

We prove part (2) as follows. If

$$\frac{p_-}{p_+} \geq 1 + \frac{2\alpha_f}{\alpha(1 + \alpha + \alpha_f)}, \tag{2-29}$$

by the Lemma, we know that $v_- < \bar{v} \leq v_+$. In this case, we use the proof by contradiction to prove (2) as follows. Suppose that the problem (1-12) and (1-13) has a solution $v(\xi)$. Since, in this case, $v_- < \bar{v} \leq v_+$, and $f'(v) < 0$, we have $f(v_-) > 0 \geq f(v_+)$. We may write (2-3) as

$$2\sigma f(v) \frac{dv}{d\xi} = G(v). \tag{2-30}$$

Since $v(-\infty) = v_-$ and $f(v) > 0$ for $v_- < v < \bar{v}$ and $G(v) > 0$ for $v_- < v < v_+$, we have $dv/d\xi > 0$ when $v_- < v < \bar{v} \leq v_+$. For a constant v_1 satisfying $v_- < v_1 < \bar{v}$, there exists $\xi_1 \in (-\infty, +\infty)$ such that $v(\xi_1) = v_1$. It follows from (2-30) that

$$\int_{v_1}^v \frac{2\sigma f(w)}{G(w)} dw = \xi - \xi_1. \tag{2-31}$$

By (1-14), we know that $f(v)$ is a linear function of v in the form

$$f(v) = -k(v - \bar{v}), \tag{2-32}$$

where $k = \sigma^2(1 + \alpha)$. It follows from (2-23), and the fact that $v_- < v < \bar{v} \leq v_+$ (when (2-29) holds), that

$$\int_{v_1}^{\bar{v}} \frac{2\sigma f(w)}{G(w)} dw < +\infty. \quad (2-33)$$

We let

$$\bar{\xi} = \xi_1 + \int_{v_1}^{\bar{v}} \frac{2\sigma f(w)}{G(w)} dw.$$

By (2-33),

$$-\infty < \bar{\xi} < \infty. \quad (2-34)$$

It follows from (2-31) that, as

$$v(\xi) \rightarrow \bar{v}, \quad \xi \rightarrow \bar{\xi}. \quad (2-35)$$

This will lead to a contradiction by the following argument. By (2-30), (2-32) and (2-22), we have

$$\frac{dv}{d\xi} = \frac{G(v)}{2\sigma f(v)} = \frac{\beta}{2\sigma} \frac{(v - v_-)(v - v_+)}{v - \bar{v}}. \quad (2-36)$$

Therefore, if

$$\frac{p_-}{p_+} > 1 + \frac{2\alpha_f}{\alpha(1 + \alpha + \alpha_f)},$$

then $\bar{v} < v_+$, and then by (2-35) and (2-36), we have $dv(\xi)/d\xi \rightarrow +\infty$ as $\xi \rightarrow \bar{\xi}$. This is a contradiction due to (2-34) because the solution $v(\xi)$ is smooth, so its derivative cannot tend to $+\infty$ for finite ξ .

If

$$\frac{p_-}{p_+} = 1 + \frac{2\alpha_f}{\alpha(1 + \alpha + \alpha_f)},$$

then $\bar{v} = v_+$, and then (2-36) reduces to

$$\frac{dv}{d\xi} = \frac{\beta}{2\sigma}(v - v_-). \quad (2-37)$$

So $dv/(v - v_-) = (\beta/2\sigma) d\xi$. In this case, (2-31) becomes

$$\int_{v_1}^v \frac{dw}{w - v_-} dw = \frac{\beta}{2\sigma}(\xi - \xi_1). \quad (2-38)$$

This implies that

$$\ln(v - v_-) - \ln(v_1 - v_-) = (\beta/2\sigma)(\xi - \xi_1).$$

Solving this for v , we obtain

$$v(\xi) = v_- + (v_1 - v_-)e^{(\beta/2\sigma)(\xi - \xi_1)}.$$

Hence, $v(\xi) \rightarrow \infty$ as $\xi \rightarrow \infty$. Therefore, it is impossible that $v(+\infty) = v_+$. This is a contradiction. Thus, part (2) of the Theorem is proved by the above argument.

We can prove part (3) as follows. We have already proved that, if

$$\frac{p_-}{p_+} < 1 + \frac{2\alpha_f}{\alpha(1 + \alpha + \alpha_f)},$$

the problem (1-13) and (1-12) has a solution. In this case, $v'(\xi) > 0$ is an easy consequence of the above argument in (i). So $v_- < v(\xi) < v_+$ for $-\infty < \xi < +\infty$. Next, we prove (1-17). We may write (2-26) as, in view of (2-26) and (2-24),

$$\int_{v_0}^v \frac{2f(w)}{(w - v_-)(w - v_+)} dw = -\sigma(1 + \alpha + \alpha_f)\xi. \tag{2-39}$$

It is easy to verify that, by noting that $f(w) = (1 + \alpha/2)(\sigma m + P) - \sigma^2(1 + \alpha)w$ (see (1-14)),

$$\frac{2f(w)}{(w - v_-)(w - v_+)} = \frac{-2f(v_-)}{(w - v_-)} \frac{1}{(v_+ - v_-)} + \frac{2f(v_+)}{(w - v_+)} \frac{1}{(v_+ - v_-)}. \tag{2-40}$$

Equation (1-17) then follows from (2-39) and (2-40). From (1-17), we can easily get the bounds for $v_+ - v(\xi)$ in (1-20). Similarly, we can get the bounds for $v(\xi) - v_-$ in (1-21). By (1-17), we have

$$\left(\frac{2f(v_+)}{v_+ - v} + \frac{2f(v_-)}{v - v_-} \right) v'(\xi) = -\sigma(1 + \alpha + \alpha_f)(v_+ - v_-).$$

Therefore, the bounds for $v'(\xi)$ in (1-20) and (1-21) can be derived from the bounds of $v_+ - v(\xi)$ and $v(\xi) - v_-$ which we have just proved. This finishes the proof of the Theorem. □

Acknowledgement

This work was done under the supervision of Professor Tao Luo. The author would like to thank the referee for the suggestions which have helped to improve the presentation of the paper greatly.

References

[Courant and Friedrichs 1948] R. Courant and K. O. Friedrichs, *Supersonic flow and shock waves*, Pure and Applied Mathematics **1**, Interscience, New York, 1948. MR 10,637c Zbl 0041.11302

[Whitham 1974] G. B. Whitham, *Linear and nonlinear waves*, Pure and Applied Mathematics **42**, Wiley, New York, 1974. MR 58 #3905 Zbl 0373.76001

[Yong and Zumbrun 2000] W.-A. Yong and K. Zumbrun, "Existence of relaxation shock profiles for hyperbolic conservation laws", *SIAM J. Appl. Math.* **60**:5 (2000), 1565–1575. MR 2001b:35208 Zbl 0959.35116

Received: 2012-05-24 Revised: 2012-10-05 Accepted: 2012-10-10

xwang1994@gmail.com

*Sidwell Friends Upper School, 3825 Wisconsin Avenue,
Washington, DC 20016, United States*

Expected conflicts in pairs of rooted binary trees

Timothy Chu and Sean Cleary

(Communicated by Robert W. Robinson)

Rotation distance between rooted binary trees measures the extent of similarity of two trees with ordered leaves. There are no known polynomial-time algorithms for computing rotation distance. If there are common edges or immediately changeable edges between a pair of trees, the rotation distance problem breaks into smaller subproblems. The number of crossings or conflicts of a tree pair also gives some measure of the extent of similarity of two trees. Here we describe the distribution of common edges and immediately changeable edges between randomly selected pairs of trees via computer experiments, and examine the distribution of the amount of conflicts between such pairs.

1. Introduction

Binary trees are used in a broad spectrum of computational and mathematical applications. Binary search trees, for example, are widely used in databases and can be used to ensure efficient searches. The shape of a binary search tree is important in guaranteeing this efficiency—a balanced binary tree guarantees worst-case search time on the order of $\log(n)$, whereas a tree with a stringy shape will have worst-case search time on the order of n , where n is the number of nodes in the tree, or equivalently, items to be stored. Because of such applications, there has been a great deal of interest in operations which preserve the left-to-right order of the leaves of a tree while adjusting the shape of the tree. See [Knuth 1973] for background and numerous algorithms related to tree shape and balance. One widely studied approach to adjust tree shape uses rotations in binary trees where there is a left-to-right order on the leaves. A rotation is a single move at a particular node which promotes one of the grandchild nodes to a child node, switches another grandchild to have a different parent, and demotes a child node to a grandchild node, while preserving the order. Such an operation is pictured in Figure 1.

MSC2010: 05C05, 68P05.

Keywords: random binary tree pairs.

The authors gratefully acknowledge support from the National Science Foundation under grant 0811002.

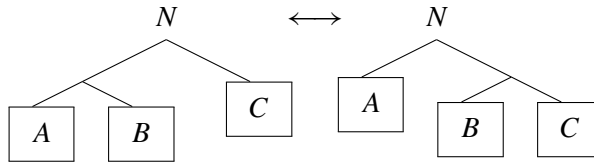


Figure 1. Rotation at a node N . Right rotation at N transforms the left tree to the right one, and left rotation at N is the inverse operation which transforms the right tree to the left one. A , B , and C represent leaves or subtrees, and the node N could be at the root or any other position in the tree.

Any shape tree of size n nodes can be converted to any other tree of the same size via a sequence of rotations, as described in [Culik and Wood 1982]. The minimum length of possible sequences of rotations converting a tree S with n nodes to a tree T with n nodes is the *rotation distance* between S and T . Though there are some properties of rotation distance that are well understood, there is no known effective algorithm for computing rotation distance. Sleator, Tarjan and Thurston [STT 1988] showed that the distance is never more than $2n - 6$, and furthermore that for very large n that bound is achieved.

Here, we investigate some measures of tree similarity which are related to rotation distance. When there are common edges, described below, this reduces rotation distance and allows breaking of the problem into smaller parts. When there are one-off edges, described below, there is an immediate essential possible first move which then results in a common edge, again allowing reduction into parts. Another measure of tree similarity is the count of the number of conflicting edge pairs, described below. For each of these quantities, we investigate with a large number of computational experiments how quickly these quantities grow with tree size. In

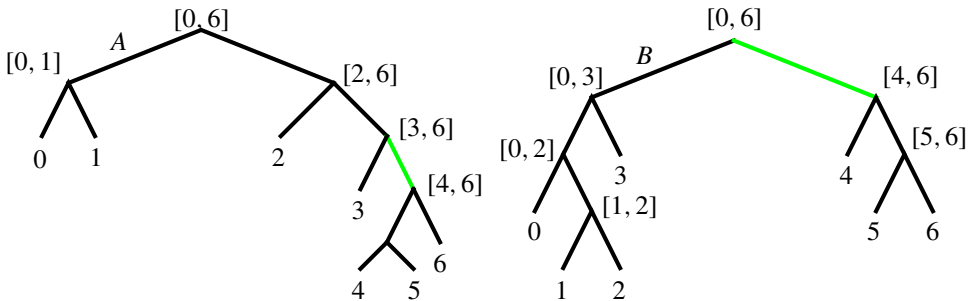


Figure 2. A common edge between a pair of trees. The green edge is common to both trees and separates leaves 4–6 from the other leaves in both trees. The root node interval is always $[0, n]$, and we do not consider that to represent a common edge.

the case of common edges and one-off edges, the growth is linear with tree size and in a manner consistent with the asymptotic behavior understood combinatorially. In the case of conflicting edges, we see growth which appears to lie between linear and quadratic.

By *binary tree of size n* , we mean a rooted binary tree with n leaves arranged in a left-to-right order, with leaves numbered from 0 to $n - 1$. To each edge, we associate an interval $[i, j]$, where i is the leftmost leaf in the subtree attached to that edge's lower side, and similarly j is the rightmost such leaf. A pair of trees (S, T) has a *common edge* if an edge $[i, j]$ is present in both trees, as illustrated in Figure 2. An edge $[i, j]$ in S is a *one-off edge* with respect to T if it is itself not a common edge of S with respect to T , but there is a single rotation in S which changes $[i, j]$ to a new edge which is now in common with T .

An edge $[i, j]$ is *in conflict* with an edge $[l, m]$ if it is not possible for both edges to exist simultaneously in the same tree. We can readily detect edge conflicts by noting that each edge partitions the set of leaves into two sets, obtained by considering connected components of the forest obtained by deleting that edge. If the partitions of leaves are incompatible, the edges had a conflict. For example, in a tree with six leaves, an edge with interval label $[2, 5]$ conflicts with an edge $[0, 3]$. The edge $[2, 5]$ partitions the leaves into two sets: $\{0, 1\}$ and $\{2, 3, 4, 5\}$ and the

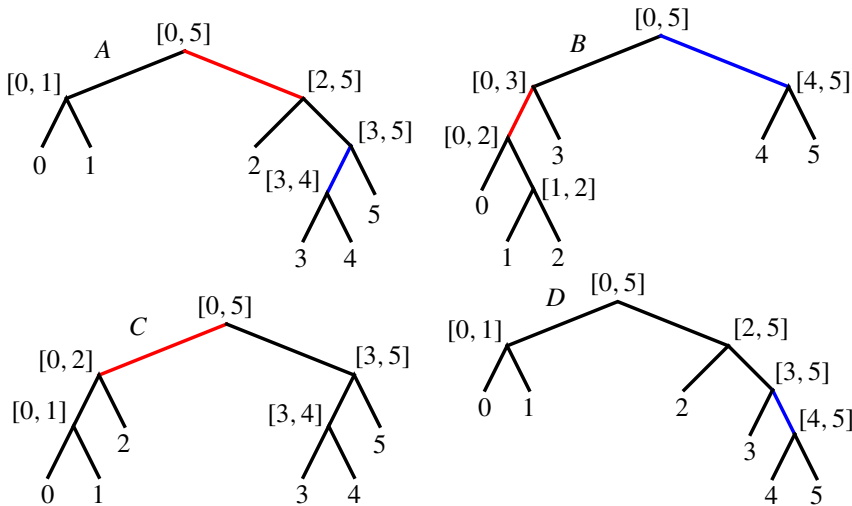


Figure 3. The tree pair (A, B) has two one-off edges in A , marked in red and blue. The tree pair (A, B) has no edges in common, but left rotation at the root of A gives tree C , which has the red edge $[0, 2]$ in common with B . Similarly, right rotation at the node marked $[3, 5]$ in A gives tree D which has the blue edge $[4, 5]$ in common with B .

edge $[0, 3]$ partitions the leaves into two sets: $\{0, 1, 2, 3\}$ and $\{4, 5\}$. There is no overall partition compatible with both such partitions, so that edge pair is in conflict, as it would not be possible for those two edges to be present in the same tree simultaneously. An example illustrating this particular edge pair in conflict is given as trees A and B in Figure 3. Using the bijection between trees and triangulations of regular polygons, described in [STT 1988], each conflict can be counted as an intersection between edges of superimposed triangulations.

Since the number of trees of size n is the n -th Catalan number C_n , and C_n grows exponentially on the order of $4^n n^{-3/2}$, the number of pairs of trees of size n grows on the order of $16^n n^{-3}$. Thus, computing these quantities exhaustively is not possible except for very small n . Instead, we use sampling techniques, experimenting computationally by repeatedly choosing pairs of trees of size n uniformly at random and computing and tabulating the results.

2. Conflicts and one-off edges

As described in [Cleary and St. John 2010], common edges permit the subdivision of the rotation distance problem into smaller pieces. From [STT 1988], one-off edges can be moved immediately to find a geodesic, and the resulting common edge will then subdivide the problem as well.

The existence of common edges of a particular peripheral type was investigated by Cleary, Elder, Rechnitzer and Taback, who showed in [CERT 2010], in connection with using tree-pair diagrams to represent elements of Thompson's group F , that a randomly selected tree pair has at least one common peripheral edge. The number of such common edges with respect to trees generated randomly by the Yule process was investigated experimentally by Cleary, Passaro and Toruno [CPT 2013].

To understand the typical behavior of common edges, one-off edges, and conflicts between tree pairs, we performed a range of computational experiments to investigate. In each case, we generated tree pairs of a particular size randomly using Rémy's bijection [Rémy 1985], which allows efficient generation of trees of size n uniformly at random through an iterative process. After generating two trees randomly, we collected the relevant information about common edges, one-off edges, and conflicts and then iterated to collect large-sample data. As anticipated, the various measures of complexity grew with tree size. We present summaries of those experiments below.

We considered approximately 10 million tree pairs total of sizes ranging from 10 to 12,000. The bulk of the computational effort lay for trees of size 20 to 800. These results are presented in Tables 1–3.

The number of common edges grows linearly with size as shown in Figure 4, and the line of best fit for the data is an excellent match with the asymptotic exact

Tree size range	Average common edge fraction	σ edge fraction
≤ 40	0.1361	0.09462
41–80	0.1052	0.04494
81–120	0.1004	0.03422
121–200	0.09720	0.02613
201–400	0.09534	0.01945
401–1000	0.09409	0.01358
1001–12000	0.09310	0.004324

Table 1. Fractions of tree common edges and their standard deviations. The asymptotic fraction is known to be about 0.092958.

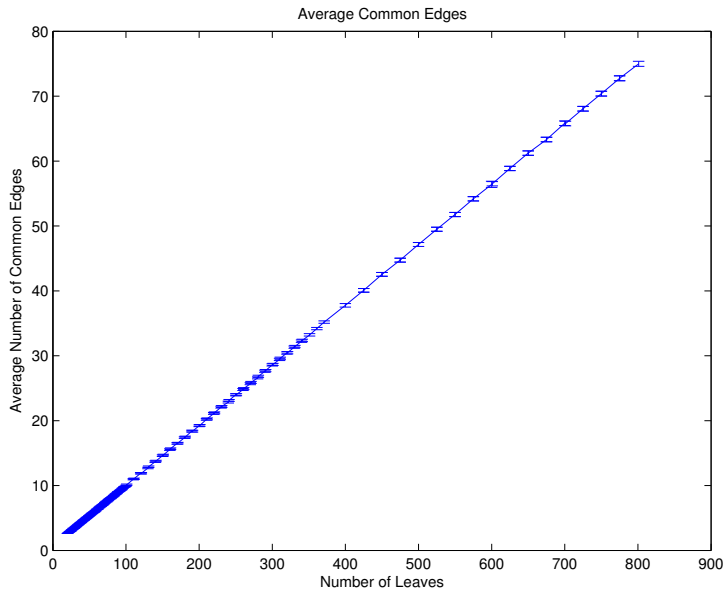


Figure 4. The average number of common edges grows linearly with tree size, with tight error bars from the large sample sizes used over this range. The slope of this line is very close to the expected 0.093 from the asymptotic analysis.

growth proven by Cleary, Rechnitzer and Wong in [CRW 2013].

The number of one-off edges grows linearly with size as shown in Figure 5, and the line of best fit for the data shows very close agreement with the number of common edges. This experimental, numerical observation led to renewed efforts using asymptotic combinatorial methods, and that equivalence is now proven asymptotically in [CRW 2013] by a delicate analysis of some of the relevant generating functions. We note that though the means are asymptotically the same,

Tree size range	Average one-off fraction	σ one-off fraction
≤ 40	0.1362	0.04890
41–80	0.1053	0.02591
81–120	0.1004	0.01986
121–200	0.09725	0.01516
201–400	0.09536	0.01129
401–1000	0.09408	0.007932
1001–12000	0.09307	0.002619

Table 2. Fractions of tree one-off edges and their standard deviations. The asymptotic fraction is known to be about 0.092958.

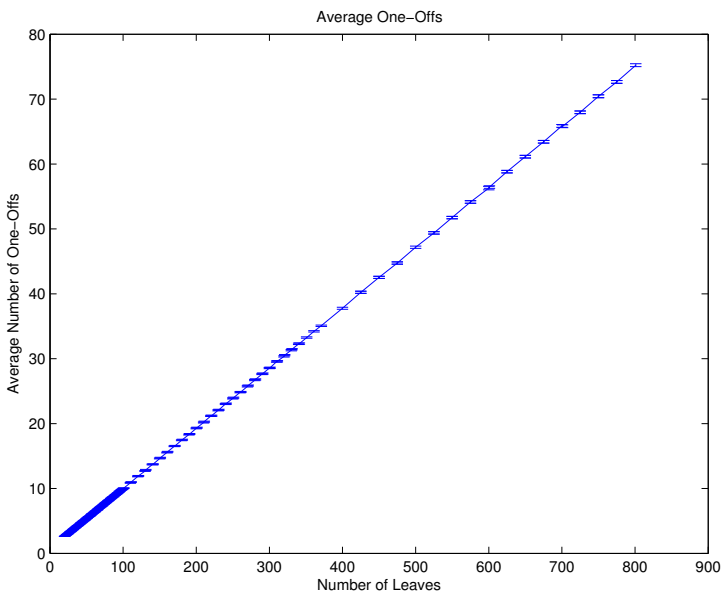


Figure 5. The average number of one-off edges grows linearly with tree size, again with tight error bars from the large sample sizes used over this range and this quantity is very close to the average number of common edges of similarly sized tree pairs. The slope of this line is very close to the expected 0.093 from the asymptotic analysis.

the distributions appear to be significantly different. The standard deviation for the number of one-offs generally has a standard deviation of a little more than half that of the number of common edges. The combinatorial analysis of [CRW 2013] only applies to the means — it appears that the distributions are genuinely different.

Tree size range	Average conflicts per edge	σ conflicts per edge
≤ 40	3.2418	0.9985
41–80	5.837	1.320
*81–120	6.968	1.409
121–200	8.321	1.533
201–400	9.768	1.628
*401–1000	11.71	1.792
*1001–12000	17.45	1.887

Table 3. Average number of conflicts per edge and their standard deviations.

The asymptotic analysis of [CRW 2013] shows that for large n , the expected number of common edges is

$$\frac{16 - 5\pi}{\pi}n + \frac{7\pi - 20}{\pi} + O\left(\frac{\log n}{n}\right),$$

which is approximately

$$0.092958n + 0.633802 + O\left(\frac{\log n}{n}\right).$$

For the average number of common edges in a tree of size n , this experimental data yields a best linear fit of $0.092950n + 0.643$, and similarly for the average number of one-off edges, the experimental data yields a best linear fit of $0.092867n + 0.711$.

We now turn to the number of conflicts between randomly selected pairs of trees, shown in Figure 6. It is apparent from this data that the typical number of conflicts per edge grows quite slowly. Even in trees of size multiple thousands, where in theory an edge could cross hundreds of other edges, typically the mean number of conflicts per edge is quite small, for example about 17. This illustrates that a tree of size n selected uniformly at random tends to be rather “stringy” rather than balanced (see [Knuth 1969]), and a pair of such stringy trees is not likely to have edges that conflict with large swaths of the other trees. Though it is possible to construct tree pairs of increasing size whose number of conflicts grows quadratically, these constructions do not represent typical behavior of randomly selected tree pairs.

This data shows that the average number of conflicts grows more than linearly with n , but subquadratically. The maximum possible number of conflicts is bounded above by a quadratic function — each edge could conflict with at most $n - 1$ other edges, giving a crude upper bound of $n^2 - n$. Since each unmatched edge gives at least one conflict, the average number of conflicts thus is growing somewhere between linearly and quadratically. It is difficult to ascertain the exact growth of the mean number of conflicts. Using the data set over the range from 5 to 12,000, a log-log analysis, as shown in Figure 7, suggests that the power law of best fit over

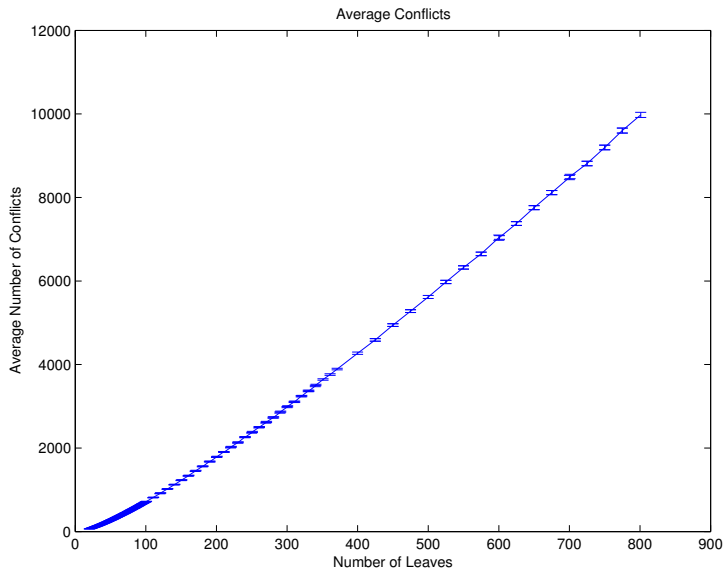


Figure 6. The number of conflicts grows with tree size in a manner which appears to be between linear and quadratic, with a slight upward concavity apparent over this range.

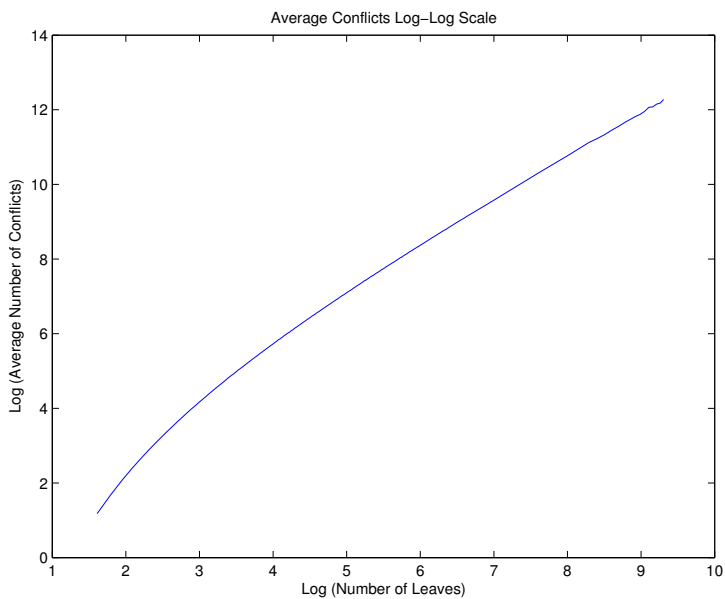


Figure 7. Log-log plot of the average number of conflicts against size. This relationship appears to be slightly concave downward, indicating that the asymptotic behavior is probably a lower-degree power law than the straight-line fit analysis would indicate.

the pictured range is 1.3173. There may also be logarithmic terms present in the growth which are difficult to detect experimentally.

3. Discussion

For common edges and one-off edges, these experiments worked well to establish the behavior for growing tree size. These computational experiments confirm close agreement to the asymptotic behavior of common edges, with relatively quick convergence to the asymptotic limit. Furthermore, if we ignore the smaller tree pairs of size 16 and less, the agreement is even stronger with the asymptotic behavior. These experiments also suggested that the average number of one-off edges was the same as common edges, which in other work has now been proven asymptotically to be the case. Again we saw close agreement with the asymptotic limit and relatively quick convergence.

For conflicts between tree pairs, these experiments gave some indication of the order of growth, with some insight coming from the relatively low overall average conflicts between randomly selected tree pairs. But there was not conclusive enough behavior to establish a likely asymptotic estimate for the growth of the number of conflicts as tree size increases. The possibility of logarithmic terms in the asymptotic terms suggests that it may be difficult to detect the asymptotic behavior more precisely with experimental methods. With fixed computational resources and computation time, investigating larger size trees gives a significant increase in the resulting error bars. Nevertheless, the power-law behavior is apparent from the analysis and we expect the possible logarithmic correction terms, for example, to not be dramatic.

References

- [CERT 2010] S. Cleary, M. Elder, A. Rechnitzer, and J. Taback, "Random subgroups of Thompson's group F ", *Groups Geom. Dyn.* **4**:1 (2010), 91–126. MR 2011e:20062 Zbl 1226.20034
- [Cleary and St. John 2010] S. Cleary and K. St. John, "A linear-time approximation for rotation distance", *J. Graph Algorithms Appl.* **14**:2 (2010), 385–390. MR 2011m:68205 Zbl 1215.68271
- [CPT 2013] S. Cleary, J. Passaro, and Y. Toruno, "Average reductions in Yule-generated binary trees", *Involve* **6**:4 (2013).
- [CRW 2013] S. Cleary, A. Rechnitzer, and T. Wong, "Common edges in rooted trees and polygonal triangulations", *Electron. J. Combin.* **20**:1 (2013), Paper 39. MR 3035049
- [Culik and Wood 1982] K. Culik, II and D. Wood, "A note on some tree similarity measures", *Inform. Process. Lett.* **15**:1 (1982), 39–42. MR 83k:68059 Zbl 0489.68058
- [Knuth 1969] D. E. Knuth, *The art of computer programming, I: Fundamental algorithms*, Second printing, Addison-Wesley, Reading, Massachusetts, 1969. MR 44 #3530 Zbl 0895.68055
- [Knuth 1973] D. E. Knuth, *The art of computer programming, III: Sorting and searching*, Addison-Wesley, Reading, Massachusetts, 1973. MR 56 #4281

[Rémy 1985] J.-L. Rémy, “Un procédé itératif de dénombrement d’arbres binaires et son application à leur génération aléatoire”, *RAIRO Inform. Théor.* **19**:2 (1985), 179–195. MR 87h:68132 Zbl 0565.05037

[STT 1988] D. D. Sleator, R. E. Tarjan, and W. P. Thurston, “Rotation distance, triangulations, and hyperbolic geometry”, *J. Amer. Math. Soc.* **1**:3 (1988), 647–681. MR 90h:68026 Zbl 0653.51017

Received: 2012-06-26 Revised: 2012-10-22 Accepted: 2012-10-23

timchu100@gmail.com

*Department of Computer Science,
The City College of New York, City University of New York,
160 Convent Avenue, New York, NY 10031, United States*

cleary@sci.ccny.cuny.edu

*Department of Mathematics, The City College of New York,
City University of New York, 160 Convent Avenue,
New York, NY 10031, United States
<http://www.sci.ccny.cuny.edu/~cleary>*

Hyperbolic construction of Cantor sets

Zair Ibragimov and John Simanyi

(Communicated by Kenneth S. Berenhaut)

In this paper we present a new construction of the ternary Cantor set within the context of Gromov hyperbolic geometry. Unlike the standard construction, where one proceeds by removing middle-third intervals, our construction uses the collection of the removed intervals. More precisely, we first hyperbolize (in the sense of Gromov) the collection of the removed middle-third open intervals, then we define a visual metric on its boundary at infinity and then we show that the resulting metric space is isometric to the Cantor set.

1. The ternary Cantor set

The ternary Cantor set \mathcal{C} is one of the most familiar fractals in mathematics. Recall its standard construction, which is based on the Euclidean notion of length. Begin with the closed unit interval $C_0 = [0, 1] \subseteq \mathbb{R}$, then remove the open middle-third interval, constructing $C_1 = [0, \frac{1}{3}] \cup [\frac{2}{3}, 1]$. We then remove the middle-third of each resulting closed interval again, finding

$$C_2 = [0, \frac{1}{9}] \cup [\frac{2}{9}, \frac{1}{3}] \cup [\frac{2}{3}, \frac{7}{9}] \cup [\frac{8}{9}, 1].$$

Continuing in this manner, we construct \mathcal{C} by taking the intersection of all C'_k s,

$$\mathcal{C} = \bigcap_{k=1}^{\infty} C_k.$$

Graphically, C_0 through C_6 are shown in Figure 1. The ternary Cantor set has many interesting properties. As the intersection of closed intervals in $(\mathbb{R}, | \cdot |)$, it is compact. It is also perfect (i.e., it contains no isolated points), uncountable and totally disconnected. The complement of the ternary Cantor set in $[0, 1]$, \mathcal{CS} , is called the *Cantor string*. It consists of the countable union of the removed open middle-third intervals. Cantor strings are subjects of study in fractal geometry [Lapidus and van Frankenhuijsen 2006].

MSC2010: primary 30C65; secondary 05C25.

Keywords: Cantor set, Gromov hyperbolic spaces.

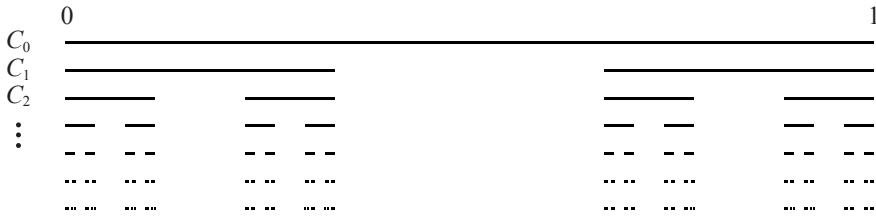


Figure 1. Sets C_0 through C_6 .

2. Hyperbolic construction

We begin with a brief discussion of Gromov hyperbolic spaces. A metric space (X, d) is called *Gromov δ -hyperbolic* (or *δ -hyperbolic*) if there exists a $\delta \geq 0$ such that for all $x, y, z, w \in X$,

$$d(x, y) + d(z, w) \leq \max\{d(x, z) + d(y, w), d(x, w) + d(y, z)\} + 2\delta. \tag{2-1}$$

For $x, y, z \in X$, the *Gromov product* of x and y with respect to z is defined by

$$(x|y)_z = \frac{1}{2}[d(x, z) + d(y, z) - d(x, y)]. \tag{2-2}$$

Alternatively, the space (X, d) is δ -hyperbolic if

$$(x|y)_v \geq \min\{(x|z)_v, (z|y)_v\} - \delta,$$

for all $x, y, z, v \in X$ (see, for example, [Väisälä 2005]). A bounded metric space X is always δ -hyperbolic with $\delta \leq \text{diam } X$, so only unbounded metric spaces may have more interesting characteristics.

To each Gromov hyperbolic space X , we associate a boundary at infinity, ∂X (also called the *Gromov boundary*). Fix a base point $v \in X$. A sequence $\{a_i\}$ in X is said to *converge at infinity* if $(a_i|a_j)_v \rightarrow \infty$ as $i, j \rightarrow \infty$. Two such sequences $\{a_i\}$ and $\{b_i\}$ are *equivalent* if $(a_i|b_i)_v \rightarrow \infty$ as $i \rightarrow \infty$. The boundary at infinity is defined to be the equivalence classes of sequences converging at infinity. The boundary at infinity supports a family of so-called *visual metrics*. A metric d on ∂X is called a visual metric if there exists a $v \in X$, $C \geq 1$ and $\epsilon > 0$ such that for all $x, y \in \partial X$,

$$\frac{1}{C} \rho_{\epsilon, v}(x, y) \leq d(x, y) \leq C \rho_{\epsilon, v}(x, y), \quad \text{where } \rho_{\epsilon, v}(x, y) = e^{-\epsilon(x|y)_v}.$$

Here $(x|y)_v$ is the Gromov product on ∂X , defined by

$$(x|y)_v = \inf\{\liminf_{i \rightarrow \infty} (a_i|b_i)_v : a_i \in x, b_i \in y\}$$

and we set $e^{-\infty} = 0$. The boundary at infinity of any Gromov hyperbolic space endowed with a visual metric is bounded and complete [Bonk and Schramm 2000].

Our goal is to produce the ternary Cantor set within the framework of Gromov hyperbolic spaces. As mentioned above, we do this by hyperbolizing the collection of the removed middle-third intervals. Let X be the collection of all such intervals. Hence, X contains intervals such as $(\frac{1}{3}, \frac{2}{3}), (\frac{1}{9}, \frac{2}{9}), (\frac{7}{9}, \frac{8}{9})$ and so on. Note that

$$\mathcal{C} = [0, 1] \setminus \bigcup_{I \in X} I.$$

We now proceed to construct a metric h on X so that the space (X, h) is Gromov hyperbolic. Let u_H be a distance function defined on the set of all nonempty subsets of $[0, 1]$, defined by

$$u_H(A, B) = \sup\{|x - y| : x \in A \text{ and } y \in B\}.$$

This distance function is called the *upper Hausdorff* distance (see, for instance, [Hausdorff 1957; Ibragimov 2011a]). If $I, J \in X$ with $I = (a, b), J = (c, d)$ and $b < c$, then $u_H = |a - d|$. Note also that for each $I, J \in X$, we have

$$u_H(I, J) \geq l(I) \vee l(J) \geq \sqrt{l(I) \cdot l(J)}, \tag{2-3}$$

where the first equality holds only if $I = J$ and the second equality holds only if $l(I) = l(J)$. Here, and in what follows, $l(I)$ denotes the Euclidean length of $I \in X$ and $a \vee b = \max\{a, b\}$ for positive numbers $a, b \in \mathbb{R}$.

Observe that since X consists of a disjoint collection of open intervals, it has a natural order \preceq induced by the usual order \leq on \mathbb{R} . Namely, we say that $I \preceq J$ if I is to the left of J or if $I = J$. Observe also that if $I \preceq J \preceq K$, then

$$u_H(I, K) \geq u_H(I, J). \tag{2-4}$$

Now we define a distance function h on X . Given $I, J \in X$, let

$$h(I, J) = 2 \log \frac{u_H(I, J)}{\sqrt{l(I) \cdot l(J)}}.$$

It is an immediate consequence of (2-3) that h is nonnegative, symmetric and $h(I, J) = 0$ if and only if $I = J$. To show that h also satisfies the triangle inequality, let I, J and K be arbitrary elements of X . Then the triangle inequality $h(I, J) \leq h(I, K) + h(K, J)$ is equivalent to

$$\begin{aligned} 2 \log \frac{u_H(I, J)}{\sqrt{l(I) \cdot l(J)}} &\leq 2 \log \frac{u_H(I, K)}{\sqrt{l(I) \cdot l(K)}} + 2 \log \frac{u_H(K, J)}{\sqrt{l(K) \cdot l(J)}} \\ &= 2 \log \frac{u_H(I, K) \cdot u_H(K, J)}{l(K) \sqrt{l(I) \cdot l(J)}}. \end{aligned}$$

This is true if and only if

$$l(K) \cdot u_H(I, J) \leq u_H(I, K) \cdot u_H(K, J). \tag{2-5}$$

It is also a consequence of (2-3) and (2-4) that inequality (2-5) holds if either $K \preceq I$ and $K \preceq J$ or $I \preceq K$ and $J \preceq K$. Therefore, due to symmetry, it is enough to verify the validity of (2-5) when $I \preceq K \preceq J$. In this case, since

$$u_H(I, J) = u_H(I, K) + u_H(J, K) - l(K),$$

inequality (2-5) is equivalent to $(u_H(I, K) - l(K))(u_H(J, K) - l(K)) \geq 0$, whose validity follows from (2-3). Thus, h is a metric on X .

Next, we will show that h satisfies the Gromov hyperbolicity condition (2-1) with $\delta = \log 2$. We will need the following lemma.

Lemma 2.6. For all $I, J, K, L \in X$, we have

$$u_H(I, J) \cdot u_H(K, L) \leq u_H(I, K) \cdot u_H(J, L) + u_H(I, L) \cdot u_H(J, K).$$

Proof. Without loss of generality we can assume that $I \preceq J \preceq K \preceq L$. Then inequality (2-4) implies that

$$u_H(I, K) \cdot u_H(J, L) \geq u_H(I, J) \cdot u_H(K, L).$$

It also implies that

$$(u_H(I, K) - u_H(J, K))(u_H(J, L) - u_H(J, K)) \geq 0,$$

which is equivalent to

$$u_H(I, K) \cdot u_H(J, L) \geq u_H(J, K)((u_H(I, K) + u_H(J, L) - u_H(J, K))).$$

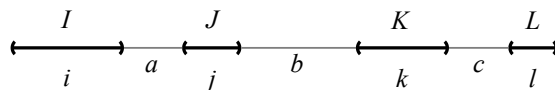
Since $u_H(I, L) = u_H(I, K) + u_H(J, L) - u_H(J, K)$, we obtain that

$$u_H(I, K) \cdot u_H(J, L) \geq u_H(J, K) \cdot u_H(I, L).$$

Therefore, to prove the lemma it is enough to show that

$$u_H(I, K) \cdot u_H(J, L) \leq u_H(I, L) \cdot u_H(J, K) + u_H(I, K) \cdot u_H(J, L).$$

Let i, j, k, l denote the lengths of I, J, K, L and let a, b, c denote the distances between I and J, J and K, K and L , respectively:



Then

$$\begin{aligned}
 u_H(I, K) \cdot u_H(J, L) &= (i+a+j+b+k)(j+b+k+c+l) \\
 &= (i+a+j+b+k)(j+b+k) + (i+a+j+b+k)(c+l) \\
 &= (i+a+j+b+k)(j+b+k) + (c+l)(j+b+k) + (i+a)(c+l) \\
 &< (i+a+k+b+j+c+l)(j+b+k) + (i+a+j)(k+c+l) \\
 &= u_H(I, L) \cdot u_H(J, K) + u_H(I, J) \cdot u_H(K, L),
 \end{aligned}$$

completing the proof. □

Theorem 2.7. The metric space (X, h) is Gromov δ -hyperbolic with $\delta \leq \log 2$.

Proof. Let $I, J, K, L \in X$ be arbitrary. Lemma 2.6 implies that

$$u_H(I, J) \cdot u_H(K, L) \leq 2[u_H(I, K) \cdot u_H(J, L) \vee u_H(I, L) \cdot u_H(J, K)].$$

Hence

$$\begin{aligned}
 h(I, J) + h(K, L) &= 2 \log \frac{u_H(I, J)}{\sqrt{l(I) \cdot l(J)}} + 2 \log \frac{u_H(K, L)}{\sqrt{l(K) \cdot l(L)}} \\
 &= 2 \log \frac{u_H(I, J) \cdot u_H(K, L)}{\sqrt{l(I) \cdot l(J) \cdot l(K) \cdot l(L)}} \\
 &\leq 2 \log \frac{2([u_H(I, K) \cdot u_H(J, L)] \vee [u_H(I, L) \cdot u_H(J, K)])}{\sqrt{l(I) \cdot l(J) \cdot l(K) \cdot l(L)}} \\
 &= [h(I, K) + h(J, L)] \vee [h(I, L) + h(J, K)] + 2 \log 2,
 \end{aligned}$$

as required. □

3. The boundary at infinity

We now discuss the boundary at infinity ∂X of the Gromov hyperbolic space (X, h) . Our goal is to construct a visual metric d on ∂X so that the space $(\partial X, d)$ is isometric to the Cantor set \mathcal{C} equipped with the standard Euclidean metric of the real line. Denote the distance between real numbers x and y by $|x - y|$. Recall that ∂X is the collection of equivalence classes of sequences in X converging at infinity. Fix $V = (\frac{1}{3}, \frac{2}{3}) \in X$ to be the base point. Observe that if the sequence $\{I_n\}$ converges at infinity, then $\lim_{j,k \rightarrow \infty} (I_j | I_k)_V = \infty$.

Lemma 3.1. Given $a \in \partial X$, there exists unique $x_a \in \mathcal{C}$ with the property that

$$\lim_{n \rightarrow \infty} u_H(I_n, \{x_a\}) = 0 \quad \text{for each } I_n \in a.$$

Conversely, for each $x \in \mathcal{C}$ there exists $a \in \partial X$ such that

$$\lim_{n \rightarrow \infty} u_H(J_n, \{x\}) = 0 \quad \text{for each } J_n \in a.$$

Proof. Given $\{I_n\} \in a$, we have

$$\begin{aligned} (I_j|I_k)_V &= \frac{1}{2}(h(I_j, V) + h(I_k, V) - h(I_j, I_k)) = \log \frac{u_H(I_j, V) \cdot u_H(I_k, V)}{l(V) \cdot u_H(I_j, I_k)} \\ &\leq \log \frac{\frac{2}{3} \cdot \frac{2}{3}}{\frac{1}{3} \cdot u_H(I_j, I_k)} = \log \frac{\frac{4}{3}}{u_H(I_j, I_k)}. \end{aligned}$$

Since $\lim_{j,k \rightarrow \infty} (I_j|I_k)_V = \infty$, we obtain $\lim_{j,k \rightarrow \infty} u_H(I_j, I_k) = 0$. For each n choose some point $x_n \in I_n$.

Next, given $\epsilon > 0$, we can find $n_0 \in \mathbb{N}$ such that

$$|x_j - x_k| \leq u_H(I_j, I_k) < \epsilon \quad \text{whenever } j, k \geq n_0.$$

Hence the sequence $\{x_n\}$ is a Cauchy sequence in $[0, 1]$. Since $[0, 1]$ is complete, it converges to some point in $[0, 1]$, call it x_a . Now if we choose a different sequence $\{y_n\}$, where $y_n \in I_n$, then

$$|y_n - x_a| \leq |y_n - x_n| + |x_n - x_a| \leq u_H(I_n, I_n) + |x_n - x_a|,$$

which implies that $\{y_n\}$ also converges to x_a . Therefore, the point x_a is well defined. Finally, since

$$u_H(I_n, \{x_a\}) \leq u_H(I_n, \{x_n\}) + u_H(\{x_n\}, \{x_a\}) \leq u_H(I_n, I_n) + |x_n - x_a|,$$

we obtain that $\lim_{n \rightarrow \infty} u_H(I_n, \{x_a\}) = 0$, as required.

Now let $\{K_n\}$ be another sequence converging at infinity and equivalent to $\{I_n\}$, i.e., $\{K_n\} \in a$. Then we need to show that $\lim_{n \rightarrow \infty} u_H(K_n, \{x_a\}) = 0$. Recall that the equivalence of the two sequences $\{I_n\}$ and $\{K_n\}$ means that $\lim_{n \rightarrow \infty} (I_n|K_n)_V = \infty$. The latter implies, by the same argument as above, that $\lim_{n \rightarrow \infty} u_H(I_n, K_n) = 0$. Since

$$u_H(K_n, \{x_a\}) \leq u_H(K_n, I_n) + u_H(I_n, \{x_a\}),$$

we obtain that $\lim_{n \rightarrow \infty} u_H(K_n, \{x_a\}) = 0$. Thus, we have shown the existence and uniqueness of x_a .

It remains to show that $x_a \in \mathcal{C}$. Assume by contrary that $x \in [0, 1] \setminus \mathcal{C}$. Then $x_a \in I$ for some $I \in X$. Since

$$0 < \frac{l(I)}{2} \leq u_H(I_n, \{x_a\}) \quad \text{and} \quad \lim_{n \rightarrow \infty} u_H(I_n, \{x_a\}) = 0,$$

we obtain the required contradiction. Thus, $x_a \in \mathcal{C}$, completing the proof of the first part.

To prove the second part, we first show that there exists a sequence $\{J_n\}$ in X converging at infinity and such that $\lim_{n \rightarrow \infty} u_H(J_n, \{x\}) = 0$. To construct such a sequence, index X as follows: let $J_{i,j} \in X$, where 3^{-i} is the length of the interval $J_{i,j}$ and j represents each interval in X of length 3^{-i} . Here

$$i = 1, 2, 3, \dots \quad \text{and} \quad j = 1, 2, \dots, 2^{i-1}.$$

Note that $J_{1,1} = V$ and that $u_H(\{x\}, J_{1,1}) \leq 2/3$ while $l(J_{1,1}) = 1/3$. We can then find J_{2,j_2} such that $u_H(\{x\}, J_{2,j_2}) \leq \frac{2}{9}$ and $l(J_{2,j_2}) = \frac{1}{9}$. Continuing in this manner, for each $n \in \mathbb{N}$, there exists j_n such that

$$u_H(\{x\}, J_{n,j_n}) \leq \frac{2}{3^n} \quad \text{and} \quad l(J_{n,j_n}) = 3^{-n}.$$

Put $J_n = J_{n,j_n}$. Then $\lim_{n \rightarrow \infty} u_H(J_n, \{x\}) = 0$, as required. Observe that since $u_H(J_j, J_k) \leq u_H(J_j, \{x\}) + u_H(J_k, \{x\})$, we have $\lim_{j,k \rightarrow \infty} u_H(J_j, J_k) = 0$. Also, since

$$(J_j|J_k)_V = \log \frac{u_H(J_j, V) \cdot u_H(J_k, V)}{l(V) \cdot u_H(J_j, J_k)}$$

and $u_H(J_j, V) \cdot u_H(J_k, V) \leq \frac{4}{9}$, we obtain that the sequence $\{J_n\}$ converges at infinity.

Finally, we let $a \in \partial X$ to be the equivalence class of sequences converging at infinity and equivalent to $\{J_n\}$. Then it follows from the first part that

$$\lim_{n \rightarrow \infty} u_H(J_n, \{x\}) = 0 \quad \text{for each } J_n \in a,$$

completing the proof of the lemma. □

Lemma 3.1 implies that the map $f: \partial X \rightarrow \mathcal{C}$, given by $f(a) = x_a$, is a well defined, bijective map. Now we define a metric d on ∂X by setting $d(a, b) = |x_a - x_b|$.

Lemma 3.2. The metric d is a visual metric. More precisely,

$$\frac{1}{3}e^{-(a|b)_V} \leq d(a, b) \leq 3e^{-(a|b)_V} \quad \text{for all } a, b \in \partial X.$$

Proof. Recall that $V = (\frac{1}{3}, \frac{2}{3})$ and

$$(a|b)_V = \inf \{ \liminf_{n \rightarrow \infty} (I_n|J_n)_V : I_n \in a, J_n \in b \}.$$

Given $a, b \in \partial X$, let $I_n \in a$ and $J_n \in b$ be arbitrary sequences. Then

$$(I_n|J_n)_V = \log \frac{u_H(I_n, V) \cdot u_H(I_n, V)}{l(V) \cdot u_H(I_n, J_n)}.$$

Lemma 3.1 implies that

$$\lim_{n \rightarrow \infty} u_H(I_n, \{x_a\}) = 0 \quad \text{and} \quad \lim_{n \rightarrow \infty} u_H(J_n, \{x_b\}) = 0.$$

In particular, since

$$|u_H(I_n, J_n) - |x_a - x_b|| \leq u_H(I_n, \{x_a\}) + u_H(J_n, \{x_b\}),$$

we have

$$\lim_{n \rightarrow \infty} u_H(I_n, J_n) = |x_a - x_b| = d(a, b).$$

Also, since

$$|u_H(V, I_n) - u_H(V, \{x_a\})| \leq u_H(I_n, \{x_a\}),$$

we have

$$\lim_{n \rightarrow \infty} u_H(V, I_n) = u_H(V, \{x_a\}) \quad \text{and} \quad \lim_{n \rightarrow \infty} u_H(V, J_n) = u_H(V, \{x_b\}).$$

Therefore, as the sequences $\{I_n\} \in a$ and $\{J_n\} \in b$ were arbitrary, we obtain

$$(a|b)_V = \log \frac{u_H(V, \{x_a\}) \cdot u_H(V, \{x_b\})}{l(V) \cdot d(a, b)}.$$

Finally, since $l(V) = \frac{1}{3}$ and since $\frac{1}{3} \leq u_H(V, \{x\}) \leq \frac{2}{3}$ for all $x \in [0, 1]$, we have

$$\frac{1}{3}d(a, b) \leq \frac{3}{4}d(a, b) = \frac{\frac{1}{3}}{\frac{2}{3} \cdot \frac{2}{3}}d(a, b) \leq e^{-(a|b)_V} \leq \frac{1}{\frac{1}{3} \cdot \frac{1}{3}}d(a, b) = 3d(a, b).$$

Equivalently,

$$\frac{1}{3}e^{-(a|b)_V} \leq d(a, b) \leq 3e^{-(a|b)_V},$$

completing the proof. □

As an immediate consequence of Lemma 3.2 we obtain our main result.

Theorem 3.1. The spaces $(\partial X, d)$ and $(\mathcal{C}, | - |)$ are isometric.

4. Further remarks

Although this particular geometric approach was successful, there is no guarantee that *any* such construction will produce the desired results. Consider, for example, the following seemingly natural distance function \hat{h} , defined for any $I, J \in X$ by

$$\hat{h}(I, J) = 2 \log \frac{l(I \cup J)}{\sqrt{l(I) \cdot l(J)}}.$$

Since the distinct intervals in X are disjoint, $l(I \cup J) = l(I) + l(J)$ whenever $I \neq J$, from which it follows that $\hat{h}(I, J) \leq \hat{h}(I, K) + \hat{h}(K, J)$, for all $I, J, K \in X$. Hence the space (X, \hat{h}) is a metric space. In fact, it is Gromov hyperbolic. Indeed, by setting $\mu(I, J) = l(I \cup J)$, we find that $\mu(I, I) > 0$, $\mu(I, J) = \mu(J, I)$

and $\mu(I, J) \leq \mu(I, K) + \mu(K, J)$, for all $I, J, K \in X$. By [Ibragimov 2011a, Lemma 3.7], we have

$$\mu(I, J) \cdot \mu(K, L) \leq 4[(\mu(I, K) \cdot \mu(J, L)) \vee (\mu(I, L) \cdot \mu(J, K))],$$

for all $I, J, K, L \in X$. Hence the space (X, \hat{h}) is δ -hyperbolic with $\delta \leq \log 4$ (see, for example, the proof of [Ibragimov 2011b, Theorem 2.1(2)]).

Next, we investigate the boundary at infinity of (X, \hat{h}) . Observe that

$$m(I, J) \leq \hat{h}(I, J) \leq m(I, J) + \log 4 \quad \text{for all } I, J \in X,$$

where

$$m(I, J) = \log \frac{\max\{l(I), l(J)\}}{\min\{l(I), l(J)\}}.$$

Fix $V = (\frac{1}{3}, \frac{2}{3}) \in X$ to be the base point. Then we have the following estimates for the Gromov products in (X, \hat{h}) with respect to V :

$$(I|J)_V = \frac{1}{2}[\hat{h}(I, V) + \hat{h}(J, V) - \hat{h}(I, J)] \leq \frac{1}{2}[m(I, V) + m(J, V) - m(I, J)] + \log 4,$$

for all $I, J \in X$ and, similarly

$$(I|J)_V = \frac{1}{2}[\hat{h}(I, V) + \hat{h}(J, V) - \hat{h}(I, J)] \geq \frac{1}{2}[m(I, V) + m(J, V) - m(I, J)] - \log 2.$$

Since

$$\frac{1}{2}[m(I, V) + m(J, V) - m(I, J)] = \log \frac{1}{l(I) \vee l(J)} - \log 3,$$

we find

$$\log \frac{1}{l(I) \vee l(J)} - \log 6 \leq (I|J)_V \leq \log \frac{1}{l(I) \vee l(J)} + \log \frac{4}{3}.$$

Hence a sequence $\{I_n\}$ in (X, \hat{h}) converges at infinity if and only if

$$\max\{l(I_n), l(I_k)\} \rightarrow 0 \quad \text{as } n, k \rightarrow \infty.$$

But all such sequences are equivalent and, consequently, we obtain that the boundary at infinity of (X, \hat{h}) consists of a single point.

We would like to also point out that this geometric construction differs from a topological approach. Topologically, the Cantor set can be viewed as the end space of the infinite binary tree, known as the Cantor tree (Figure 2), when the latter is endowed with a path metric. The end space of such a tree is the collection of all possible infinite branches emanating from its root, and is an ultrametric space when equipped with a visual metric (see [Hughes 2004] for details). As the end space is an ultrametric space, it can not be isometric to the Cantor set, although it is homeomorphic to it.

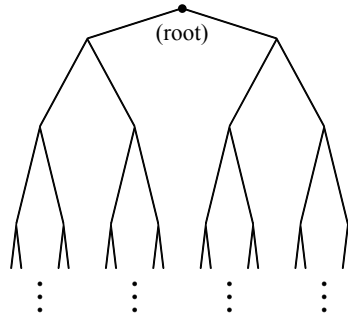


Figure 2. The Cantor tree.

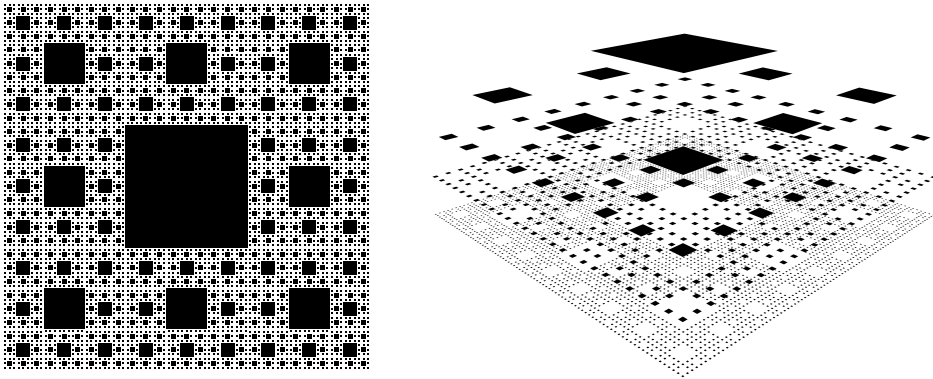


Figure 3. The standard Sierpiński carpet and some of its removed squares.

Finally, although we will not pursue it in this paper, many other fractals, such as Sierpiński carpets, can also be isometrically identified with the boundary at infinity of a similarly hyperbolized collection of removed squares (Figure 3).

References

- [Bonk and Schramm 2000] M. Bonk and O. Schramm, “Embeddings of Gromov hyperbolic spaces”, *Geom. Funct. Anal.* **10**:2 (2000), 266–306. MR 2001g:53077 Zbl 0972.53021
- [Hausdorff 1957] F. Hausdorff, *Set theory*, Chelsea, New York, 1957. MR 19,111a Zbl 0081.04601
- [Hughes 2004] B. Hughes, “Trees and ultrametric spaces: A categorical equivalence”, *Adv. Math.* **189**:1 (2004), 148–191. MR 2005m:57001 Zbl 1061.57021
- [Ibragimov 2011a] Z. Ibragimov, “Hyperbolizing hyperspaces”, *Michigan Math. J.* **60**:1 (2011), 215–239. MR 2012g:53063 Zbl 1220.30075
- [Ibragimov 2011b] Z. Ibragimov, “Hyperbolizing metric spaces”, *Proc. Amer. Math. Soc.* **139**:12 (2011), 4401–4407. MR 2012f:30084 Zbl 1244.30066

[Lapidus and van Frankenhuijsen 2006] M. L. Lapidus and M. van Frankenhuijsen, *Fractal geometry, complex dimensions and zeta functions: Geometry and spectra of fractal strings*, Springer, New York, 2006. MR 2007j:11001 Zbl 1119.28005

[Väisälä 2005] J. Väisälä, “Gromov hyperbolic spaces”, *Expo. Math.* **23**:3 (2005), 187–231. MR 2006j:53055 Zbl 1087.53039

Received: 2012-07-06 Revised: 2012-12-21 Accepted: 2013-01-06

zibragimov@fullerton.edu *Department of Mathematics, California State University,
Fullerton, McCarthy Hall 154, Fullerton, CA 92831, United States*

jsimanyi@csu.fullerton.edu *Department of Mathematics, California State University,
Fullerton, McCarthy Hall 154, Fullerton, CA 92831, United States*

Extensions of the Euler–Satake characteristic for nonorientable 3-orbifolds and indistinguishable examples

Ryan Carroll and Christopher Seaton

(Communicated by Colin Adams)

We compute the \mathbb{F}_l -Euler–Satake characteristics of an arbitrary closed, effective 3-dimensional orbifold Q where \mathbb{F}_l is a free group with l generators. We focus on the case of nonorientable orbifolds, extending previous results for the case of orientable orbifolds. Using these computations, we determine examples of distinct 3-orbifolds Q and Q' such that $\chi_\Gamma^{\text{ES}}(Q) = \chi_\Gamma^{\text{ES}}(Q')$ for every finitely generated discrete group Γ .

1. Introduction

This paper completes a program to determine what information about the singular set of an effective, low-dimensional orbifold is determined by the collection of Γ -extensions of the Euler–Satake characteristic. For a finitely generated discrete group Γ and an orbifold Q , the *orbifold of Γ -sectors* of Q is a collection of orbifolds of different dimensions containing Q as well as finite singular covers of the singular strata of Q . The Γ -*extension* of an orbifold invariant is defined by applying the invariant to the orbifold of Γ -sectors of Q .

The *Euler–Satake characteristic* $\chi_{\text{ES}}(Q)$ of a closed orbifold Q is a rational number that corresponds to $\chi_{\text{top}}(M)/|G|$ in the case that Q is a *global quotient orbifold*, i.e., is presented by the quotient of a closed manifold M by a finite group G , where χ_{top} denotes the usual Euler characteristic. It was defined in [Satake 1957] where it is referred to as the *Euler characteristic as a V -manifold* and [Thurston 1997] where it is called the *orbifold Euler characteristic*. The Γ -extensions of the Euler–Satake characteristic of Q , denoted $\chi_\Gamma^{\text{ES}}(Q)$, include many interesting orbifold invariants. When $\Gamma = \mathbb{Z}$, $\chi_\Gamma^{\text{ES}}(Q)$ coincides with the Euler characteristic of

MSC2010: primary 57R18, 57R20; secondary 22A22, 57S17.

Keywords: orbifold, 3-orbifold, Euler–Satake characteristic, orbifold Euler characteristic.

The first author was supported by a Barry M. Goldwater Scholarship and a Rhodes College Fellowship. The second author was supported by a Rhodes College Faculty Development Endowment Grant.

the underlying topological space of Q . When $\Gamma = \mathbb{Z}^2$, $\chi_\Gamma^{\text{ES}}(Q)$ is the stringy orbifold Euler characteristic defined in [Dixon et al. 1985] for global quotients and [Roan 1996] for general orbifolds; see also [Adem and Ruan 2003]. Further extensions corresponding to $\Gamma = \mathbb{Z}^l$ were suggested in [Atiyah and Segal 1989] and defined for global quotients in [Bryan and Fulman 1998]. In [2001; 2003], Tamanoi introduced and studied extensions of orbifold invariants for global quotients, including the Euler–Satake characteristic, corresponding to arbitrary Γ , and this definition was extended to arbitrary orbifolds in [Farsi and Seaton 2010b; 2011].

In [Duval et al. 2010], it was demonstrated that the collection of \mathbb{Z}^l -extensions of the Euler–Satake characteristic determine the diffeomorphism type of a closed, effective, orientable 2-dimensional orbifold and that infinitely many were required to do so. In addition, it was demonstrated that the χ_Γ^{ES} corresponding to any collection of finitely generated discrete groups do not distinguish between certain effective, nonorientable 2-orbifolds.

However, in [Schulte et al. 2011], it was shown that any infinite collection $\chi_{\mathbb{Z}^l}^{\text{ES}}$ along with any infinite collection of $\chi_{\mathbb{F}_l}^{\text{ES}}$ determines the number and type of point singularities of a closed, effective, nonorientable 2-orbifold and that an infinite collection of both is required. In dimension 3, it is shown in [Carroll and Seaton 2013] that any infinite collection of the $\chi_{\mathbb{F}_l}^{\text{ES}}$ determines the number and type of point singularities of a closed, effective, orientable 3-orbifold and that infinitely many are required to do so.

Here, we study the Γ -Euler–Satake characteristics of effective, nonorientable 3-dimensional orbifolds and demonstrate that the above results do not extend to this case. For a closed, effective 3-orbifold Q , we show that the $\chi_\Gamma^{\text{ES}}(Q)$ depend only on the number and type of point singularities of Q and the Euler characteristic of the (topological manifold) boundary of the underlying space of Q . In particular, these invariants can be computed without determining the structure of the 2-dimensional sectors of Q , which can be complicated and difficult to describe in general. We detail a general computation of these invariants for $\Gamma = \mathbb{F}_l$. This computation is used to determine examples of closed, effective 3-orbifolds whose Γ -Euler–Satake characteristics coincide for every finitely generated discrete group Γ , though the point singularities and the topology of the underlying space are different.

This paper is organized as follows. In Section 2, we review the relevant background on orbifolds and Γ -sectors as well as the structure of the singular set of a closed 3-orbifold. In Section 3, we compute the \mathbb{F}_l -Euler–Satake characteristics of closed, effective 3-orbifolds. In particular, we demonstrate Proposition 3.6, which reduces the computation of the $\chi_\Gamma^{\text{ES}}(Q)$ for any finitely generated discrete Γ to an expression that does not involve the 2-dimensional sectors of Q . In Section 4, we give an example of distinct orbifolds whose Γ -Euler–Satake characteristics coincide for every Γ .

2. Background and definitions

In this section, we review the relevant background material and fix notation. In Section 2A, we recall the definition of an orbifold Q as well as the Γ -sectors \tilde{Q}_Γ of Q . Note that there are many definitions of orbifolds in the literature that are more or less equivalent and suited to different purposes. Here, we consider an orbifold to be the Morita equivalence class of a proper, étale, Lie groupoid, and the definition of the Γ -sectors is most natural from this perspective. However, we expect this work to be accessible to readers with no knowledge of groupoids, and hence adapt these definitions to the framework in which an orbifold structure is designated by an atlas of orbifold charts. Though many of the required properties of Γ -sectors are developed elsewhere using groupoid language, we explain the ingredients we will need in the language of charts below. In Section 2B, we review the classification of finite subgroups of $O(3)$, and in Section 2C, we use this classification to describe the topology of a closed, effective 3-orbifold and its singular set.

The reader is referred to [Adem et al. 2007; Moerdijk and Mrčun 2003; Moerdijk 2002] for background on orbifolds from the perspective of Lie groupoids. See [Thurston 1997; Chen and Ruan 2002; Satake 1957] for background from the perspective of orbifold charts, [Boileau et al. 2003; Scott 1983] for more discussion of 3-dimensional orbifolds and [Lerman 2010; Iglesias et al. 2010] for alternate approaches to orbifolds. Note that some of the above references restrict their attention to effective orbifolds. The Γ -sectors of an orbifold are defined for global quotient orbifolds in [Tamanoi 2001; 2003], and are defined for general orbifolds in [Farsi and Seaton 2010b]; see also [Farsi and Seaton 2010a; 2011]. Note that the Γ -sectors extend the definition of the inertia orbifold (see [Kawasaki 1978]) and multi-sectors defined in [Adem et al. 2007; Chen and Ruan 2004].

2A. Orbifolds and Γ -sectors. By an orbifold Q , we will mean a paracompact Hausdorff space \mathbb{X}_Q that is homeomorphic to the orbit space $|\mathcal{G}|$ of a proper, étale Lie groupoid \mathcal{G} . We refer to a choice of \mathcal{G} and homeomorphism between $|\mathcal{G}|$ and \mathbb{X}_Q as a *presentation* of Q . For \mathcal{G} , we may take an *orbifold atlas* for Q , consisting of charts of the form $\{V, G, \pi\}$ where V is an open neighborhood of the origin in \mathbb{R}^n equipped with the action of the finite group G , which may be taken to be a subgroup of $O(n)$ with respect to an inner product on \mathbb{R}^n , and $\pi : V \rightarrow \mathbb{X}_Q$ is a continuous function that induces a homeomorphism of $G \backslash V$ onto an open subset of \mathbb{X}_Q . When a chart is labeled $\{V_p, G_p, \pi_p\}$ for a point $p \in \mathbb{X}_Q$, we assume that $\pi_p(0) = p$ and refer to $\{V_p, G_p, \pi_p\}$ as an *orbifold chart at p* . An *injection* of orbifold charts $\{V, G, \pi\} \rightarrow \{V', G', \pi'\}$ is a pair (f, λ) where $\lambda : G \rightarrow G'$ is an injective homomorphism and $f : V \rightarrow V'$ is a λ -equivariant open embedding such that $\pi \circ f = \pi'$. Two charts $\{V, G, \pi\}$ and $\{V', G', \pi'\}$ are said to be *compatible* if for each $p \in \pi(V) \cap \pi'(V')$, there is an orbifold chart $\{V_p, G_p, \pi_p\}$ at p and a pair

of injections of $\{V_p, G_p, \pi_p\}$ into $\{V, G, \pi\}$ and $\{V', G', \pi'\}$, respectively. Then an orbifold atlas is a collection of compatible charts whose images in \mathbb{X}_Q cover \mathbb{X}_Q , and an equivalence of atlases can be defined which corresponds to Morita equivalence for groupoid presentations. *Diffeomorphic* orbifolds are those presented by Morita equivalent groupoids, e.g, equivalent orbifold atlases.

Note that any two injections (f_1, λ_1) and (f_2, λ_2) of orbifold charts $\{V, G, \pi\} \rightarrow \{V', G', \pi'\}$ are related by an element g of G' ; that is, $f_2(x) = gf_1(x)$ for each $x \in V$, and $\lambda_2(h) = g\lambda_1(h)g^{-1}$ for each $h \in G$; see [Moerdijk and Pronk 1997, Proposition A.1]. Applying this result to injections between a chart and itself, it follows that the (isomorphism class of the) *isotropy group* G_p of a point $p \in \mathbb{X}_Q$ does not depend on the choice of chart at p , and in fact can be defined as the isotropy group of an arbitrary lift of p into an arbitrary chart. Moreover, though the elements of G_p depend on the choice of chart, their G_p -conjugacy classes in a chart at p are well-defined.

An orbifold Q is *effective* if it is presented by an effective groupoid \mathcal{G} , or equivalently if it is equipped with an atlas such that the group action in each chart is effective. It is *closed* if \mathbb{X}_Q is compact and Q does not have boundary as an orbifold; note that we have only considered orbifolds without boundary in the definitions above. When Q is connected, the *dimension* of Q is the dimension of the object space of an étale presentation \mathcal{G} of Q , or equivalently the dimension of the domain of each orbifold chart.

The *Euler–Satake characteristic* $\chi_{\text{ES}}(Q)$ of a closed orbifold Q is defined in terms of a triangulation of Q such that the isomorphism class of the isotropy group is constant on the interior of each simplex. If \mathcal{T} is such a triangulation and for each $\sigma \in \mathcal{T}$, G_σ denotes the isotropy group of a point on the interior of σ , then

$$\chi_{\text{ES}}(Q) = \sum_{\sigma \in \mathcal{T}} \frac{(-1)^{\dim \sigma}}{|G_\sigma|}.$$

Let Γ be a finitely generated discrete group. The simplest description of the Γ -sectors of Q is in terms of a proper étale Lie groupoid \mathcal{G} presenting Q . In this case the collection $\text{HOM}(\Gamma, \mathcal{G})$ of groupoid homomorphisms from Γ to \mathcal{G} inherits the structure of a disjoint union of smooth manifolds, potentially of different dimensions, as well as a smooth action of \mathcal{G} . Then $\mathcal{G} \times \text{HOM}(\Gamma, \mathcal{G})$ is itself a proper étale Lie groupoid presenting the orbifold of Γ -sectors \tilde{Q}_Γ . Note that \tilde{Q}_Γ always includes a connected component diffeomorphic to Q , called the *nontwisted Γ -sector* corresponding to the trivial homomorphisms; all other sectors are called *twisted Γ -sectors*. If Q is closed, then \tilde{Q}_Γ is a finite union of connected, closed orbifolds.

Alternatively, the Γ -sectors of Q can be defined as follows. Let

$$\mathbb{X}_{\tilde{Q}_\Gamma} = \{(p, (\varphi_p)_{G_p}) : p \in \mathbb{X}_Q, \varphi_p : \Gamma \rightarrow G_p\},$$

where $(\varphi_p)_{G_p}$ denotes the G_p -conjugacy class of φ_p . Given an orbifold chart $\{V_p, G_p, \pi_p\}$ for Q at a point p , define the orbifold chart $\{V_p^{(\varphi_p)}, C_{G_p}(\varphi_p), \pi_p^{\varphi_p}\}$ for \tilde{Q}_Γ at $(p, (\varphi_p)_{G_p})$, where $V_p^{(\varphi_p)}$ denotes the points in V_p fixed by the image of φ_p , $C_{G_p}(\varphi_p)$ denotes the centralizer of φ_p in G_p , and $\pi_p^{\varphi_p} : V_p^{(\varphi_p)} \rightarrow \mathbb{X}_{\tilde{Q}_\Gamma}$ is defined as follows. Given $y \in V_p^{(\varphi_p)}$, identify the isotropy group of $\pi_p(y)$ with the isotropy group $(G_p)_y \leq G_p$, and then let $\varphi_{\pi_p(y)} : \Gamma \rightarrow (G_p)_y$ denote the homomorphism given by restricting the codomain of φ_p to this subgroup. Note that the image $\text{Im}(\varphi_p)$ of φ_p is contained in $(G_p)_y$ precisely when $y \in V_p^{(\varphi_p)}$. Note further that $\varphi_{\pi_p(y)}$ is well-defined only up to its $G_{\pi_p(x)}$ -conjugacy class. Then we define $\pi_p^{\varphi_p}(y) = (\pi_p(y), (\varphi_{\pi_p(y)})_{(G_p)_y})$. The proof that the $\{V_p^{(\varphi_p)}, C_{G_p}(\varphi_p), \pi_p^{\varphi_p}\}$ define an orbifold structure for $\mathbb{X}_{\tilde{Q}_\Gamma}$ is omitted; it is given by translating the proof in groupoid language given in [Farsi and Seaton 2010b] to this context. It is, as well, a direct generalization of the proof of [Chen and Ruan 2004, Lemma 3.1.1] (see also [Kawasaki 1978]), which is given in atlas language for the case $\Gamma = \mathbb{Z}$. We will, however, require an understanding of the injections between orbifold charts for \tilde{Q}_Γ , which we now describe.

Given an injection (f, λ) of orbifold charts $\{V_q, G_q, \pi_q\} \rightarrow \{V_p, G_p, \pi_p\}$, we say that a homomorphism $\varphi_q : \Gamma \rightarrow G_q$ is *locally covered* by a homomorphism $\varphi_p : \Gamma \rightarrow G_p$ (with respect to the choice of charts and injection) if $\lambda \circ \varphi_q = \varphi_p$. Then it is easy to see that $\{f|_{V_q^{(\varphi_q)}}, \lambda|_{C_{G_q}(\varphi_q)}\}$ is an injection of the orbifold chart $\{V_q^{(\varphi_q)}, C_{G_q}(\varphi_q), \pi_q^{\varphi_q}\}$ into the orbifold chart $\{V_p^{(\varphi_p)}, C_{G_p}(\varphi_p), \pi_p^{\varphi_p}\}$. Note that if φ_p locally covers φ_q with respect to the injection (f, λ) as above, then for any other choice of injection $(f', \lambda') : \{V_q, G_q, \pi_q\} \rightarrow \{V_p, G_p, \pi_p\}$, there is a $g \in G_p$ such that $g(\lambda' \circ \varphi_q)g^{-1} = \varphi_p$; compare [Farsi and Seaton 2010b, Definition 2.6]. In particular, if φ_p and ψ_p are both homomorphisms $\Gamma \rightarrow G_p$, then by the characterization of injections of a chart into itself given in [Moerdijk and Pronk 1997, Proposition A.1] and recalled above, φ_p locally covers ψ_p if and only if φ_p and ψ_p are G_p -conjugate. By allowing finite sequences of local coverings (in either direction), we extend the notion of local covering to an equivalence relation on $\bigcup_{p \in \mathbb{X}_Q} \text{HOM}(\Gamma, G_p)$ and let \approx denote this relation. We let $(\varphi_p)_\approx$ denote the \approx -class of a homomorphism φ_p and T_Q^Γ the set of equivalence classes. Note that φ_p and φ_q are equivalent if and only if $(p, (\varphi_p)_{G_p})$ and $(q, (\varphi_q)_{G_q})$ are in the same connected component of $\mathbb{X}_{\tilde{Q}_\Gamma}$.

2B. The finite subgroups of $O(3)$. In this section, we recall the classification of finite subgroups G of $O(3)$ given in [Benson and Grove 1971, Theorem (2.5.2)] as well as the corresponding orbifold singularities. In each case, we fix a representation of the group G to refer to in the sequel.

First, recall that every element of $SO(3)$ acts as a rotation about a line in \mathbb{R}^3 . Up to conjugation in $SO(3)$, the finite subgroups of $SO(3)$ consist of the cyclic groups

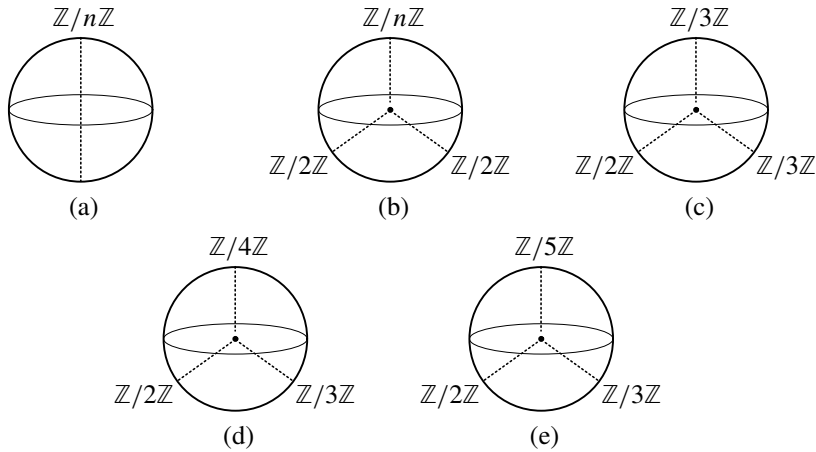


Figure 1. Singular sets in the quotients of \mathbb{R}^3 by the finite subgroups of $\text{SO}(3)$: (a) a cyclic group $\mathbb{Z}/n\mathbb{Z}$; (b) a dihedral group D_{2n} ; (c) the tetrahedral group \mathbb{T} ; (d) the octahedral group \mathbb{O} ; (e) the icosahedral group \mathbb{I} .

$\mathbb{Z}/n\mathbb{Z}$, the dihedral groups D_{2n} of order $2n$, the tetrahedral group \mathbb{T} of order 12, the octahedral group \mathbb{O} of order 24, and the icosahedral group \mathbb{I} of order 60. The quotient $G \backslash \mathbb{R}^3$ is homeomorphic to \mathbb{R}^3 in each case; see [Boileau et al. 2003]. In $\mathbb{Z}_n \backslash \mathbb{R}^3$ the singular set is a line fixed by the entire group \mathbb{Z}_n , while for the other groups, the singular set is the origin as well as three rays fixed by cyclic groups; see Figure 1. The Γ -Euler–Satake characteristics of orientable 3-orbifolds, which contain only these singularities, are studied in [Carroll and Seaton 2013].

Let J denote the negative identity element in $\text{O}(3)$. A finite subgroup of $\text{O}(3)$ generated by J and a finite subgroup G of $\text{SO}(3)$ is called a *full group*, denoted G^* . Note that as J is central and $J^2 = I$ is the identity in $\text{O}(3)$, G^* is isomorphic to $G \times \mathbb{Z}/2\mathbb{Z}$. There are five classes of full groups corresponding to the five classes of subgroups of $\text{SO}(3)$. See Figure 2 for diagrams of the quotient spaces and singular sets in each case, and note that they refer to mixed groups and $\mathcal{P}_{\text{proj}}$, which are defined below. Note that the quotient space $G^* \backslash \mathbb{R}^3$ is homeomorphic to closed half-space in \mathbb{R}^3 except in the case of $G = (\mathbb{Z}/n\mathbb{Z})^*$ with n odd, where $(\mathbb{Z}/n\mathbb{Z})^* \backslash \mathbb{R}^3$ is homeomorphic to the cone on $\mathbb{R}P^2$.

- A *full cyclic group* $(\mathbb{Z}/n\mathbb{Z})^*$ has order $2n$ and is generated by A_n and J , where

$$A_n = \begin{bmatrix} \cos(2\pi/n) & -\sin(2\pi/n) & 0 \\ \sin(2\pi/n) & \cos(2\pi/n) & 0 \\ 0 & 0 & 1 \end{bmatrix}$$

satisfies $A_n^n = I$.

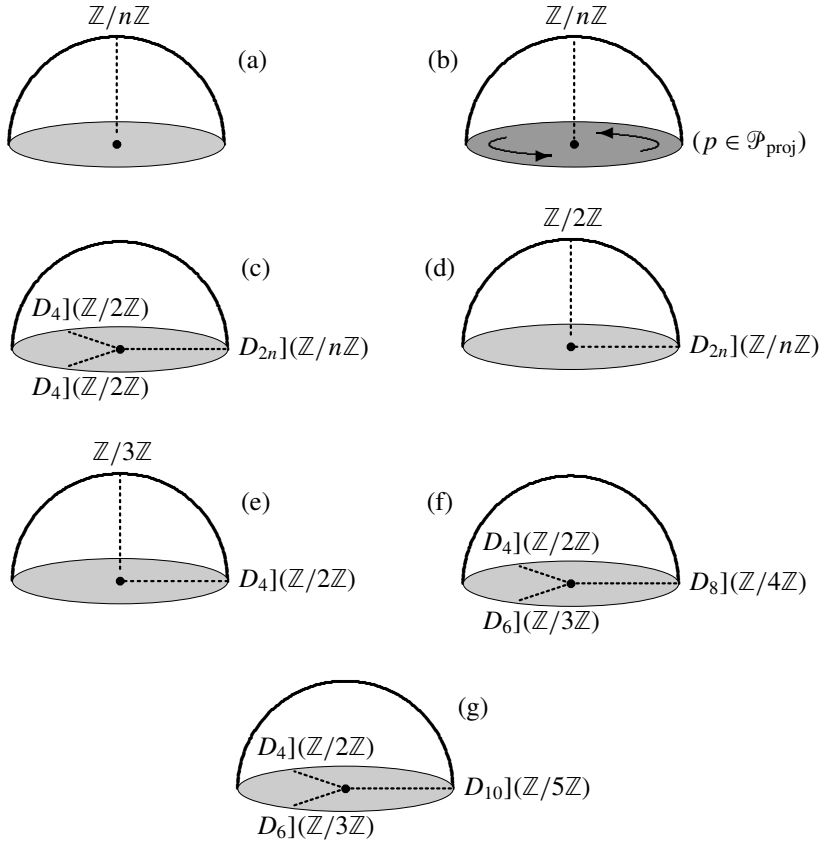


Figure 2. Singular sets corresponding to the finite full subgroups of $O(3)$, where the lightly shaded boundary disks have generic isotropy $\mathbb{Z}/2\mathbb{Z}$ and the darkly shaded boundary disk is identified via the antipodal map as indicated by curved arrows: (a) a full cyclic group $(\mathbb{Z}/n\mathbb{Z})^*$ for n even; (b) a full cyclic group $(\mathbb{Z}/n\mathbb{Z})^*$ for n odd; (c) a full dihedral group D_{2n}^* for n even; (d) a full dihedral group D_{2n}^* for n odd; (e) the full tetrahedral group \mathbb{T}^* ; (f) the full octahedral group \mathbb{O}^* ; (g) the full icosahedral group \mathbb{I}^* .

- A full dihedral group D_{2n}^* has order $4n$ and is generated by A_n , B , and J , where A_n is as above and

$$B = \begin{bmatrix} 1 & 0 & 0 \\ 0 & -1 & 0 \\ 0 & 0 & -1 \end{bmatrix}$$

is a rotation about the x -axis through an angle of π . Note that $A_n B = B A_n^{n-1}$.

- The *full tetrahedral group* \mathbb{T}^* has order 24 and is generated by C , D , and J , where

$$C = \begin{bmatrix} -1 & 0 & 0 \\ 0 & -1 & 0 \\ 0 & 0 & 1 \end{bmatrix} \quad \text{and} \quad D = \begin{bmatrix} 0 & -1 & 0 \\ 0 & 0 & -1 \\ 1 & 0 & 0 \end{bmatrix}.$$

Note that $C^2 = D^3 = (CD)^3 = I$.

- The *full octahedral group* \mathbb{O}^* has order 48 and is generated by R , S , and J , where

$$R = \begin{bmatrix} 0 & 1 & 0 \\ 1 & 0 & 0 \\ 0 & 0 & -1 \end{bmatrix} \quad \text{and} \quad S = \begin{bmatrix} 1 & 0 & 0 \\ 0 & 0 & 1 \\ 0 & -1 & 0 \end{bmatrix}.$$

Note that $R^2 = S^4 = (RS)^3 = I$.

- The *full icosahedral group* \mathbb{I}^* is generated by B , E , and J , where B is as above and

$$E = \begin{bmatrix} +\phi/2 & +\bar{\phi}/2 & +1/2 \\ +\bar{\phi}/2 & +1/2 & -\phi/2 \\ -1/2 & +\phi/2 & +\bar{\phi}/2 \end{bmatrix}.$$

Here, $\phi = (1 + \sqrt{5})/2$ and $\bar{\phi} = (1 - \sqrt{5})/2$. Note that $B^2 = E^5 = (BE)^3 = I$.

A finite subgroup $G < O(3)$ that is not full or contained in $SO(3)$ is a *mixed group*. A mixed group G is denoted $H]K$, where H and K are finite subgroups of $SO(3)$ such that K is a subgroup of H of index 2. Then G is isomorphic to H as a group, but the representation of G on \mathbb{R}^3 is given by multiplying those elements in the nontrivial coset of H/K by J . The quotient spaces and singular sets of $G \setminus \mathbb{R}^3$ for mixed groups G are pictured in Figure 3. Again, each quotient space is homeomorphic to closed half-space in \mathbb{R}^3 with the exception of $(\mathbb{Z}/2n\mathbb{Z}][\mathbb{Z}/n\mathbb{Z}] \setminus \mathbb{R}^3$ for n even, which is homeomorphic to the cone on $\mathbb{R}P^2$. The four families of mixed subgroups of $O(3)$ are as follows:

- A *mixed cyclic group* $(\mathbb{Z}/2n\mathbb{Z}][\mathbb{Z}/n\mathbb{Z}]$ has order $2n$ and is generated by $A_{2n}J$ where A_{2n} is as above.
- A *mixed dihedral group* $D_{4n}]D_{2n}$ of order $4n$ is generated by $A_{2n}J$ and B .
- A *dihedral extending cyclic group* $D_{2n}][\mathbb{Z}/n\mathbb{Z}]$ of order $2n$ is generated by A_n and BJ .
- The *octahedral extending tetrahedral group* $\mathbb{O}]\mathbb{T}$ is generated by RJ and SJ .

Every finite subgroup of $O(3)$ is conjugate to one of the groups listed above. When referring to these groups, we will always mean the group as well as its standard representation on \mathbb{R}^3 in coordinates as described above.

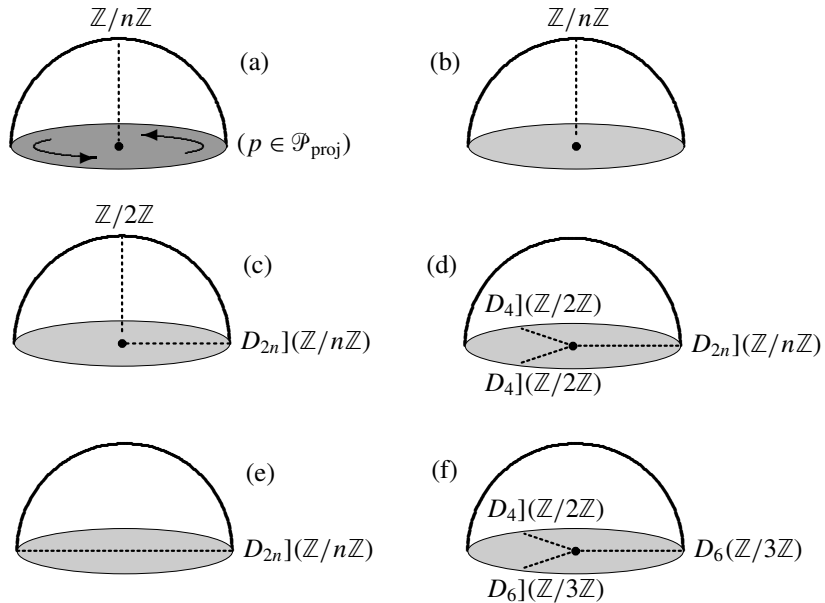


Figure 3. Singular sets corresponding to the finite mixed subgroups of $O(3)$, where the lightly shaded boundary disks have generic isotropy $\mathbb{Z}/2\mathbb{Z}$ and the darkly shaded boundary disk is identified via the antipodal map as indicated by curved arrows: (a) a mixed cyclic group $(\mathbb{Z}/2n\mathbb{Z}][\mathbb{Z}/n\mathbb{Z}$ for n even; (b) a mixed cyclic group $(\mathbb{Z}/2n\mathbb{Z}][\mathbb{Z}/n\mathbb{Z}$ for n odd; (c) a mixed dihedral group $D_{4n}]D_{2n}$ for n even; (d) a mixed dihedral group $D_{4n}]D_{2n}$ for n odd; (e) a dihedral extending cyclic group $D_{2n}][\mathbb{Z}/n\mathbb{Z}$ for n of either parity; (f) the octahedral extending tetrahedral group $\mathbb{O}][\mathbb{T}$.

2C. Closed, effective 3-dimensional orbifolds. Let Q be a closed, effective 3-orbifold. Then each point of Q is contained in a neighborhood that is homeomorphic to $G \backslash \mathbb{R}^3$ where G is a finite subgroup of $O(3)$. Inspecting the possible homeomorphism classes of $G \backslash \mathbb{R}^3$, it follows that there is a finite, possibly empty collection $\mathcal{P}_{\text{proj}} = \{p_1, \dots, p_k\}$ of points in Q such that $\mathbb{X}_Q \setminus \mathcal{P}_{\text{proj}}$ is a topological 3-manifold, potentially with boundary. In particular, $\mathcal{P}_{\text{proj}}$ consists of those points with isotropy group $(\mathbb{Z}/n\mathbb{Z})^*$ for n odd or $(\mathbb{Z}/2n\mathbb{Z}][\mathbb{Z}/n\mathbb{Z}$ for n even. Note that Q is orientable if and only if $\mathcal{P}_{\text{proj}} = \emptyset$ and \mathbb{X}_Q is an orientable 3-manifold without boundary. In the case that \mathbb{X}_Q has boundary as a topological manifold, we let $\partial_{\text{top}} Q$ denote the boundary and caution the reader that Q does not have boundary as an orbifold.

The singular set of Q consists of $\partial_{\text{top}} Q \cup \mathcal{P}_{\text{proj}}$ along with a disjoint collection of circles in the interior of $\mathbb{X}_Q \setminus \mathcal{P}_{\text{proj}}$ and a not-necessarily connected graph \mathfrak{G} that is trivalent on the interior of $\mathbb{X}_Q \setminus \mathcal{P}_{\text{proj}}$ and has univalent vertices in $\mathcal{P}_{\text{proj}}$ and $\partial_{\text{top}} Q$. Note that the (isomorphism class of the) isotropy group is constant on each circle as well as the interior of each edge; however, it need not be constant on $\partial_{\text{top}} Q$. Rather, $\partial_{\text{top}} Q$ itself contains a union of circles and a (not necessarily connected) graph with trivalent vertices as well as univalent vertices where \mathfrak{G} intersects $\partial_{\text{top}} Q$. The isotropy type is constant on the circles and the interiors of the edges of this graph and is $\mathbb{Z}/2\mathbb{Z}$ elsewhere in $\partial_{\text{top}} Q$.

By a *point singularity* of Q , we mean a point $p \in \mathbb{X}_Q$ contained in a neighborhood U such that the isotropy group of p is strictly larger than all points in $U \setminus \{p\}$. Equivalently, a point singularity corresponds to a 0-dimensional stratum of \mathbb{X}_Q with respect to the stratification by orbit types. Note that the point singularities of Q correspond to the vertices of the graphs described above.

In the sequel, we will let \mathcal{P} denote the set of point singularities of Q and \mathcal{P}_{∂} denote the set of point singularities that occur on $\partial_{\text{top}} Q$. Note that $\mathcal{P}_{\text{proj}}$ is the set of point singularities that occur on nonmanifold points of \mathbb{X}_Q . Then $\mathcal{P} \setminus (\mathcal{P}_{\partial} \cup \mathcal{P}_{\text{proj}})$ is exactly the set of point singularities at which Q is *locally orientable*, i.e., with isotropy group contained in $\text{SO}(3)$.

The Γ -sectors of a closed, effective 3-orbifold Q include the nontwisted Γ -sector of dimension 3 and may include twisted Γ -sectors of dimensions 0, 1, or 2. Each Γ -sector is a closed orbifold, and only the nontwisted Γ -sector is effective. Sectors of dimension 0 are points equipped with the trivial action of a finite group, and it is easy to see that such sectors correspond to homomorphisms $\varphi_p : \Gamma \rightarrow G_p$ where p is a point singularity of the orbifold and the image of φ_p fixes a single point. The only closed, effective 1-dimensional orbifolds are circles or mirrored intervals, i.e., intervals with $\mathbb{Z}/2\mathbb{Z}$ -isotropy at the endpoints, and so all closed 1-dimensional sectors are given by circles with the trivial action of a finite group or noneffective mirrored intervals.

The 2-dimensional sectors correspond to homomorphisms $\varphi_p : \Gamma \rightarrow G_p$ where $p \in \partial_{\text{top}} Q$ and the image of φ_p fixes a plane. However, the 2-dimensional sectors of Q need not correspond to entire connected components of $\partial_{\text{top}} Q$. In fact, the 0- and 1-dimensional singular strata contained in $\partial_{\text{top}} Q$ divide $\partial_{\text{top}} Q$ into regions, and the closures of these regions can be covered by distinct sectors. We illustrate this with the following, considering an open orbifold for simplicity.

Example 2.1. Let $n \geq 4$ be even and let Q denote the orbifold given by the quotient of \mathbb{R}^3 by the full dihedral group D_{2n}^* ; see Figure 2(c). Then Q is homeomorphic to closed half-space, and the singular strata divide $\partial_{\text{top}} Q$ into three dense regions with isotropy $\mathbb{Z}/2\mathbb{Z}$.

Let $\Gamma = \mathbb{Z}$, and then there are three 2-dimensional sectors. The first, corresponding to homomorphisms that map $1 \in \mathbb{Z}$ to the central element $A_n^{n/2} J \in D_{2n}^*$, is given by the quotient of a plane \mathbb{R}^2 by the action of $D_{2n} \times (\mathbb{Z}/2\mathbb{Z})$, where the D_{2n} -factor acts via the standard effective action of a dihedral group on \mathbb{R}^2 , and the $\mathbb{Z}/2\mathbb{Z}$ -factor acts trivially. The resulting orbifold is homeomorphic to a closed quadrant in \mathbb{R}^2 , where the origin is a *corner reflector* with isotropy $D_{2n} \times (\mathbb{Z}/2\mathbb{Z})$, other points on the (topological) boundary have isotropy $(\mathbb{Z}/2\mathbb{Z})^2$, and points on the interior have isotropy $\mathbb{Z}/2\mathbb{Z}$. The map $(p, (\varphi_p)_{G_p}) \mapsto p$ is a bijection between this sector and the single closed region in $\partial_{\text{top}} Q$ bounded by the two rays with isotropy $D_4](\mathbb{Z}/2\mathbb{Z})$.

The other 2-dimensional sectors cover the respective closures of the other two regions in $\partial_{\text{top}} Q$. They corresponds to the two conjugacy classes of homomorphisms that map $1 \in \mathbb{Z}$ to $A_n^k B J \in D_{2n}^*$ where $k \neq n/2$. Each is given by the quotient of \mathbb{R}^2 by $\langle A_n^{n/2}, A_n^k B J, J \rangle \cong (\mathbb{Z}/2\mathbb{Z})^3$, where $A_n^k B J$ acts trivially and the other two factors act via the standard action of $(\mathbb{Z}/2\mathbb{Z})^2 \cong D_4$ on \mathbb{R}^2 . These sectors are also each homeomorphic to a closed quadrant in \mathbb{R}^2 , where the origin is a corner reflector with isotropy $D_4 \times (\mathbb{Z}/2\mathbb{Z})$, other points on the (topological) boundary have isotropy $(\mathbb{Z}/n\mathbb{Z})^2$, and points on the interior have isotropy $\mathbb{Z}/2\mathbb{Z}$. The map $(p, (\varphi_p)_{G_p}) \mapsto p$ is a bijection from each of these sectors to the closures of the corresponding regions in $\partial_{\text{top}} Q$.

From this example, it is clear that a description of the 2-dimensional sectors of an arbitrary closed, effective 3-orbifold Q would require a detailed description of the topology of $\partial_{\text{top}} Q$ as well as the configuration of the singular strata it contains. As we will see in Section 3A, however, the sum of the Euler–Satake characteristics of the 2-dimensional sectors of Q depends only on $\chi_{\text{top}}(\partial_{\text{top}} Q)$ and the number and type of point singularities in Q , and hence can be computed using only this information.

3. Computation of $\chi_{\mathbb{F}_l}^{\text{ES}}(Q)$

In this section, we compute the \mathbb{F}_l -Euler–Satake characteristics of a closed, effective 3-orbifold Q where \mathbb{F}_l is the free group with l generators. In Section 3A, we simplify this computation by demonstrating Proposition 3.6, which expresses the Γ -Euler–Satake characteristic in terms of quantities involving only the number and type of point singularities of Q as well as $\chi_{\text{top}}(\partial_{\text{top}} Q)$. In Section 3B, we compute these quantities for each of the finite subgroups of $O(3)$ when $\Gamma = \mathbb{F}_l$. The formulas for the \mathbb{F}_l -Euler–Satake characteristics are given in Section 3C.

3A. General observations. Let Γ be a finitely generate discrete group and Q a closed, effective 3-orbifold. The Γ -Euler–Satake characteristic of Q is given by

$$\chi_{\Gamma}^{\text{ES}}(Q) = \chi_{\text{ES}}(\tilde{Q}_{\Gamma}),$$

the usual Euler–Satake characteristic of the orbifold of Γ -sectors \tilde{Q}_Γ of Q . We let $\tilde{Q}_{\Gamma,d}$ denote the collection of Γ -sectors of Q of dimension d , and then

$$\tilde{Q}_\Gamma = \tilde{Q}_{\Gamma,0} \sqcup \tilde{Q}_{\Gamma,1} \sqcup \tilde{Q}_{\Gamma,2} \sqcup \tilde{Q}_{\Gamma,3},$$

where $\tilde{Q}_{\Gamma,3} = Q$ consists only of the nontwisted sector. By [Satake 1957, Theorem 4], the Euler–Satake characteristic of an odd-dimensional closed orbifold vanishes; note that Satake assumes that orbifolds do not have singular strata of codimension 1, but his result can be applied to the orientable double-cover of an orbifold and hence extended to arbitrary orbifolds. Therefore, we have that

$$\chi_\Gamma^{\text{ES}}(Q) = \chi_{\text{ES}}(\tilde{Q}_{\Gamma,0}) + \chi_{\text{ES}}(\tilde{Q}_{\Gamma,2}). \tag{3-1}$$

As was illustrated in Example 2.1 above, the structure of $\tilde{Q}_{\Gamma,2}$ is complicated and depends heavily on the graph structure of the singular strata in $\partial_{\text{top}} Q$. However, our first goal of this section is to indicate how $\chi_\Gamma^{\text{ES}}(Q)$ can be computed without determining the structure or number of components of $\tilde{Q}_{\Gamma,2}$. First, we have the following.

Lemma 3.1. *Let Q be a closed, effective, 3-dimensional orbifold with underlying space \mathbb{X}_Q and let $\mathcal{P}_{\text{proj}}$ denote the finite set of projective points of Q . Then*

$$\chi_{\text{top}}(\mathbb{X}_Q) = \frac{1}{2} \chi_{\text{top}}(\partial_{\text{top}} Q) + \frac{1}{2} |\mathcal{P}_{\text{proj}}|.$$

Proof. For each $p \in \mathcal{P}_{\text{proj}}$, choose a neighborhood U_p of p homeomorphic to $G_p \setminus \mathbb{R}^3$ and small enough so that $U_p \cap U_q = \emptyset$ for $p \neq q$, each $U_p \cap \partial_{\text{top}} Q = \emptyset$, and $\partial(\bar{U}_p)$ is homeomorphic to $G_p \setminus \mathbb{S}^2$, where by $\partial(\bar{U}_p)$, we mean the boundary of the manifold $\bar{U}_p \setminus \{p\}$. Then the topological space $X = \mathbb{X}_Q \setminus \bigcup_{p \in \mathcal{P}_{\text{proj}}} U_p$ is a topological 3-manifold with boundary given by $\partial X = \partial_{\text{top}} Q \cup \bigcup_{p \in \mathcal{P}_{\text{proj}}} \partial(U_p)$. Note that each $\partial(\bar{U}_p)$ is homeomorphic to $\mathbb{R}P^2$ and hence $\chi_{\text{top}}(\partial(\bar{U}_p)) = 1$. Expressing \mathbb{X}_Q as $X \cup \bigcup_{p \in \mathcal{P}_{\text{proj}}} \bar{U}_p$ and noting that the intersection of each \bar{U}_p with X is $\partial(\bar{U}_p)$, we have

$$\chi_{\text{top}}(\mathbb{X}_Q) = \chi_{\text{top}}(X) + \sum_{p \in \mathcal{P}_{\text{proj}}} \chi_{\text{top}}(\bar{U}_p) - \sum_{p \in \mathcal{P}_{\text{proj}}} \chi_{\text{top}}(\partial(\bar{U}_p)).$$

However, as \bar{U}_p is homeomorphic to the cone on $\mathbb{R}P^2$ and hence is contractible, we have $\chi_{\text{top}}(\bar{U}_p) = 1 = \chi_{\text{top}}(\partial(\bar{U}_p))$. It follows that

$$\chi_{\text{top}}(\mathbb{X}_Q) = \chi_{\text{top}}(X).$$

As the Euler characteristic of a 3-manifold is half that of its boundary, we then have

$$\chi_{\text{top}}(\mathbb{X}_Q) = \chi_{\text{top}}(X) = \frac{1}{2} \chi_{\text{top}}(\partial X) = \frac{1}{2} (\chi_{\text{top}}(\partial_{\text{top}} Q) + |\mathcal{P}_{\text{proj}}|). \quad \square$$

Using the fact that $\chi_{\text{top}}(\mathbb{X}_Q) = \chi_{\mathbb{Z}}^{\text{ES}}(Q)$ (see [Farsi and Seaton 2011] or [Seaton 2008]), we have the following.

Corollary 3.2. *Let Q be a closed, effective, 3-dimensional orbifold with underlying space \mathbb{X}_Q and let $\mathcal{P}_{\text{proj}}$ denote the finite set of projective points of Q . Then*

$$\chi_{\mathbb{Z}}^{\text{ES}}(Q) = \frac{1}{2}\chi_{\text{top}}(\partial_{\text{top}} Q) + \frac{1}{2}|\mathcal{P}_{\text{proj}}|.$$

In particular, as $\chi_{\mathbb{Z}}^{\text{ES}}(Q) = \chi_{\text{ES}}(\tilde{Q}_{\mathbb{Z},0}) + \chi_{\text{ES}}(\tilde{Q}_{\mathbb{Z},2})$, we have

$$\chi_{\text{ES}}(\tilde{Q}_{\mathbb{Z},2}) = \frac{1}{2}\chi_{\text{top}}(\partial_{\text{top}} Q) + \frac{1}{2}|\mathcal{P}_{\text{proj}}| - \chi_{\text{ES}}(\tilde{Q}_{\mathbb{Z},0}). \tag{3-2}$$

Hence, using Corollary 3.2, we can compute the Euler–Satake characteristic of the 2-dimensional \mathbb{Z} -sectors in terms of the 0-dimensional \mathbb{Z} -sectors and $\chi_{\text{top}}(\partial Q)$. We can use this to compute the Euler–Satake characteristic of the 2-dimensional Γ -sectors for arbitrary Γ using the following. For $p \in Q$, let $\text{HOM}(\Gamma, G_p)_d$ denote the collection of homomorphisms $\Gamma \rightarrow G_p$ whose image fix a d -dimensional subspace in a chart at p .

Lemma 3.3. *Let Q be a closed, effective, 3-dimensional orbifold and let Γ be a finitely generated discrete group. Then the 2-dimensional Γ -sectors of Q consist of $|\text{HOM}(\Gamma, \mathbb{Z}/2\mathbb{Z})| - 1$ identical copies of the 2-dimensional \mathbb{Z} -sectors of Q . In particular, the 2-dimensional \mathbb{F}_1 -sectors of Q consist of $2^l - 1$ copies of the 2-dimensional \mathbb{Z} -sectors of Q .*

Proof. By inspection, the only elements of $O(3)$ that fix planes are reflections that generate a subgroup isomorphic to $\mathbb{Z}/2\mathbb{Z}$. Hence each element in the union $\bigcup_{p \in Q} \text{HOM}(\Gamma, G_p)_2$ has image isomorphic to $\mathbb{Z}/2\mathbb{Z}$. Define the map

$$\Psi : \bigcup_{p \in Q} \text{HOM}(\Gamma, G_p)_2 \longrightarrow \bigcup_{p \in Q} \text{HOM}(\mathbb{Z}, G_p)_2$$

by sending $\varphi_p \in \text{HOM}(\Gamma, G_p)_2$ to the homomorphism in $\text{HOM}(\mathbb{Z}, G_p)_2$ that maps the generator of \mathbb{Z} to the unique generator of the image $\text{Im}(\varphi_p)$ of φ_p . Then as the image of a homomorphism $\mathbb{Z} \rightarrow \mathbb{Z}/2\mathbb{Z}$ uniquely characterizes the homomorphism, we have for each $\psi_p \in \text{HOM}(\mathbb{Z}, G_p)_2$ that $\Psi^{-1}(\psi_p)$ consists of every element of $\text{HOM}(\Gamma, \text{Im}(\psi_p))$ except the trivial homomorphism. Therefore, Ψ is a $(|\text{HOM}(\Gamma, \mathbb{Z}/2\mathbb{Z})| - 1)$ -to-1 map. It is clear from its construction that Ψ is equivariant with respect to the G_p -actions by conjugation on $\text{HOM}(\mathbb{Z}, G_p)_2$ and $\text{HOM}(\Gamma, G_p)_2$, and moreover that the centralizer of each ψ_p in G_p coincides with the centralizer of $\Psi^{-1}(\psi_p)$ in G_p , so that Ψ induces a $(|\text{HOM}(\Gamma, \mathbb{Z}/2\mathbb{Z})| - 1)$ -to-1 map

$$\tilde{\Psi} : \tilde{Q}_{\Gamma,2} \rightarrow \tilde{Q}_{\mathbb{Z},2}, \quad (p, (\varphi_p)_{G_p}) \mapsto (p, (\Psi(\varphi_p))_{G_p}).$$

To complete the proof, we demonstrate that the restriction of $\tilde{\Psi}$ to each 2-dimensional Γ -sector of Q is a diffeomorphism onto a \mathbb{Z} -sector of Q . In groupoid language, this can be accomplished by extending Ψ to a map $\text{HOM}(\Gamma, \mathcal{G})_2 \rightarrow \text{HOM}(\mathbb{Z}, \mathcal{G})_2$, where $\text{HOM}(\Gamma, \mathcal{G})_2$ denotes the groupoid homomorphisms corresponding to points in 2-dimensional sectors, and then computing directly that the resulting map is in fact equivariant with respect to the \mathcal{G} -actions, and hence a Lie groupoid isomorphism when restricted to each sector.

To demonstrate this in terms of an atlas, suppose $(p, (\varphi_p)_{G_p})$ and $(q, (\varphi_q)_{G_q})$ are points in $\mathbb{X}_{\tilde{Q}_\Gamma}$ contained in orbifold charts for \tilde{Q}_Γ related by an injection. Specifically, suppose $(f, \lambda) : \{V_q, G_q, \pi_q\} \rightarrow \{V_p, G_p, \pi_p\}$ is an injection of orbifold charts with respect to which $\varphi_p : \Gamma \rightarrow G_p$ locally covers $\varphi_q : \Gamma \rightarrow G_q$ for $\varphi_p \in \text{HOM}(\Gamma, G_p)_2$ and $\varphi_q \in \text{HOM}(\Gamma, G_q)_2$. Then

$$\{f|_{V_q^{(\varphi_q)}}, \lambda|_{C_{G_q}(\varphi_q)}\}$$

is an injection of the orbifold chart $\{V_q^{(\varphi_q)}, C_{G_q}(\varphi_q), \pi_q^{(\varphi_q)}\}$ for \tilde{Q}_Γ at $(q, (\varphi_q)_{G_q})$ into the chart $\{V_p^{(\varphi_p)}, C_{G_p}(\varphi_p), \pi_p^{(\varphi_p)}\}$ for \tilde{Q}_Γ at $(p, (\varphi_p)_{G_p})$. As Ψ preserves images of homomorphisms, it is easy to see that

$$V_p^{(\varphi_p)} = V_p^{(\Psi(\varphi_p))} \quad \text{and} \quad C_{G_p}(\varphi_p) = C_{G_p}(\Psi(\varphi_p)).$$

Moreover, from $\lambda \circ \varphi_q = \varphi_p$, it is easy to see that $\lambda \circ \Psi(\varphi_q) = \Psi(\varphi_p)$. It follows that

$$\{f|_{V_q^{(\Psi(\varphi_q))}}, \lambda|_{C_{G_q}(\Psi(\varphi_q))}\}$$

is an injection of the chart $\{V_q^{(\Psi(\varphi_q))}, C_{G_q}(\Psi(\varphi_q)), \pi_q^{(\Psi(\varphi_q))}\}$ for $\tilde{Q}_\mathbb{Z}$ at $(q, (\Psi(\varphi_q))_{G_q})$ into the chart $\{V_p^{(\Psi(\varphi_p))}, C_{G_p}(\Psi(\varphi_p)), \pi_p^{(\Psi(\varphi_p))}\}$ for $\tilde{Q}_\mathbb{Z}$ at $(p, (\Psi(\varphi_p))_{G_p})$. With this, it follows that there is a bijection between orbifold charts and injections for each connected component of $\tilde{Q}_{\Gamma,2}$ and its image under $\tilde{\Psi}$, completing the proof. \square

We conclude that for a 3-dimensional closed, effective orbifold Q , the Γ -Euler–Satake characteristics can be determined from the number and type of point singularities of Q as well as the Euler characteristic $\chi_{\text{top}}(\partial_{\text{top}} Q)$. We recall the following, which was also observed in [Carroll and Seaton 2013, Proposition 2.1].

Lemma 3.4. *Let Q be a closed, effective 3-orbifold, let \mathcal{P} denote the collection of point singularities of Q and let Γ be a finitely generated discrete group. Then*

$$\chi_{\text{ES}}(\tilde{Q}_{\Gamma,0}) = \sum_{p \in \mathcal{P}} \frac{|\text{HOM}(\Gamma, G_p)_0|}{|G_p|}.$$

Proof. First, we have by definition of the Euler–Satake characteristic that

$$\chi_{\text{ES}}(\tilde{Q}_{\Gamma,0}) = \sum_{p \in \mathcal{P}} \sum_{(\varphi_p)_{G_p} \in \text{HOM}(\Gamma, G_p)_0 / G_p} \frac{1}{|C_{G_p}(\varphi_p)|}.$$

Using the fact that $|C_{G_p}(\varphi_p)| |(\varphi_p)_{G_p}| = |G_p|$, this is equal to

$$\sum_{p \in \mathcal{P}} \sum_{(\varphi_p)_{G_p} \in \text{HOM}(\Gamma, G_p)_0 / G_p} \frac{|(\varphi_p)_{G_p}|}{|G_p|} = \sum_{p \in \mathcal{P}} \frac{|\text{HOM}(\Gamma, G_p)_0|}{|G_p|}. \quad \square$$

Lemma 3.5. *Let Q be a closed, effective 3-orbifold and let \mathcal{P}_∂ denote the set of point singularities contained in $\partial_{\text{top}} Q$. Then*

$$\chi_{\text{ES}}(\tilde{Q}_{\mathbb{Z},0}) = \frac{1}{2} |\mathcal{P}_{\text{proj}}| + \sum_{p \in \mathcal{P}_\partial} \frac{|\text{HOM}(\mathbb{Z}, G_p)_0|}{|G_p|}.$$

Proof. For each $p \in \mathcal{P}$ such that $G_p \leq \text{SO}(3)$, each element of G_p is a rotation and hence fixes a line. As the image of any element of $\text{HOM}(\mathbb{Z}, G_p)$ must be cyclic, it follows that $\text{HOM}(\mathbb{Z}, G_p)_0 = \emptyset$ for each such p . Recalling that all other point singularities are elements of $\mathcal{P}_{\text{proj}} \cup \mathcal{P}_\partial$ and applying Lemma 3.4, we have

$$\chi_{\text{ES}}(\tilde{Q}_{\mathbb{Z},0}) = \sum_{p \in \mathcal{P}_{\text{proj}}} \frac{|\text{HOM}(\mathbb{Z}, G_p)_0|}{|G_p|} + \sum_{p \in \mathcal{P}_\partial} \frac{|\text{HOM}(\mathbb{Z}, G_p)_0|}{|G_p|}.$$

If $p \in \mathcal{P}_{\text{proj}}$, then G_p is given either by $(\mathbb{Z}/n\mathbb{Z})^*$ for n odd or $(\mathbb{Z}/2n\mathbb{Z})][\mathbb{Z}/n\mathbb{Z}]$ for n even. In the former case, it is easy to see that all elements of $(\mathbb{Z}/n\mathbb{Z})^*$ of the form $A_n^k J$ fix a point, while nontrivial elements of the form A_n^k fix a line, so that

$$\frac{|\text{HOM}(\mathbb{Z}, (\mathbb{Z}/n\mathbb{Z})^*)_0|}{|(\mathbb{Z}/n\mathbb{Z})^*|} = \frac{n}{2n} = \frac{1}{2}.$$

In the latter case, $(\mathbb{Z}/2n\mathbb{Z})][\mathbb{Z}/n\mathbb{Z}]$ is generated by $A_{2n} J$, and odd powers of $A_n J$ fix a point while nontrivial even powers fix a line. We have again

$$\frac{|\text{HOM}(\mathbb{Z}, (\mathbb{Z}/2n\mathbb{Z})][\mathbb{Z}/n\mathbb{Z}])_0|}{|(\mathbb{Z}/2n\mathbb{Z})][\mathbb{Z}/n\mathbb{Z}]|} = \frac{n}{2n} = \frac{1}{2}.$$

The claim follows. □

With this, combining Equation (3-2) and Lemma 3.5 yields

$$\chi_{\text{ES}}(\tilde{Q}_{\mathbb{Z},2}) = \frac{1}{2} \chi_{\text{top}}(\partial_{\text{top}} Q) - \sum_{p \in \mathcal{P}_\partial} \frac{|\text{HOM}(\mathbb{Z}, G_p)_0|}{|G_p|}.$$

Along with Equation (3-1) and Lemmas 3.3 and 3.4, this establishes the following.

Proposition 3.6. *Let Q be a closed, effective 3-orbifold and let Γ be a finitely generated discrete group. Then*

$$\chi_\Gamma^{\text{ES}}(Q) = (|\text{HOM}(\Gamma, \mathbb{Z}/2\mathbb{Z})| - 1) \left(\frac{1}{2} \chi_{\text{top}}(\partial_{\text{top}} Q) - \sum_{p \in \mathcal{P}_\partial} \frac{|\text{HOM}(\mathbb{Z}, G_p)_0|}{|G_p|} \right) + \sum_{p \in \mathcal{P}} \frac{|\text{HOM}(\Gamma, G_p)_0|}{|G_p|}. \quad (3-3)$$

In particular, $\chi_\Gamma^{\text{ES}}(Q)$ depends only on $\chi_{\text{top}}(\partial_{\text{top}} Q)$ and the number and type of point singularities of Q . For $\Gamma = \mathbb{F}_l$, we have

$$\chi_{\mathbb{F}_l}^{\text{ES}}(Q) = \frac{2^l - 1}{2} \chi_{\text{top}}(\partial_{\text{top}} Q) + \sum_{p \in \mathcal{P} \setminus \mathcal{P}_\partial} \frac{|\text{HOM}(\mathbb{F}_l, G_p)_0|}{|G_p|} + \sum_{p \in \mathcal{P}_\partial} \frac{|\text{HOM}(\mathbb{F}_l, G_p)_0| - (2^l - 1)|\text{HOM}(\mathbb{Z}, G_p)_0|}{|G_p|}.$$

3B. Counting point-fixing homomorphisms. In view of Proposition 3.6, to complete the computation of the \mathbb{F}_l -Euler-Satake characteristic of an arbitrary closed, effective 3-orbifold Q , we need only determine the value of $|\text{HOM}(\mathbb{F}_l, G_p)_0|/|G_p|$ for each G_p corresponding to $p \in \mathcal{P} \setminus \mathcal{P}_\partial$ and that of

$$\left(|\text{HOM}(\mathbb{F}_l, G_p)_0| - (2^l - 1)|\text{HOM}(\mathbb{Z}, G_p)_0| \right) / |G_p|$$

for $p \in \mathcal{P}_\partial$. To organize the computations of these quantities, we make the following observations.

Given an arbitrary finitely generated discrete group Γ , for each finite subgroup $G < \text{O}(3)$ corresponding to a point singularity, we have

$$\text{HOM}(\Gamma, G) = \text{HOM}(\Gamma, G)_0 + \text{HOM}(\Gamma, G)_1 + \text{HOM}(\Gamma, G)_2 + \text{HOM}(\Gamma, G)_3.$$

Clearly, $|\text{HOM}(\Gamma, G)_3| = 1$, as only the trivial homomorphism fixes all of \mathbb{R}^3 . Similarly, as the only plane-fixing elements of $\text{O}(3)$ generate a subgroup isomorphic to $\mathbb{Z}/2\mathbb{Z}$, and as a plane in \mathbb{R}^3 is fixed by exactly one nontrivial element of $\text{O}(3)$, $\text{HOM}(\Gamma, G)_2$ contains $c(|\text{HOM}(\Gamma, \mathbb{Z}/2\mathbb{Z})| - 1)$ homomorphisms where c is the number of planes in \mathbb{R}^3 fixed by an element of G . Finally, by inspection, any 1-dimensional singular stratum of $G \backslash \mathbb{R}^3$ has isotropy group $D_{2n}[\mathbb{Z}/n\mathbb{Z}]$ or $\mathbb{Z}/n\mathbb{Z}$. Hence, as each such subgroup fixes a unique line, we have

$$|\text{HOM}(\Gamma, G)_1| = \sum_{n=2}^{\infty} a_n |\text{HOM}(\Gamma, D_{2n}[\mathbb{Z}/n\mathbb{Z}])_1| + b_n |\text{HOM}(\Gamma, \mathbb{Z}/n\mathbb{Z})_1|,$$

where a_n denotes the number of distinct lines in \mathbb{R}^3 with isotropy group $D_{2n}[\mathbb{Z}/n\mathbb{Z}]$ and b_n denotes the number of distinct lines in \mathbb{R}^3 with isotropy group $\mathbb{Z}/n\mathbb{Z}$.

With this, we note that if $\Gamma = \mathbb{F}_l$, then by considering the images of a chosen set of generators for \mathbb{F}_l , it is easy to compute that

$$|\text{HOM}(\mathbb{F}_l, \mathbb{Z}/n\mathbb{Z})_1| = n^l - 1.$$

Recall that $D_{2n}](\mathbb{Z}/n\mathbb{Z})$ is generated by A_n and BJ , where A_n acts as a rotation about the z -axis and BJ as a reflection through the yz -plane. Then there are n plane-fixing elements of the form $A_n^k BJ$ for $0 \leq k \leq n - 1$, and hence $n(2^l - 1)$ elements of $\text{HOM}(\mathbb{F}_l, D_{2n}](\mathbb{Z}/n\mathbb{Z})_2$. Then as each element of $D_{2n}](\mathbb{Z}/n\mathbb{Z})$ fixes the z -axis, there are no point-fixing elements, so that

$$|\text{HOM}(\mathbb{F}_l, D_{2n}](\mathbb{Z}/n\mathbb{Z}))_1| = (2n)^l - n(2^l - 1) - 1.$$

We summarize these observations with the following.

Lemma 3.7. *Let G be a finite subgroup of $O(3)$. For each $n \geq 2$, let a_n denote the number of lines in \mathbb{R}^3 with isotropy group $D_{2n}](\mathbb{Z}/n\mathbb{Z})$, let b_n denote the number of lines in \mathbb{R}^3 with isotropy group $\mathbb{Z}/n\mathbb{Z}$, and let c denote the number of planes in \mathbb{R}^3 fixed by a nontrivial element of G . Then for each $l \geq 1$,*

$$|\text{HOM}(\mathbb{F}_l, G)_0| = |G|^l - c(2^l - 1) - 1 - \sum_{n=2}^{\infty} a_n((2n)^l - 2^l n + n - 1) + b_n(n^l - 1).$$

We will now apply this result to each of the point-fixing subgroups of $O(3)$. To simplify the notation, for a finite $G < O(3)$ such that $G \setminus \mathbb{R}^3$ has nonempty topological boundary (i.e., G is the isotropy group of a point singularity $p \in \mathcal{P}_\partial$), we let

$$\mathbf{S}_\partial(G) := \frac{|\text{HOM}(\mathbb{F}_l, G)_0| - (2^l - 1)|\text{HOM}(\mathbb{Z}, G)_0|}{|G|}$$

denote the corresponding term of $\chi_{\mathbb{F}_l}^{\text{ES}}(Q)$ in Proposition 3.6.

$G = (\mathbb{Z}/n\mathbb{Z})^*$. Recall that $(\mathbb{Z}/n\mathbb{Z})^*$ has order $2n$, and first assume n is even. Then $(\mathbb{Z}/n\mathbb{Z})^*$ contains one plane-fixing element $A_n^{n/2} J$ so that $c = 1$, and a point with isotropy group $(\mathbb{Z}/n\mathbb{Z})^*$ is contained in \mathcal{P}_∂ . The z -axis is the only line in \mathbb{R}^3 with nontrivial isotropy $\mathbb{Z}/n\mathbb{Z}$, and so $a_k = 0$ for each k , $b_n = 1$, and $b_k = 0$ for $k \neq n$. Applying Lemma 3.7,

$$|\text{HOM}(\mathbb{F}_l, (\mathbb{Z}/n\mathbb{Z})^*)_0| = (n^l - 1)(2^l - 1) \quad (n \text{ even}),$$

and in particular $|\text{HOM}(\mathbb{Z}, (\mathbb{Z}/n\mathbb{Z})^*)_0| = n - 1$. Then

$$\mathbf{S}_\partial(((\mathbb{Z}/n\mathbb{Z})^*)_0) = \frac{2^l - 1}{2}(n^{l-1} - 1), \quad (n \text{ even}). \tag{3-4}$$

For n odd, $(\mathbb{Z}/n\mathbb{Z})^*$ contains no plane-fixing elements so that $c = 0$, and a point with isotropy group $(\mathbb{Z}/n\mathbb{Z})^*$ is an element of $\mathcal{P} \setminus \mathcal{P}_\partial$. The z -axis is again the only

line in \mathbb{R}^3 with nontrivial isotropy $\mathbb{Z}/n\mathbb{Z}$ so the a_k and b_k vanish except for $b_n = 1$. Again applying Lemma 3.7,

$$|\text{HOM}(\mathbb{F}_l, (\mathbb{Z}/n\mathbb{Z})^*)_0| = n^l(2^l - 1) \quad (n \text{ odd}),$$

and so

$$\frac{|\text{HOM}(\mathbb{F}_l, (\mathbb{Z}/n\mathbb{Z})^*)_0|}{|(\mathbb{Z}/n\mathbb{Z})^*|} = \frac{2^l - 1}{2} n^{l-1} \quad (n \text{ odd}). \tag{3-5}$$

$G = (\mathbb{Z}/2n\mathbb{Z})][\mathbb{Z}/n\mathbb{Z}]$. We again have $(\mathbb{Z}/2n\mathbb{Z})][\mathbb{Z}/n\mathbb{Z}]$ has order $2n$. Assume n is even. Then $(\mathbb{Z}/2n\mathbb{Z})][\mathbb{Z}/n\mathbb{Z}]$ contains no plane-fixing elements, so $c = 0$, and the corresponding point singularity is in $\mathcal{P} \setminus \mathcal{P}_\partial$. Other than the origin, only the z -axis has nontrivial isotropy $\mathbb{Z}/n\mathbb{Z}$, so the computation is identical to the case of $(\mathbb{Z}/n\mathbb{Z})^*$ for n odd given in Equation (3-5) above. That is,

$$\frac{|\text{HOM}(\mathbb{F}_l, (\mathbb{Z}/2n\mathbb{Z})][\mathbb{Z}/n\mathbb{Z}])_0|}{|(\mathbb{Z}/2n\mathbb{Z})][\mathbb{Z}/n\mathbb{Z}]|} = \frac{2^l - 1}{2} n^{l-1} \quad (n \text{ even}). \tag{3-6}$$

If n is odd, then $(\mathbb{Z}/2n\mathbb{Z})][\mathbb{Z}/n\mathbb{Z}]$ contains one plane-fixing element $(A_{2n}J)^n$, and one line in \mathbb{R}^3 is fixed by $\mathbb{Z}/n\mathbb{Z}$. The point singularity is contained in \mathcal{P}_∂ , and the computation is identical to the case of $(\mathbb{Z}/n\mathbb{Z})^*$ for n even in Equation (3-4). Hence,

$$\mathbf{S}_\partial((\mathbb{Z}/2n\mathbb{Z})][\mathbb{Z}/n\mathbb{Z}]) = \frac{2^l - 1}{2} (n^{l-1} - 1) \quad (n \text{ odd}). \tag{3-7}$$

$G = D_{2n}^*$. Recall that D_{2n}^* has order $4n$. Suppose n is even. There are $n + 1$ plane-fixing elements given by $A_n^{n/2}J$ and A_n^kBJ for $k = 0, \dots, n - 1$ so that $c = n + 1$ and the point singularity is an element of \mathcal{P}_∂ . The z -axis has isotropy $D_{2n}][\mathbb{Z}/n\mathbb{Z}]$, and the n lines spanned by $(\cos(k\pi/n), \sin(k\pi/n), 0)$ for $0 \leq k \leq n - 1$ have isotropy $D_4][\mathbb{Z}/2\mathbb{Z}]$. Therefore, $a_2 = n$, $a_n = 1$, and the other a_k and b_k vanish, so that by Lemma 3.7,

$$|\text{HOM}(\mathbb{F}_l, D_{2n}^*)_0| = (2^l - 1)((2n)^l - 2^l n + n - 1), \quad (n \text{ even}).$$

Therefore,

$$\mathbf{S}_\partial(D_{2n}^*) = 2^{l-2}(2^l - 1)(n^{l-1} - 1) \quad (n \text{ even}). \tag{3-8}$$

If n is odd, there are n plane-fixing elements A_n^kBJ for $k = 0, \dots, n - 1$ so $c = n$. A $D_{2n}][\mathbb{Z}/n\mathbb{Z}]$ subgroup fixes the z -axis, and n lines in the xy -plane have isotropy $\langle A^k B \rangle \cong \mathbb{Z}/2\mathbb{Z}$, so that $a_n = 1$, $b_2 = n$, and all others vanish. This yields

$$|\text{HOM}(\mathbb{F}_l, D_{2n}^*)_0| = (2^l - 1)((2n)^l - n), \quad (n \text{ odd}),$$

and so

$$\mathbf{S}_\partial(D_{2n}^*) = \frac{2^l - 1}{2} ((2n)^{l-1} - 1), \quad (n \text{ odd}). \tag{3-9}$$

$G = \mathbb{T}^*$. In this case, the plane fixing elements are the three conjugates of CJ . We have $c = 3$, $a_2 = 3$, $b_3 = 4$, and all a_k and b_k vanish. Then Lemma 3.7 yields

$$|\text{HOM}(\mathbb{F}_l, \mathbb{T}^*)_0| = (24)^l - 3 \cdot 4^l + 3 \cdot 2^l + 3,$$

and

$$\mathbf{S}_\partial(\mathbb{T}^*) = \frac{1}{2}(2 \cdot 24^{l-1} - 4^{l-1} - 3^{l-1} - 2^{l-1} + 1). \tag{3-10}$$

$G = \mathbb{O}^*$. Here, the plane fixing elements are the three conjugates of S^2J and the six conjugates of RJ . We have $c = 9$, $a_2 = 6$, $a_3 = 4$, $a_4 = 3$, and all others vanish. Applying Lemma 3.7,

$$|\text{HOM}(\mathbb{F}_l, \mathbb{O}^*)_0| = 48^l - 3 \cdot 8^l - 4 \cdot 6^l - 6 \cdot 4^l + 27 \cdot 2^l - 15,$$

and

$$\mathbf{S}_\partial(\mathbb{O}^*) = 2^{l-2}(2 \cdot 24^{l-1} - 4^{l-1} - 3^{l-1} - 2^{l-1} + 1). \tag{3-11}$$

$G = \mathbb{I}^*$. The plane fixing elements are the fifteen conjugates of BJ . We have $c = 15$, $a_2 = 15$, $a_3 = 10$, $a_5 = 6$, and the others vanish, so by Lemma 3.7,

$$|\text{HOM}(\mathbb{F}_l, \mathbb{I}^*)_0| = 120^l - 6 \cdot 10^l - 10 \cdot 6^l - 15 \cdot 4^l + 75 \cdot 2^l - 45,$$

and

$$\mathbf{S}_\partial(\mathbb{I}^*) = 2^{l-2}(2 \cdot 60^{l-1} - 5^{l-1} - 3^{l-1} - 2^{l-1} + 1). \tag{3-12}$$

$G = D_{4n}]D_{2n}$. Assume n is even, and then the plane fixing elements are $(A_{2n}J)^k B$ for k odd. Then $c = n$, $a_n = 1$, $b_2 = n$, and the other a_k and b_k vanish. Hence

$$|\text{HOM}(\mathbb{F}_l, D_{4n}]D_{2n})_0| = (2^l - 1)((2n)^l - n) \quad (n \text{ even}),$$

and

$$\mathbf{S}_\partial(D_{4n}]D_{2n}) = \frac{2^l - 1}{2}((2n)^{l-1} - 1) \quad (n \text{ even}). \tag{3-13}$$

If n is odd, then the plane fixing elements are $(A_{2n}J)^n$ and $(A_{2n}J)^k B$ for k odd. Hence $c = n + 1$, $a_2 = n$, $a_n = 1$, and the other a_k and b_k vanish so that

$$|\text{HOM}(\mathbb{F}_l, D_{4n}]D_{2n})_0| = (2^l - 1)((2n)^l - 2^l n + n - 1), \quad (n \text{ odd}),$$

and

$$\mathbf{S}_\partial(D_{4n}]D_{2n}) = 2^{l-2}(2^l - 1)(n^{l-1} - 1), \quad (n \text{ odd}). \tag{3-14}$$

$G = \mathbb{O}] \mathbb{T}$. In this case, the six plane fixing elements are the conjugates of RJ . We have $c = 6$, $a_2 = 3$, $a_3 = 4$, and the other a_k and b_k vanish. Therefore

$$|\text{HOM}(\mathbb{F}_l, \mathbb{O}] \mathbb{T})_0| = 24^l - 4 \cdot 6^l - 3 \cdot 4^l + 3 \cdot 2^{l+2} - 6,$$

and

$$\mathbf{S}_\partial(\mathbb{O}] \mathbb{T}) = 2^{l-2}(2 \cdot 12^{l-1} - 2 \cdot 3^{l-1} - 2^{l-1} + 1). \tag{3-15}$$

3C. The \mathbb{F}_l -Euler–Satake characteristics of a closed, effective 3-orbifold. Combining Proposition 3.6 with Equations (3-4) through (3-15) as well as [Carroll and Seaton 2013, Theorem 3.1], which computes the terms associated to the finite subgroups of $\mathrm{SO}(3)$, we have the following.

Theorem 3.8. *Let Q be a closed, effective 3-orbifold with:*

- \mathfrak{t} point singularities with isotropy \mathbb{T} ;
- \mathfrak{o} point singularities with isotropy \mathbb{O} ;
- \mathfrak{i} point singularities with isotropy \mathbb{I} ;
- \mathfrak{d} point singularities with isotropy D_{2n} for each n ;
- \mathfrak{c}_n^{e*} point singularities with isotropy $(\mathbb{Z}/n\mathbb{Z})^*$ for each even n ;
- \mathfrak{c}_n^{o*} point singularities with isotropy $(\mathbb{Z}/n\mathbb{Z})^*$ for each odd n ;
- \mathfrak{t}^* point singularities with isotropy \mathbb{T}^* ;
- \mathfrak{o}^* point singularities with isotropy \mathbb{O}^* ;
- \mathfrak{i}^* point singularities with isotropy \mathbb{I}^* ;
- \mathfrak{d}_n^{e*} point singularities with isotropy D_{2n}^* for each even n ;
- \mathfrak{d}_n^{o*} point singularities with isotropy D_{2n}^* for each odd n ;
- \mathfrak{c}_n^{em} point singularities with isotropy $(\mathbb{Z}/2\mathbb{Z}][\mathbb{Z}/n\mathbb{Z})$ for each even n ;
- \mathfrak{c}_n^{om} point singularities with isotropy $(\mathbb{Z}/2n\mathbb{Z}][\mathbb{Z}/n\mathbb{Z})$ for each odd n ;
- \mathfrak{d}_n^{em} point singularities with isotropy $D_{4n}][D_{2n}$ for each even n ;
- \mathfrak{d}_n^{om} point singularities with isotropy $D_{4n}][D_{2n}$ for each odd n ;
- \mathfrak{o}^m point singularities with isotropy $\mathbb{O}][\mathbb{T}$.

Then

$$\begin{aligned} \chi_{\mathbb{F}_l}^{\mathrm{ES}}(Q) &= \frac{2^l - 1}{2} \chi_{\mathrm{top}}(\partial_{\mathrm{top}} Q) + \frac{\mathfrak{t}}{2} (2 \cdot 12^{l-1} - 2 \cdot 3^{l-1} - 2^{l-1} + 1) \\ &\quad + \frac{\mathfrak{o}}{2} (2 \cdot 24^{l-1} - 4^{l-1} - 3^{l-1} - 2^{l-1} + 1) \\ &\quad + \frac{\mathfrak{i}}{2} (2 \cdot 60^{l-1} - 5^{l-1} - 3^{l-1} - 2^{l-1} + 1) \\ &\quad + \frac{\mathfrak{t}^*}{2} (2 \cdot 24^{l-1} - 4^{l-1} - 3^{l-1} - 2^{l-1} + 1) \\ &\quad + 2^{l-2} \mathfrak{o}^* (2 \cdot 24^{l-1} - 4^{l-1} - 3^{l-1} - 2^{l-1} + 1) \\ &\quad + 2^{l-2} \mathfrak{i}^* (2 \cdot 60^{l-1} - 5^{l-1} - 3^{l-1} - 2^{l-1} + 1) \\ &\quad + \mathfrak{o}^m [2^{l-2} (2 \cdot 12^{l-1} - 2 \cdot 3^{l-1} - 2^{l-1} + 1)] \\ &\quad + \left(\frac{2^l - 1}{2} \right) \sum_{n=1}^{\infty} (\mathfrak{d}_n (n^{l-1} - 1) + \mathfrak{c}_n^{e*} (n^{l-1} - 1) + \mathfrak{c}_n^{o*} n^{l-1} \\ &\quad + \mathfrak{d}_n^{e*} 2^{l-1} (n^{l-1} - 1) + \mathfrak{d}_n^{o*} ((2n)^{l-1} - 1) + \mathfrak{c}_n^{em} n^{l-1} \\ &\quad + \mathfrak{c}_n^{om} (n^{l-1} - 1) + \mathfrak{d}_n^{em} ((2n)^{l-1} - 1) + \mathfrak{c}_n^{om} 2^{l-1} (n^{l-1} - 1)). \end{aligned}$$

We note that a closed orbifold Q has a finite number of point singularities, and hence there is a finite number of nonzero terms in the sum over n .

4. Indistinguishable orbifolds

Based on Theorem 3.8, it is easy to see that, in contrast with the orientable case, no collection of the $\chi_{\Gamma}^{\text{ES}}(Q)$ determine the point singularities of the closed, effective 3-orbifold Q . In fact, in this section, we describe a pair of closed, effective 3-orbifolds Q_1 and Q_2 such that $\chi_{\Gamma}^{\text{ES}}(Q_1) = \chi_{\Gamma}^{\text{ES}}(Q_2)$ for every finitely generated discrete group Γ .

Let n be an odd integer and let \bar{B}^3 denote the closed unit ball in \mathbb{R}^3 . Let Q_1 be the orbifold formed by gluing together two copies of $(\mathbb{Z}/n\mathbb{Z})^* \setminus \bar{B}^3$ along $(\mathbb{Z}/n\mathbb{Z})^* \setminus \mathbb{S}^2$ so that Q_1 has two point singularities with isotropy $(\mathbb{Z}/n\mathbb{Z})^*$ connected by a segment with isotropy $\mathbb{Z}/n\mathbb{Z}$. See Figure 4, left.

Let Q_2 be the orbifold formed by gluing together two copies of

$$(\mathbb{Z}/2n\mathbb{Z}) \rfloor (\mathbb{Z}/n\mathbb{Z}) \setminus \bar{B}^3$$

along $(\mathbb{Z}/2n\mathbb{Z}) \rfloor (\mathbb{Z}/n\mathbb{Z}) \setminus \mathbb{S}^2$ so that $\partial_{\text{top}} Q_2$ is homomorphic to \mathbb{S}^2 and contains two point singularities with isotropy $(\mathbb{Z}/2n\mathbb{Z}) \rfloor (\mathbb{Z}/n\mathbb{Z})$ connected by a segment with isotropy $\mathbb{Z}/n\mathbb{Z}$ contained in the complement of $\partial_{\text{top}} Q_2$. See Figure 4, right.

Let Γ be an arbitrary finitely generated discrete group. Note that $\partial_{\text{top}} Q_1$ is empty so that Proposition 3.6 yields

$$\chi_{\Gamma}^{\text{ES}}(Q_1) = 2 \frac{|\text{HOM}(\Gamma, (\mathbb{Z}/n\mathbb{Z})^*)_0|}{|(\mathbb{Z}/n\mathbb{Z})^*|} = \frac{|\text{HOM}(\Gamma, (\mathbb{Z}/n\mathbb{Z})^*)_0|}{n}.$$

A nontrivial homomorphism $\varphi : \Gamma \rightarrow (\mathbb{Z}/n\mathbb{Z})^*$ corresponds to a 1-dimensional

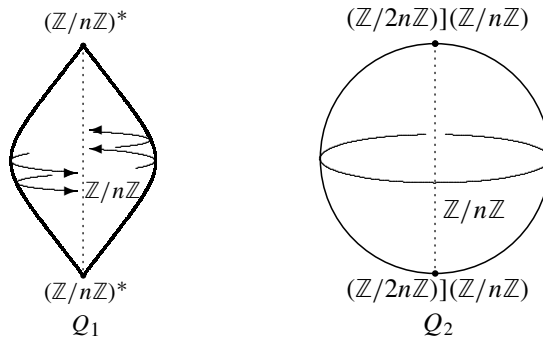


Figure 4. The orbifolds Q_1 and Q_2 . Note that the boundary of the region describing Q_1 is identified antipodally in horizontal planes as indicated by the curved arrows, while Q_2 has (topological) boundary homeomorphic to \mathbb{S}^2 .

sector if its image is contained in $(\mathbb{Z}/n\mathbb{Z})^* \cap \mathrm{SO}(3) = \mathbb{Z}/n\mathbb{Z}$. So using the fact that $(\mathbb{Z}/n\mathbb{Z})^*$ is isomorphic to $\mathbb{Z}/2n\mathbb{Z}$, we have

$$\chi_{\Gamma}^{\mathrm{ES}}(Q_1) = \frac{|\mathrm{HOM}(\Gamma, \mathbb{Z}/2n\mathbb{Z})| - |\mathrm{HOM}(\Gamma, \mathbb{Z}/n\mathbb{Z})|}{n}.$$

In the case of Q_2 , we have $\partial_{\mathrm{top}} Q_2 = \mathbb{S}^2$ so that $\chi_{\mathrm{top}}(\partial_{\mathrm{top}} Q_2) = 2$. Therefore, Proposition 3.6 yields

$$\begin{aligned} \chi_{\Gamma}^{\mathrm{ES}}(Q_2) = (|\mathrm{HOM}(\Gamma, \mathbb{Z}/2\mathbb{Z})| - 1) & \left(1 - 2 \frac{|\mathrm{HOM}(\mathbb{Z}, (\mathbb{Z}/2n\mathbb{Z})[(\mathbb{Z}/n\mathbb{Z}))_0]|}{|(\mathbb{Z}/2n\mathbb{Z})[(\mathbb{Z}/n\mathbb{Z})]} \right) \\ & + 2 \frac{|\mathrm{HOM}(\Gamma, (\mathbb{Z}/2n\mathbb{Z})[(\mathbb{Z}/n\mathbb{Z}))_0]|}{|(\mathbb{Z}/2n\mathbb{Z})[(\mathbb{Z}/n\mathbb{Z})]} . \end{aligned}$$

Then $\mathrm{HOM}(\mathbb{Z}, (\mathbb{Z}/2n\mathbb{Z})[(\mathbb{Z}/n\mathbb{Z})])$ contains $2n$ elements, of which the $n-1$ nontrivial elements of $(\mathbb{Z}/2n\mathbb{Z})[(\mathbb{Z}/n\mathbb{Z})] \cap \mathrm{SO}(3) = \mathbb{Z}/n\mathbb{Z}$ correspond to 1-dimensional sectors, so that $|\mathrm{HOM}(\mathbb{Z}, (\mathbb{Z}/2n\mathbb{Z})[(\mathbb{Z}/n\mathbb{Z}))_0]| = n$. It follows that

$$1 - 2 \frac{|\mathrm{HOM}(\mathbb{Z}, (\mathbb{Z}/2n\mathbb{Z})[(\mathbb{Z}/n\mathbb{Z}))_0]|}{|(\mathbb{Z}/2n\mathbb{Z})[(\mathbb{Z}/n\mathbb{Z})]} = 0.$$

Therefore, as $(\mathbb{Z}/2n\mathbb{Z})[(\mathbb{Z}/n\mathbb{Z})]$ is isomorphic to $\mathbb{Z}/2n\mathbb{Z}$,

$$\chi_{\Gamma}^{\mathrm{ES}}(Q_2) = \frac{|\mathrm{HOM}(\Gamma, \mathbb{Z}/2n\mathbb{Z})| - |\mathrm{HOM}(\Gamma, \mathbb{Z}/n\mathbb{Z})|}{n}.$$

Hence $\chi_{\Gamma}^{\mathrm{ES}}(Q_1) = \chi_{\Gamma}^{\mathrm{ES}}(Q_2)$ for every finitely generated discrete group Γ .

Acknowledgements

This paper is the result of the first author's honors research project in the Rhodes College Department of Mathematics and Computer Science, and the authors gratefully acknowledge the support of the department and college for these activities. In addition, the authors would like to thank Silvio Levy for assistance with the figures in this paper.

References

- [Adem and Ruan 2003] A. Adem and Y. Ruan, "Twisted orbifold K -theory", *Comm. Math. Phys.* **237**:3 (2003), 533–556. MR 2004e:19004 Zbl 1051.57022
- [Adem et al. 2007] A. Adem, J. Leida, and Y. Ruan, *Orbifolds and stringy topology*, Cambridge Tracts in Mathematics **171**, Cambridge University Press, 2007. MR 2009a:57044 Zbl 1157.57001
- [Atiyah and Segal 1989] M. Atiyah and G. Segal, "On equivariant Euler characteristics", *J. Geom. Phys.* **6**:4 (1989), 671–677. MR 92c:19005 Zbl 0708.19004
- [Benson and Grove 1971] C. T. Benson and L. C. Grove, *Finite reflection groups*, Bogden & Quigley, Publishers, Tarrytown-on-Hudson, N.Y., 1971. MR 52 #4099

- [Boileau et al. 2003] M. Boileau, S. Maillot, and J. Porti, *Three-dimensional orbifolds and their geometric structures*, Panoramas et Synthèses **15**, Soc. Math. de France, Paris, 2003. MR 2005b:57030 Zbl 1058.57009
- [Bryan and Fulman 1998] J. Bryan and J. Fulman, “Orbifold Euler characteristics and the number of commuting m -tuples in the symmetric groups”, *Ann. Comb.* **2**:1 (1998), 1–6. MR 2000f:20002 Zbl 0921.55003
- [Carroll and Seaton 2013] R. Carroll and C. Seaton, “Extensions of the Euler–Satake characteristic determine point singularities of orientable 3-orbifolds”, *Kodai Math. J.* **36**:1 (2013), 179–188. MR 3043409 Zbl 06165622
- [Chen and Ruan 2002] W. Chen and Y. Ruan, “Orbifold Gromov–Witten theory”, pp. 25–85 in *Orbifolds in mathematics and physics* (Madison, WI, 2001), edited by A. Adem et al., Contemp. Math. **310**, Amer. Math. Soc., Providence, RI, 2002. MR 2004k:53145 Zbl 1091.53058
- [Chen and Ruan 2004] W. Chen and Y. Ruan, “A new cohomology theory of orbifold”, *Comm. Math. Phys.* **248**:1 (2004), 1–31. MR 2005j:57036 Zbl 1063.53091
- [Dixon et al. 1985] L. Dixon, J. A. Harvey, C. Vafa, and E. Witten, “Strings on orbifolds”, *Nuclear Phys. B* **261**:4 (1985), 678–686. MR 87k:81104a
- [Duval et al. 2010] W. Duval, J. Schulte, C. Seaton, and B. Taylor, “Classifying closed 2-orbifolds with Euler characteristics”, *Glasg. Math. J.* **52**:3 (2010), 555–574. MR 2011g:57029 Zbl 1211.57016
- [Farsi and Seaton 2010a] C. Farsi and C. Seaton, “Generalized twisted sectors of orbifolds”, *Pacific J. Math.* **246**:1 (2010), 49–74. MR 2011g:57030 Zbl 1189.22004
- [Farsi and Seaton 2010b] C. Farsi and C. Seaton, “Nonvanishing vector fields on orbifolds”, *Trans. Amer. Math. Soc.* **362**:1 (2010), 509–535. MR 2011a:57051 Zbl 1196.57025
- [Farsi and Seaton 2011] C. Farsi and C. Seaton, “Generalized orbifold Euler characteristics for general orbifolds and wreath products”, *Algebr. Geom. Topol.* **11**:1 (2011), 523–551. MR 2012h:57048 Zbl 1213.22005
- [Iglesias et al. 2010] P. Iglesias, Y. Karshon, and M. Zadka, “Orbifolds as diffeologies”, *Trans. Amer. Math. Soc.* **362**:6 (2010), 2811–2831. MR 2011d:57067 Zbl 1197.57025
- [Kawasaki 1978] T. Kawasaki, “The signature theorem for V -manifolds”, *Topology* **17**:1 (1978), 75–83. MR 57 #14072 Zbl 0392.58009
- [Lerman 2010] E. Lerman, “Orbifolds as stacks?”, *Enseign. Math.* (2) **56**:3-4 (2010), 315–363. MR 2012c:18010 Zbl 1221.14003
- [Moerdijk 2002] I. Moerdijk, “Orbifolds as groupoids: an introduction”, pp. 205–222 in *Orbifolds in mathematics and physics* (Madison, WI, 2001), edited by A. Adem et al., Contemp. Math. **310**, Amer. Math. Soc., Providence, RI, 2002. MR 2004c:22003 Zbl 1041.58009
- [Moerdijk and Mrčun 2003] I. Moerdijk and J. Mrčun, *Introduction to foliations and Lie groupoids*, Cambridge Studies in Advanced Mathematics **91**, Cambridge University Press, 2003. MR 2005c:58039
- [Moerdijk and Pronk 1997] I. Moerdijk and D. A. Pronk, “Orbifolds, sheaves and groupoids”, *K-Theory* **12**:1 (1997), 3–21. MR 98i:22004 Zbl 0883.22005
- [Roan 1996] S.-S. Roan, “Minimal resolutions of Gorenstein orbifolds in dimension three”, *Topology* **35**:2 (1996), 489–508. MR 97c:14013 Zbl 0872.14034
- [Satake 1957] I. Satake, “The Gauss–Bonnet theorem for V -manifolds”, *J. Math. Soc. Japan* **9** (1957), 464–492. MR 20 #2022 Zbl 0080.37403
- [Schulte et al. 2011] J. Schulte, C. Seaton, and B. Taylor, “Free and free abelian Euler–Satake characteristics of nonorientable 2-orbifolds”, *Topology Appl.* **158**:16 (2011), 2244–2255. MR 2831914 Zbl 1237.57029

[Scott 1983] P. Scott, “The geometries of 3-manifolds”, *Bull. London Math. Soc.* **15**:5 (1983), 401–487. MR 84m:57009 Zbl 0561.57001

[Seaton 2008] C. Seaton, “Two Gauss–Bonnet and Poincaré–Hopf theorems for orbifolds with boundary”, *Differential Geom. Appl.* **26**:1 (2008), 42–51. MR 2009b:53135

[Tamanoi 2001] H. Tamanoi, “Generalized orbifold Euler characteristic of symmetric products and equivariant Morava K -theory”, *Algebr. Geom. Topol.* **1** (2001), 115–141. MR 2002e:57052 Zbl 0965.57033

[Tamanoi 2003] H. Tamanoi, “Generalized orbifold Euler characteristics of symmetric orbifolds and covering spaces”, *Algebr. Geom. Topol.* **3** (2003), 791–856. MR 2005j:57025 Zbl 1037.57022

[Thurston 1997] W. P. Thurston, *Three-dimensional geometry and topology*, vol. 1, Princeton Mathematical Series **35**, Princeton University Press, 1997. MR 97m:57016 Zbl 0873.57001

Received: 2012-08-10 Accepted: 2012-10-10

racarrol@ucsc.edu

*Department of Mathematics, University of California,
Santa Cruz, CA 95064, United States*

seatonc@rhodes.edu

*Department of Mathematics and Computer Science,
Rhodes College, 2000 North Parkway, Memphis, TN 38112,
United States*

Rank numbers of graphs that are combinations of paths and cycles

Brianna Blake, Elizabeth Field and Jobby Jacob

(Communicated by Joseph A. Gallian)

A k -ranking of a graph G is a function $f : V(G) \rightarrow \{1, 2, \dots, k\}$ such that if $f(u) = f(v)$, then every u - v path contains a vertex w such that $f(w) > f(u)$. The rank number of G , denoted $\chi_r(G)$, is the minimum k such that a k -ranking exists for G . It is shown that given a graph G and a positive integer t , the question of whether $\chi_r(G) \leq t$ is NP-complete. However, the rank number of numerous families of graphs have been established. We study and establish rank numbers of some more families of graphs that are combinations of paths and cycles.

1. Introduction

Let G be an undirected graph with no loops and no multiple edges. A function $f : V(G) \rightarrow \{1, 2, \dots, k\}$ is a (vertex) k -ranking of G if for $u, v \in V(G)$, $f(u) = f(v)$ implies that every u - v path contains a vertex w such that $f(w) > f(u)$. By definition, every ranking is a proper coloring. The *rank number* of G , denoted $\chi_r(G)$, is the minimum value of k such that G has a k -ranking. If the value of k is not important then f will be referred to simply as a ranking of G .

Interest in rankings of graphs was sparked by its many applications to other fields, including designs of very large scale integration (VLSI) layouts, Cholesky factorizations of matrices in parallel, and scheduling problems of assembly steps in manufacturing systems [Duff and Reid 1983; Iyer et al. 1991; Leiserson 1980; Liu 1990; Sen et al. 1992]. The optimal tree node ranking problem is identical to the problem of generating a minimum-height node separator tree for a tree. Node separator trees are extensively used in VLSI layout [Leiserson 1980]. Ranking of graphs is used in communication networks in which information flow between the nodes has to be monitored. An application of graph ranking to scheduling of assembly steps in manufacturing system is discussed in [Iyer et al. 1991].

MSC2010: primary 05C15, 05C78; secondary 05C38.

Keywords: ranking, k -ranking, rank number, paths, cycles.

Research was supported by the National Science Foundation and the Department of Defense under the NSF-REU site award 1062128.

Bodlaender et al. [1995] show that for a graph G and a positive integer t , the question of whether $\chi_r(G) \leq t$ is NP-complete. However, the rank number of numerous families of graphs have been established [Alpert 2010; Bruoth and Horňák 1999; Dereniowski and Nadolski 2006; Hsieh 2002; Novotny et al. 2009; Ortiz et al. 2010; Sergel et al. 2011]. Bodlaender et al. [1995] established that $\chi_r(P_n) = \lfloor \log_2 n \rfloor + 1$, where P_n is a path on n vertices. They showed that a k -ranking for $P_n = v_1 v_2 \cdots v_n$, where $k = \chi_r(P_n)$, can be obtained by labeling v_i with $\gamma + 1$, where 2^γ is the largest power of 2 that divides i . Throughout this paper, this particular scheme of ranking of a path will be referred as a standard ranking.

In this paper, we study and establish rank numbers of some more families of graphs, called flower graphs, lollipop graphs, star-flower graphs, and spider-flower graphs, which are defined in the following sections. These graphs can be considered as combinations of paths and cycles. We restate some known results that are used throughout this paper.

Lemma 1 [Ghoshal et al. 1996]. *Let H be a subgraph of G . Then $\chi_r(H) \leq \chi_r(G)$.*

Lemma 2 [Sergel et al. 2011]. *Let H_1 and H_2 be two vertex-disjoint graphs such that $\chi_r(H_1) = \chi_r(H_2) = k$. Let G be a connected supergraph of $H_1 \cup H_2$. Then $\chi_r(G) \geq k + 1$.*

Theorem 3 [Bodlaender et al. 1995]. *$\chi_r(P_n) = \lfloor \log_2 n \rfloor + 1$, where P_n is a path on n vertices.*

If z is an integer, any ranking of P_{2^z} must have a label $r > z$. Hence:

Lemma 4. *Let $\chi_r(P_n) = j$, and let f be a χ_r -ranking of P_n such that $f(v_n) = k < j$, where v_n is an end vertex of P_n . Then $n \leq \sum_{i=k}^j 2^{i-1}$.*

The rank number of a cycle on n vertices, where $n \geq 3$, is as follows:

Theorem 5 [Bruoth and Horňák 1999]. *$\chi_r(C_n) = \lceil \log_2 n \rceil + 1$, where C_n is a cycle on $n > 2$ vertices.*

2. Flower graphs

A *flower graph* is a graph consisting of c cycles that share a common vertex. Figure 1 gives an example.

Theorem 6. *Let G be a flower graph where C_n is the largest cycle in G . Then $\chi_r(G) = \chi_r(C_n)$.*

Proof. Let G be a flower graph with largest cycle C_n and let $\chi_r(C_n) = k$. Since C_n is a subgraph of G , we have $\chi_r(G) \geq k$ by Lemma 1.

Now, consider a labeling f such that each cycle is given its χ_r -ranking so that the vertex with the largest label would be the center vertex x . Then, let $f(x) = k$. This is a valid k -ranking of G , since for any two vertices u, v on the same cycle in G , if

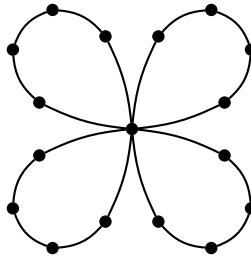


Figure 1. A flower graph where all of the cycles are the same size.

$f(u) = f(v)$, then any u - v path will contain some vertex w such that $f(w) > f(u)$ because f restricted to each cycle is a valid ranking. In addition, if the two vertices are on different cycles, then any u - v path will contain x , and $f(x) = k > f(u)$.

Therefore, $k \leq \chi_r(G) \leq k$ and $\chi_r(G) = \chi_r(C_n)$. □

3. Lollipop graphs

A lollipop graph $L_{a,b}$ consists of a path of order a and a cycle of order b joined by an edge, as shown in Figure 2.

In this section, we determine the rank number of $L_{a,b}$ for all values of a and b . In determining the rank number of lollipop graphs, we consider three cases: $\chi_r(P_a) < \chi_r(C_b)$, $\chi_r(P_a) = \chi_r(C_b)$, and $\chi_r(P_a) > \chi_r(C_b)$.

Theorem 7. *Let $L_{a,b}$ be a lollipop graph where $\chi_r(P_a) < \chi_r(C_b)$. Then $\chi_r(L_{a,b}) = \chi_r(C_b)$.*

Proof. Let $L_{a,b}$ be a lollipop graph with $\chi_r(P_a) < \chi_r(C_b)$ and let $\chi_r(C_b) = k$. Since C_b is a subgraph of $L_{a,b}$, $\chi_r(L_{a,b}) \geq k$ by Lemma 1.

Now, consider a labeling f of $L_{a,b}$ where P_a is labeled according to the standard ranking of a path and the cycle C_b is given a valid k -ranking such that the vertex adjacent to P_a is labeled k . Note that f restricted to C_b and P_a respectively are valid rankings. Also, for any two vertices u, v where one is on P_a and the other is on C_b , if $f(u) = f(v)$, then any u - v path will contain the vertex on C_b labeled k , and $k > f(u)$. Thus f is a valid k -ranking.

Thus $k \leq \chi_r(L_{a,b}) \leq k$, and so if $\chi_r(P_a) < \chi_r(C_b)$, then $\chi_r(L_{a,b}) = \chi_r(C_b)$. □

Theorem 8. *If $\chi_r(P_a) = \chi_r(C_b)$, then $\chi_r(L_{a,b}) = \chi_r(P_a) + 1$.*

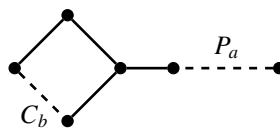


Figure 2. Lollipop graph.

Proof. Let $L_{a,b}$ be a lollipop graph and let $\chi_r(P_a) = \chi_r(C_b) = k$. Since $L_{a,b}$ is the connected supergraph of P_a and C_b , and since $\chi_r(P_a) = \chi_r(C_b) = k$, we have $\chi_r(L_{a,b}) \geq k + 1$ by Lemma 2.

Now, consider a labeling f of $L_{a,b}$ as in the proof of Theorem 7, and let $f(x) = k + 1$, where x is the vertex on C_b that is adjacent to P_a . Clearly f is a valid $(k + 1)$ -ranking, since the restrictions of f to C_b and P_a are valid rankings, and for any two vertices u, v , one on P_a and the other on C_b , if $f(u) = f(v)$, then any u - v path will contain x which is labeled $k + 1$ and $k + 1 > f(u)$.

Therefore $k + 1 \leq \chi_r(L_{a,b}) \leq k + 1$, and so if $\chi_r(P_a) = \chi_r(C_b)$, then $\chi_r(L_{a,b}) = \chi_r(P_a) + 1$. □

Theorem 9. *If $\chi_r(P_a) > \chi_r(C_b)$, then*

$$\chi_r(L_{a,b}) = \begin{cases} \chi_r(P_a) & \text{if } 2^{\chi_r(P_a)-1} \leq a \leq \left(\sum_{i=\chi_r(C_b)}^{\chi_r(P_a)} 2^{i-1} \right) - 1, \\ \chi_r(P_a) + 1 & \text{otherwise.} \end{cases}$$

Proof. Let $L_{a,b}$ be a lollipop graph where $\chi_r(P_a) > \chi_r(C_b)$, and let $\chi_r(P_a) = j$ and $\chi_r(C_b) = k$. Since $L_{a,b}$ can be labeled to have a valid $(j + 1)$ -ranking by giving C_b a valid k -ranking, P_a a valid j -ranking, and by changing the label of the vertex on C_b adjacent to P_a to $j + 1$, we have $\chi_r(L_{a,b}) \leq j + 1$. Also, since P_a is a subgraph of $L_{a,b}$, we have $\chi_r(L_{a,b}) \geq j$ by Lemma 1. Thus, $j \leq \chi_r(L_{a,b}) \leq j + 1$.

Let $L_{a,b}$ be a lollipop graph such that

$$2^{j-1} \leq a \leq \left(\sum_{i=k}^j 2^{i-1} \right) - 1.$$

Now consider a labeling f of $L_{a,b}$ defined as follows. Label C_b so that it has a valid k -ranking, with the vertex adjacent to P_a labeled k . Beginning with the vertex of P_a that is joined to C_b , label the vertices of P_a starting with the label of the $(2^{k-1} + 1)$ -st vertex in the standard ranking of $P_{a+2^{k-1}}$. Since

$$2^{j-1} \leq a \leq \left(\sum_{i=k}^j 2^{i-1} \right) - 1,$$

we have

$$a + 2^{k-1} \leq \left(\sum_{i=k}^j 2^{i-1} \right) - 1 + 2^{k-1} = 2^j - 1.$$

However, $\chi_r(P_{2^j-1}) = j$, which means $\chi_r(P_{a+2^{k-1}}) \leq j$ and thus f uses at most j labels.

Let x be the vertex on C_b that is adjacent to P_a . The restriction of f to P_{a+1} , the induced subgraph induced by $V(P_a) \cup \{x\}$, is part of the standard ranking of $P_{a+2^{k-1}}$ and hence is a valid ranking. Also, f restricted to C_b is a valid ranking, and for any two vertices u, v , one on P_a and the other in $V(C_b) \setminus \{x\}$, if $f(u) = f(v)$, then

any $u-v$ path contains the x and $f(x) = k > f(u)$. Thus f is a valid j -ranking.

Thus, if $\chi_r(P_a) > \chi_r(C_b)$ and $2^{j-1} \leq a \leq (\sum_{i=k}^j 2^{i-1}) - 1$, then $j \leq \chi_r(L_{a,b}) \leq j$, and hence $\chi_r(L_{a,b}) = \chi_r(P_a)$ in this case.

Now, let $L_{a,b}$ be a lollipop graph such that $a > (\sum_{i=k}^j 2^{i-1}) - 1$. Consider any χ_r -ranking of $L_{a,b}$. Since $\chi_r(C_b) = k$, a label of at least $k + \delta < j$, where $\delta \geq 0$, must go on C_b . (Note that if C_b has a label j , and since $\chi_r(P_a) = j$, there must be a label $j + 1$.) Assume, without loss of generality, that $k + \delta$ is the largest label on C_b and that the vertex labeled $k + \delta$ is the vertex which is adjacent to P_a . Then by Lemma 4, if there is no vertex with label $j + 1$ on P_a , then

$$a < \sum_{i=k+\delta}^j 2^{i-1}.$$

This is a contradiction, and thus a vertex on P_a must have label $j + 1$. This means $\chi_r(L_{a,b}) \geq j + 1$. Thus if $\chi_r(P_a) > \chi_r(C_b)$ and $a > (\sum_{i=k}^j 2^{i-1}) - 1$, then $\chi_r(L_{a,b}) = \chi_r(P_a) + 1$. □

4. Star-flower graphs

A star-flower graph is a graph that consists of c vertex-disjoint cycles each appended to a center vertex x by an edge. The largest cycle in a star-flower graph will be referred to as C_n . An example of a star-flower graph is shown in Figure 3.

Theorem 10. *Let G be a star-flower graph such that no two cycles in G have the same rank number. Then $\chi_r(G) = \chi_r(C_n)$.*

Proof. Let G be a star-flower graph where no two cycles in G have the same rank number and let $\chi_r(C_n) = k$. Since C_n is a subgraph of G , $\chi_r(G) \geq k$ by Lemma 1.

Consider a labeling f of G in which each cycle is labeled using its χ_r -ranking such that the vertices which are adjacent to x are labeled with the highest label

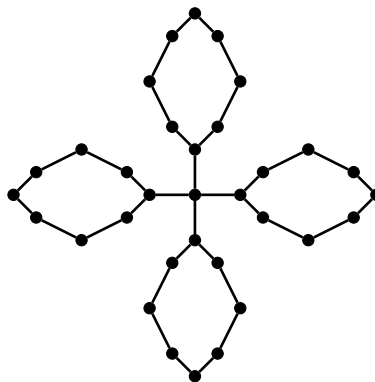


Figure 3. Star-flower graph.

needed in each cycle. Now let $f(x) = 1$. This is a valid k -ranking of G , since f restricted to each cycle is a valid ranking and because for any two vertices u, v with $f(u) = f(v)$, if u and v are on different cycles or one of them is x , then any u - v path contains the vertex on the larger cycle adjacent to x which is greater than $f(u)$. Thus $k \leq \chi_r(G) \leq k$, and hence if no cycles in G have the same rank number, then $\chi_r(G) = \chi_r(C_n)$. \square

Theorem 11. *Let G be a star-flower graph such that G has two or more cycles with the same rank number, and let w be the largest repeated rank number among the cycles. Then, $\chi_r(G) = \chi_r(C_n)$ if there exists q such that $w < q < \chi_r(C_n)$ and such that there is no cycle C in G with $\chi_r(C) = q$. In the opposite case, $\chi_r(G) = \chi_r(C_n) + 1$.*

Proof. Let G be a star-flower graph with two or more cycles with the same rank number, and let w be the largest repeated rank number among the cycles. Also, let $\chi_r(C_n) = k$. Note that $k \leq \chi_r(G) \leq k + 1$. The lower bound follows from Lemma 1, since C_n is a subgraph of G . The upper bound follows from the fact that G can be given a valid $(k + 1)$ -ranking by giving the cycles valid k -rankings and labeling x with $k + 1$.

Suppose G is a star-flower graph such that there exists some q , where $w < q < k$, for which there is no cycle with a rank number q . Consider a labeling f of G as follows. Label each cycle using its χ_r -ranking so that the vertices adjacent to x are given the highest label needed in each cycle. Now let $f(x) = q$.

The restriction of f to each cycle is a valid ranking. For any two vertices u and v , where both are on different cycles with rank number less than q , any u - v path contains x and $f(x) = q > f(u)$ if $f(u) = f(v)$. Also, if both u and v are on different cycles where one or both of the cycles have a rank number greater than q , and if $f(u) = f(v)$, then any u - v path contains the vertex on the larger cycle which is greater than $f(u)$. Thus f is a valid k -ranking, and therefore $\chi_r(G) \leq k$. Hence in this case $\chi_r(G) = \chi_r(C_n)$.

Now, let G be a star-flower graph such that for all integers q in $w \leq q \leq k$ there is at least one cycle with rank number q . If there are two or more cycles in G with rank number k (that is, $w = k$), then by Lemma 2 we have $\chi_r(G) \geq k + 1$. Otherwise, since there are at least two cycles with a rank number of w , the connected supergraph of these cycles must have a rank number of at least $w + 1$ by Lemma 2. Since there is a cycle with a rank number of $w + 1$, the subgraph of G formed by taking the connected supergraph of this cycle and the subgraph with rank number $w + 1$ must have a rank number of at least $w + 2$, also by Lemma 2. Continuing this argument, since there are cycles with rank numbers of $w + 2$ through k , we see that $\chi_r(G) \geq k + 1$. Thus, if G is a star-flower graph with two or more cycles with the same rank number and if there is at least one cycle with rank number q for all integers q in $w \leq q \leq k$, then $\chi_r(G) = \chi_r(C_n) + 1$. \square

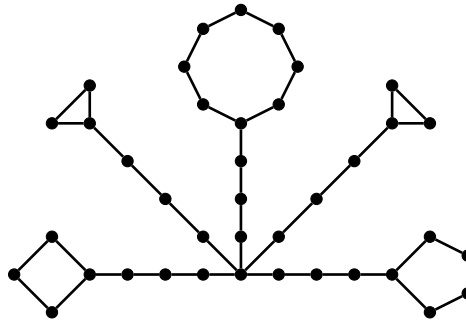


Figure 4. Spider-flower graph.

5. Spider-flower graphs

A spider-flower graph consists of three or more lollipop graphs

$$L_{a,b_1}, L_{a,b_2}, L_{a,b_3}, \dots, L_{a,b_n}$$

that are appended to a center vertex x (the pendant vertex in each lollipop graph is adjacent to x in the spider-flower graph). Figure 4 illustrates a spider-flower graph which consists of five lollipop graphs. The paths of the lollipop graphs comprising the spider-flower graph are of the same length by definition. The largest cycle in a spider-flower graph will be referred to as C_n , and the paths of the lollipop graphs which comprise the spider-flower graph will be referred to as P_a and are the arms of the spider-flower graph. Note that any spider-flower graph has at least three arms by definition.

To determine the rank number of a spider-flower graph, as with lollipop graphs, we will consider three main cases of spider-flower graphs: $\chi_r(C_n) < \chi_r(P_a)$, $\chi_r(C_n) = \chi_r(P_a)$, and $\chi_r(C_n) > \chi_r(P_a)$.

Theorem 12. *Let G be a spider-flower graph such that $\chi_r(C_n) < \chi_r(P_a)$. Then*

$$\chi_r(G) = \begin{cases} \chi_r(P_a) + 1 & \text{if } 2^{\chi_r(P_a)-1} \leq a < \sum_{i=\chi_r(C_n)}^{\chi_r(P_a)} 2^{i-1}, \\ \chi_r(P_a) + 2 & \text{otherwise.} \end{cases}$$

Proof. Suppose G is a spider-flower graph with $\chi_r(C_n) < \chi_r(P_a)$. Let $\chi_r(P_a) = j$ and let $\chi_r(C_n) = k$. Then $j + 1 \leq \chi_r(G) \leq j + 2$. The lower bound follows from Lemma 2 since there are at least two vertex-disjoint copies of P_a in G . The upper bound is true because G can be given a valid $(j + 2)$ -ranking as follows. Label each of the cycles in G using its χ_r -ranking, label the vertex on each arm that is adjacent to the cycles with $j + 1$, label the remaining vertices of each arm using the standard ranking of a path, and label x with $j + 2$.

Now, suppose G has arms of order a such that

$$2^{\chi_r(P_a)-1} \leq a < \sum_{i=\chi_r(C_n)}^{\chi_r(P_a)} 2^{i-1}.$$

Consider a labeling f of G as follows. Label the cycles in G using a k -ranking where the vertices on each cycle that are adjacent to the arms are labeled with k . Label each arm using the labeling scheme described in the proof of Theorem 9. Finally, let $f(x) = j + 1$.

The restriction of f to each lollipop graph is a valid ranking by similar arguments as in the proof of Theorem 9. Also, for any two vertices u, v with $f(u) = f(v)$, if u and v occur on different cycles or on different arms, or if one is on a cycle and the other is on a nonadjacent arm, then any u - v path contains x and $f(x) = j + 1 > f(u)$. This means f is a valid $j + 1$ -ranking. Thus $\chi_r(G) \leq j + 1$, and hence if

$$\chi_r(C_n) < \chi_r(P_a) \quad \text{and} \quad 2^{j-1} \leq a < \sum_{i=w}^j 2^{i-1},$$

then $\chi_r(G) = \chi_r(P_a) + 1$.

Suppose $a \geq \sum_{i=k}^j 2^{i-1}$. Since $\chi_r(P_a) = j$, we have $2^{j-1} \leq a < 2^j$, so

$$\sum_{i=k}^j 2^{i-1} \leq a < 2^j.$$

There is at least one lollipop graph $L_{a,b}$ which is a subgraph of G that has rank number $j + 1$ by Theorem 9. There are also at least two other arms in G which are vertex-disjoint from $L_{a,b}$, and the rank number of the connected supergraph H of these two arms must also be at least $j + 1$ by Lemma 2. So, by applying Lemma 2 again, the rank number of the connected supergraph of $L_{a,b}$ and H must be at least $j + 2$, and thus $\chi_r(G) \geq j + 2$. Therefore, if

$$\chi_r(C_n) < \chi_r(P_a) \quad \text{and} \quad \sum_{i=w}^j 2^{i-1} \leq a < 2^j,$$

then $\chi_r(G) = \chi_r(P_a) + 2$. □

Theorem 13. *Let G be a spider-flower graph such that $\chi_r(C_n) = \chi_r(P_a)$. Then $\chi_r(G) = \chi_r(C_n) + 2$.*

Proof. Let $\chi_r(P_a) = \chi_r(C_n) = k$. Using the same arguments as in the proof of the second case in Theorem 12, we have $\chi_r(G) \geq k + 2$.

Now consider a labeling f of G as follows. Label the largest cycle(s) using a valid k -ranking, where the vertex which is adjacent to the arm of G is labeled k .

Label all of the other cycles using their χ_r -ranking and placing the largest label on the vertex adjacent to the arm. Now, label the vertex on each of the arms which is adjacent to the cycles $k + 1$. Label the remainder of each of the arms according to the standard labeling of a path. Finally, let $f(x) = k + 2$.

Note that f restricted to a cycle or an arm is a valid ranking. Also, for any two vertices u, v where both are on different cycles or both are on different arms, if $f(u) = f(v)$ then any $u-v$ path will contain x and $f(x) = k + 2 > f(u)$. Finally, for any two vertices u, v where one is on a cycle and the other is on an adjacent arm, if $f(u) = f(v)$, then any $u-v$ path will contain the vertex on the arm of G which is adjacent to the cycle and is labeled $k + 1 > f(u)$. Hence, f is a valid $(k + 2)$ -ranking and thus $\chi_r(G) \leq k + 2$.

Therefore if $\chi_r(C_n) = \chi_r(P_a)$, then $\chi_r(G) = \chi_r(C_n) + 2$. □

Now we consider the case where $\chi_r(C_n) > \chi_r(P_n)$ in a spider-flower graph.

Lemma 14. *Let G be a spider-flower graph such that $\chi_r(C_n) > \chi_r(P_a)$. Then $\chi_r(C_n) \leq \chi_r(G) \leq \chi_r(C_n) + 1$.*

Proof. C_n is a subgraph of G , and thus by Lemma 1, $\chi_r(C_n) \leq \chi_r(G)$.

Consider a labeling f of G as follows. Label all cycles using their χ_r -ranking by placing the highest label on the vertices adjacent to the arms, and then relabel these vertices with $\chi_r(C_n)$. Label the arms of G according to the standard labeling of a path, and then label x with $\chi_r(C_n) + 1$. Note that f restricted to a cycle or an arm is a valid ranking. If two vertices u, v are on different cycles, different arms, or one on a cycle and the other on a nonadjacent arm, then any $u-v$ path contains the vertex x , and $f(x) = \chi_r(C_n) + 1 > f(u)$. Also, since $\chi_r(C_n) > \chi_r(P_a)$, if u is on a cycle and v is on an adjacent arm, then any $u-v$ path contains vertex adjacent to the arm labeled $\chi_r(C_n) > f(v)$.

Therefore f is a valid $(\chi_r(C_n) + 1)$ -ranking of G , and so $\chi_r(G) \leq \chi_r(C_n) + 1$. □

For the rest of the paper, we consider d the largest repeated rank number among the cycles. If no two cycles have the same rank number, then we assume $d = 0$.

Theorem 15. *Let G be a spider-flower graph such that $\chi_r(C_n) > \chi_r(P_a)$. Suppose G has two or more cycles with the same rank number, the greatest of these being d . Let $\chi_r(P_a) < d \leq \chi_r(C_n)$. Then $\chi_r(G) = \chi_r(C_n)$ if there exists t such that $d < t < \chi_r(C_n)$ and such that there is no cycle C in G with $\chi_r(C) = t$. In the opposite case, $\chi_r(G) = \chi_r(C_n) + 1$.*

Proof. Let G be a spider-flower graph where two or more cycles have the same rank number, the greatest of these being d , and $\chi_r(P_a) < d \leq \chi_r(C_n)$. Also, let $\chi_r(C_n) = k$. Suppose there exists some t such that $d < t < k$ and there is no cycle with rank number t in G . Consider the labeling f of G as follows. The cycles in G are labeled using their χ_r -ranking, where the vertices adjacent to the arms are given

the largest label for each cycle. For those cycles with rank numbers less than d , replace the largest label with d . Label the arms using the standard labeling of a path. Finally, since there is some t , where $d < t < k$, for which there is no cycle with a rank number t , label x with the greatest such t .

Note that f restricted to a cycle or an arm is a valid ranking. For any two vertices u, v where both are on different arms of G , if $f(u) = f(v)$, then any u - v path will contain x , and $f(x) = t > \chi_r(P_a) \geq f(u)$. Also, for any two vertices u, v where both are on different cycles of G or where one is on a cycle and the other is on a nonadjacent arm, if at least one of the cycles has a rank number greater than $t > d$, then if $f(u) = f(v)$, any u - v path will contain the vertex on the larger cycle adjacent to the arm which has a label greater than $f(u)$. And, for any two vertices u, v where both are on different cycles of G or where one is on a cycle and the other is on a nonadjacent arm, if none of the cycles have a rank number greater than t , then if $f(u) = f(v)$, any u - v path will contain the center vertex x , and $f(x) = t > d \geq f(u)$. Finally, for any two vertices u, v where one is on a cycle and the other is on the arm adjacent to that cycle, if $f(u) = f(v)$, then any u - v path will contain the vertex on the cycle which is adjacent to the arm with label $q \geq d > \chi_r(P_a) \geq f(u)$. Thus f is a valid k -ranking, and hence $\chi_r(G) \leq \chi_r(C_n)$. Therefore, by Lemma 14, we have $\chi_r(G) = \chi_r(C_n)$.

Now, suppose for all t in $d < t < k$ there is a cycle with rank number t in G . If there are two or more cycles with a rank number of k , then $\chi_r(G) \geq k + 1$ by Lemma 2. Otherwise, since there are at least two cycles with a rank number of d , the rank number of the connected supergraph of these two cycles must be at least $d + 1$. Then using similar arguments as in the proof of Theorem 11, $\chi_r(G) \geq k + 1$. Thus, by Lemma 14, $\chi_r(G) = \chi_r(C_n) + 1$. \square

Theorem 16. *Let G be a spider-flower graph such that $\chi_r(C_n) > \chi_r(P_a)$. Suppose G has two or more cycles with the same rank number, the greatest of these being d , and that $d \leq \chi_r(P_a) < \chi_r(C_n)$. Let b be the largest number for which*

$$2^{\chi_r(P_a)-1} \leq a < \sum_{i=b}^{\chi_r(P_a)} 2^{i-1}.$$

Suppose there are no cycles with rank number r where $b + 1 \leq r \leq \chi_r(P_a)$. Then $\chi_r(G) = \chi_r(C_n)$ if there exists t such that $\chi_r(P_a) < t < \chi_r(C_n)$ and such that there is no cycle C in G with $\chi_r(C) = t$. In the opposite case, $\chi_r(G) = \chi_r(C_n) + 1$.

Proof. Assume that there exists t as in the statement. Let $\chi_r(P_a) = j$ and let $\chi_r(C_n) = k$. Consider a labeling f of G as follows. Label the cycles in G using their χ_r -ranking so that the vertex adjacent to the arm has the largest label on the cycle. Relabel the highest-labeled vertices in each of the cycles that have rank numbers less than b with b . Now, label the arms adjacent to cycles with rank

numbers greater than j using the standard labeling of a path. The rest of the arms are now adjacent to vertices labeled b . As there are a maximum of $\sum_{i=b}^j 2^{i-1} - 1$ vertices on each arm which remain to be labeled, these arms can be labeled with j labels using the standard labeling of a path beginning with the vertex adjacent to the cycle and treating that vertex as if it were the $(2^{b-1} + 1)$ -st vertex in the path as in the proof of Theorem 9. Finally, let $f(x) = s$, where s is the greatest t in $j < t < k$ for which there is no cycle with a rank number of t .

Note that f restricted to a cycle or an arm is a valid ranking. For any two vertices u, v where both are on different arms, both are on different cycles whose rank numbers are less than s , or one is on a cycle with rank number less than s and the other is on a nonadjacent arm, if $f(u) = f(v)$, then any $u-v$ path will contain the center vertex x , where $f(x) = s > j \geq f(u)$. For any two vertices u, v where both are on cycles where one or both of the rank numbers is greater than s or one is on a cycle with rank number greater than s and the other is on a nonadjacent arm, if $f(u) = f(v)$, then any $u-v$ path will contain the vertex that is adjacent to the arm on the larger cycle and has a label $q > f(u)$. Also, for any two vertices u, v where one is on a cycle and the other is on an adjacent arm, if the rank number of the cycle is greater than j and $f(u) = f(v)$, then any $u-v$ path will contain the vertex on the cycle adjacent to the arm which has a label $z > j \geq f(u)$. If the rank number of the cycle is less than j and $f(u) = f(v)$, then any $u-v$ path will either contain the vertex on the cycle labeled b where $b > f(u)$, or will contain the vertex with a higher label as in the proof of Theorem 9. Therefore f is a valid k -ranking, and hence $\chi_r(G) \leq \chi_r(C_n)$. Thus $\chi_r(G) = \chi_r(C_n)$ by Lemma 14.

Now, let G be a spider-flower graph where for every t such that $j < t < k$, there exists some cycle with rank number equal to t . Since there are at least two disjoint copies of P_a in G , a label of $y \geq j + 1$ must be used to separate these arms. However, since for every t in $j < t < k$ there is some cycle with rank number equal to t , $\chi_r(G) \geq k + 1$ by the same argument used in the proof of Theorem 11. Thus, by Lemma 14, $\chi_r(G) = \chi_r(C_n) + 1$. □

Theorem 17. *Let G be a spider-flower graph such that $\chi_r(C_n) > \chi_r(P_a)$. Suppose G has two or more cycles with the same rank number, the greatest of these being d , and that $d \leq \chi_r(P_a) < \chi_r(C_n)$. Let b be the largest number for which*

$$2^{\chi_r(P_a)-1} \leq a < \sum_{i=b}^{\chi_r(P_a)} 2^{i-1}.$$

Suppose there is at least one cycle with rank number r for $b + 1 \leq r \leq \chi_r(P_a)$. Then $\chi_r(G) = \chi_r(C_n)$ if there exists t such that $\chi_r(P_a) + 1 < t < \chi_r(C_n)$ and such that there is no cycle C with $\chi_r(C) = t$. In the opposite case, $\chi_r(G) = \chi_r(C_n) + 1$.

Proof. Assume there exists t as in the statement. Let $\chi_r(P_a) = j$ and let $\chi_r(C_n) = k$. Now, consider a labeling f of G as follows. Label G as in the proof of Theorem 16 except that for those cycles with rank number r , where $b + 1 \leq r \leq j$, the vertices on the arms adjacent to the cycles are labeled $j + 1$ and the remainder of the arms are labeled according to the standard labeling of a path. Finally, let $f(x) = s$, where s is the largest t in $j + 1 < t < k$ for which there is no cycle with rank number t .

For any two vertices u, v where one vertex is on a cycle with rank number r , where $b + 1 \leq r \leq j$, any u - v path will contain the vertex on the arm adjacent to the cycle labeled $j + 1$, and $j + 1 > f(u)$. For two vertices u, v in any other position of the graph, we can use the same arguments as in the proof of Theorem 16 and conclude that f is a valid k -ranking. Therefore $\chi_r(G) \leq \chi_r(C_n)$, and hence $\chi_r(G) = \chi_r(C_n)$ by Lemma 14.

Now, let G be a spider-flower graph where for every t in $j + 1 < t < k$ there is some cycle with rank number t . Since there is a cycle with rank number r for each r such that $b + 1 \leq r \leq j$, G contains a cycle with rank number j . This cycle, together with its arm P_a , forms a lollipop graph $L_{a,z}$ with rank number $j + 1$ by Theorem 8. Also, since G has at least three lollipop graphs as subgraphs, there are at least two disjoint copies of P_a , namely P and Q , which are also disjoint from $L_{a,z}$. G also has cycles of rank number t , where $j + 1 < t < k$. These cycles, P , Q , and $L_{a,z}$ are mutually vertex-disjoint. Then, using a similar argument as in Theorem 11, we get $\chi_r(G) \geq k + 1$, and hence by Lemma 14 we get $\chi_r(G) = \chi_r(C_n) + 1$. \square

6. Conclusion and future directions

We determined the rank numbers of flower graphs, lollipop graphs, star-flower graphs, and spider-flower graphs. We determined the rank number of each of these graphs for any size of cycles. The spider-flower graphs consists of at least three lollipop graphs that are appended to a vertex. However, the graph where exactly two lollipop graphs are appended to a vertex requires significantly different analysis than the spider-flower graphs. Some cases of this graph were looked into in [McClive 2010].

By definition, the arms of the spider-flower graphs are of the same length. One related graph to consider would be the graph that consists of lollipop graphs of different arm lengths appended to a center vertex. Finding the rank number of this graph requires finding the rank number of a special type of graphs called extended star graphs. We can define an extended star graph to be a graph that consists of paths of any length appended to a single vertex. It is clear that the rank number of an extended star graph is either $\chi_r(P_n)$ or $\chi_r(P_n) + 1$, where P_n is the longest path in the extended star graph. However, characterizing extended star graphs with respect to their rank numbers turned out to be extremely difficult.

References

- [Alpert 2010] H. Alpert, “Rank numbers of grid graphs”, *Discrete Math.* **310**:23 (2010), 3324–3333. MR 2012a:05264 Zbl 1221.05280
- [Bodlaender et al. 1995] H. L. Bodlaender, J. S. Deogun, K. Jansen, T. Kloks, D. Kratsch, H. Müller, and Z. Tuza, “Rankings of graphs”, pp. 292–304 in *Graph-theoretic concepts in computer science* (Herrsching, 1994), edited by E. W. Mayr et al., Lecture Notes in Comput. Sci. **903**, Springer, Berlin, 1995. MR 96h:68145
- [Bruoth and Horňák 1999] E. Bruoth and M. Horňák, “On-line ranking number for cycles and paths”, *Discuss. Math. Graph Theory* **19**:2 (1999), 175–197. MR 2002g:05109 Zbl 0958.05076
- [Dereniowski and Nadolski 2006] D. Dereniowski and A. Nadolski, “Vertex rankings of chordal graphs and weighted trees”, *Inform. Process. Lett.* **98**:3 (2006), 96–100. MR 2006j:68032 Zbl 1187.68340
- [Duff and Reid 1983] I. S. Duff and J. K. Reid, “The multifrontal solution of indefinite sparse symmetric linear equations”, *ACM Trans. Math. Software* **9**:3 (1983), 302–325. MR 86k:65030 Zbl 0515.65022
- [Ghoshal et al. 1996] J. Ghoshal, R. Laskar, and D. Pillone, “Minimal rankings”, *Networks* **28**:1 (1996), 45–53. MR 97e:05110 Zbl 0863.05071
- [Hsieh 2002] S.-y. Hsieh, “On vertex ranking of a starlike graph”, *Inform. Process. Lett.* **82**:3 (2002), 131–135. MR 2002k:05085 Zbl 1013.68141
- [Iyer et al. 1991] A. V. Iyer, H. D. Ratliff, and G. Vijayan, “On an edge ranking problem of trees and graphs”, *Discrete Appl. Math.* **30**:1 (1991), 43–52. MR 91k:90071 Zbl 0727.05053
- [Leiserson 1980] C. Leiserson, “Area efficient graph layouts for VLSI”, pp. 270–281 in *Proc. 21st Ann IEEE Symp. FOCS*, IEEE, Piscataway, NJ, 1980.
- [Liu 1990] J. W. H. Liu, “The role of elimination trees in sparse factorization”, *SIAM J. Matrix Anal. Appl.* **11**:1 (1990), 134–172. MR 91a:65115 Zbl 0697.65013
- [McClive 2010] J. N. McClive, “Rank numbers for graphs with paths and cycles”, Master’s thesis, Rochester Institute of Technology, 2010, <https://ritdml.rit.edu/handle/1850/13411>.
- [Novotny et al. 2009] S. Novotny, J. Ortiz, and D. A. Narayan, “Minimal k -rankings and the rank number of P_n^2 ”, *Inform. Process. Lett.* **109**:3 (2009), 193–198. MR 2009m:05067
- [Ortiz et al. 2010] J. Ortiz, A. Zemke, H. King, D. Narayan, and M. Horňák, “Minimal k -rankings for prism graphs”, *Involve* **3**:2 (2010), 183–190. MR 2011g:05264 Zbl 1221.05159
- [Sen et al. 1992] A. Sen, H. Deng, and S. Guha, “On a graph partition problem with application to VLSI layout”, *Inform. Process. Lett.* **43**:2 (1992), 87–94. MR 1187395 Zbl 0764.68132
- [Sergel et al. 2011] E. Sergel, P. Richter, A. Tran, P. Curran, J. Jacob, and D. A. Narayan, “Rank numbers for some trees and unicyclic graphs”, *Aequationes Math.* **82**:1-2 (2011), 65–79. MR 2012e:05331 Zbl 1232.05210

Received: 2013-04-25 Accepted: 2013-07-29

blakeb@augsbu.edu

Mathematics Department, Augsburg College,
Minneapolis, MN 55454, United States

fielde1@owls.southernct.edu

Department of Mathematics, Southern Connecticut State
University, New Haven, CT 06515, United States

jsxjsma@rit.edu

School of Mathematical Sciences, Rochester Institute of
Technology, Rochester, NY 14623, United States

Guidelines for Authors

Authors may submit manuscripts in PDF format on-line at the Submission page at the *Involve* website.

Originality. Submission of a manuscript acknowledges that the manuscript is original and is not, in whole or in part, published or under consideration for publication elsewhere. It is understood also that the manuscript will not be submitted elsewhere while under consideration for publication in this journal.

Language. Articles in *Involve* are usually in English, but articles written in other languages are welcome.

Required items. A brief abstract of about 150 words or less must be included. It should be self-contained and not make any reference to the bibliography. If the article is not in English, two versions of the abstract must be included, one in the language of the article and one in English. Also required are keywords and subject classifications for the article, and, for each author, postal address, affiliation (if appropriate), and email address.

Format. Authors are encouraged to use \LaTeX but submissions in other varieties of \TeX , and exceptionally in other formats, are acceptable. Initial uploads should be in PDF format; after the refereeing process we will ask you to submit all source material.

References. Bibliographical references should be complete, including article titles and page ranges. All references in the bibliography should be cited in the text. The use of Bib \TeX is preferred but not required. Tags will be converted to the house format, however, for submission you may use the format of your choice. Links will be provided to all literature with known web locations and authors are encouraged to provide their own links in addition to those supplied in the editorial process.

Figures. Figures must be of publication quality. After acceptance, you will need to submit the original source files in vector graphics format for all diagrams in your manuscript: vector EPS or vector PDF files are the most useful.

Most drawing and graphing packages (Mathematica, Adobe Illustrator, Corel Draw, MATLAB, etc.) allow the user to save files in one of these formats. Make sure that what you are saving is vector graphics and not a bitmap. If you need help, please write to graphics@msp.org with details about how your graphics were generated.

White space. Forced line breaks or page breaks should not be inserted in the document. There is no point in your trying to optimize line and page breaks in the original manuscript. The manuscript will be reformatted to use the journal's preferred fonts and layout.

Proofs. Page proofs will be made available to authors (or to the designated corresponding author) at a Web site in PDF format. Failure to acknowledge the receipt of proofs or to return corrections within the requested deadline may cause publication to be postponed.

involve

2013

vol. 6

no. 3

Potentially eventually exponentially positive sign patterns MARIE ARCHER, MINERVA CATRAL, CRAIG ERICKSON, RANA HABER, LESLIE HOGBEN, XAVIER MARTINEZ-RIVERA AND ANTONIO OCHOA	261
The surgery unknotting number of Legendrian links BIANCA BORANDA, LISA TRAYNOR AND SHUNING YAN	273
On duals of p -frames ALI AKBAR AREFIJAMAAL AND LEILI MOHAMMADKHANI	301
Shock profile for gas dynamics in thermal nonequilibrium WANG XIE	311
Expected conflicts in pairs of rooted binary trees TIMOTHY CHU AND SEAN CLEARY	323
Hyperbolic construction of Cantor sets ZAIR IBRAGIMOV AND JOHN SIMANYI	333
Extensions of the Euler–Satake characteristic for nonorientable 3-orbifolds and indistinguishable examples RYAN CARROLL AND CHRISTOPHER SEATON	345
Rank numbers of graphs that are combinations of paths and cycles BRIANNA BLAKE, ELIZABETH FIELD AND JOBBY JACOB	369



1944-4176(2013)6:3;1-8